UNIVERSIDADE ESTADUAL PAULISTA "JÚLIO DE MESQUITA FILHO"
FACULDADE DE ENGENHARIA
CÂMPUS DE ILHA SOLTEIRA

ELHAM MAHDAVI

RECONFIGURATION OF DISTRIBUTION NETWORKS WITH SIMULTANEOUS ALLOCATION OF DISTRIBUTED GENERATION USING THE WHALE OPTIMIZATION ALGORITHM

Ilha Solteira
2023

UNIVERSIDADE ESTADUAL PAULISTA
"JÚLIO DE MESQUITA FILHO"
Campus de Ilha Solteira

POSTGRADUATE PROGRAM IN ELECTRICAL ENGINEERING

ELHAM MAHDAVI

Reconfiguration of distribution networks with simultaneous allocation of distributed generation using the whale optimization algorithm

The category of the thesis work presented to the Faculty of Engineering, Campus of Ilha Solteira, Sao Paulo State University, as part of the requirements for obtaining the title of doctoral degree (PhD) in Electrical Engineering. Specialty: Automation.

Prof. Dr. Rubén Augusto Romero Lázaro
Advisor

Leonardo H. F. Macedo Possagnolo
Co-advisor

Ilha Solteira

2023

FICHA CATALOGRÁFICA
Desenvolvido pelo Serviço Técnico de Biblioteca e Documentação

M214r

Mahdavi, Elham.

Reconfiguration of distribution networks with simultaneous allocation of distributed generation using the whale optimization algorithm / Elham Mahdavi. -- Ilha Solteira: [s.n.], 2023

154 f. : il.

Tese (doutorado) - Universidade Estadual Paulista. Faculdade de Engenharia de Ilha Solteira. Área de conhecimento: Automação, 2023

Orientador: Rubén Augusto Romero Lázaro
Co-orientador: Leonardo Henrique Faria Macedo Possagnolo
Inclui bibliografia

1. Whale optimization algorithm. 2. Distribution network. 3. Reconfiguration. 4. Power losses. 5. Distributed generation. 6. MATLAB.

Amanda Sertori dos Santos
Bibliotecária - CRB/8-9061
Seção Técnica de Referência, Atendimento ao Usuário e Documentação
Diretoria Técnica de Biblioteca e Documentação

UNIVERSIDADE ESTADUAL PAULISTA

Câmpus de Ilha Solteira

CERTIFICADO DE APROVAÇÃO

TÍTULO DA TESE: Reconfiguration of distribution networks with simultaneous allocation of distributed generation using the whale optimization algorithm

AUTORA: ELHAM MAHDAVI
ORIENTADOR: RUBEN AUGUSTO ROMERO LAZARO
COORIENTADOR: LEONARDO HENRIQUE FARIA MACEDO POSSAGNOLO

Aprovada como parte das exigências para obtenção do Título de Doutora em Engenharia Elétrica, área: Automação pela Comissão Examinadora:

Prof. Dr. RUBEN AUGUSTO ROMERO LAZARO (Participaçao Presencial)
Departamento de Engenharia Eletrica / Faculdade de Engenharia de Ilha Solteira - UNESP

Profa. Dra. ANNA DIVA PLASENCIA LOTUFO (Participaçao Presencial)
Departamento de Engenharia Elétrica / Faculdade de Engenharia de Ilha Solteira - UNESP

Prof. Dr. JONATAS BOAS LEITE (Participaçao Presencial)
Departamento de Engenharia Elétrica / Faculdade de Engenharia de Ilha Solteira - UNESP

Prof. Dr. CARLOS ROBERTO MENDONÇA DA ROCHA (Participaçao Virtual)
Departamento de Engenharia Eletrica / Universidade Estadual do Oeste do Paraná - UNIOESTE

Prof. Dr. MOHAMMAD HOSEIN SABZALIAN (Participaçao Virtual)
Departamento de Engenharia Mecanica / Universidad de Santiago de Chile - USACH

Ilha Solteira, 24 de julho de 2023

DEDICATION

I dedicate this thesis to Mr. Seifollah Asadpour (Ph.D. student of electrical engineering at São Paulo State University (UNESP)) from the beautiful province of Mazandaran, Iran, and the land of North Savadkuh, in the village of Deraz Kola, who was always my friend, companion and supporter in achieving this success.

THANKS

To Mr. Seifollah Asadpour, for his support, friendship, understanding, and help.

To Professor Rubén Romero, for his dedication, patience, trust and friendship during the orientation.

To professors Dr. Anna Diva Plasencia Lotufo (Department of Electrical Engineering / Faculty of Engineering of Ilha Solteira - UNESP), Dr. Jonatas Boas Leite (Department of Electrical Engineering / Faculty of Engineering of Ilha Solteira - UNESP), Dr. Carlos Roberto Mendonça Da Rocha (Department of Electrical Engineering / State University of Western Paraná - UNIOESTE), and Dr. Mohammadhosein Sabzalian (Department of Mechanical Engineering / University of Santiago de Chile - USACH), as the committee of examiners for their suggestions and friendship during the development of this work.

This work was carried out with the support of the Coordination for the Improvement of Higher Education Personnel - Brazil (CAPES) - Financing Code 001.

“Human beings are members of a whole,
In creation of one essence and soul.
If one member is afflicted with pain,
Other members uneasy will remain.
If you’ve no sympathy for human pain,
The name of human you cannot retain!”. Saadi Shirazi from Iran.

ABSTRACT

Due to the economic interest of the reduction of the power losses and the regulatory requirements regarding voltage levels in steady state, this study offers a computational methodology to assist in the optimization of the power losses and voltage profile in steady state through the distribution network reconfiguration (DNR) and distributed generations (DGs). The power flow execution and the methods of the sophisticated optimization are able to investigate the big combinative problems required to study DNR. The optimization procedure kind utilized in the distribution network is determined based on the size of the network. Approaches that are expensive in terms of computation or prohibitive include direct approaches, but approaches that have acceptable results with less computational expense include heuristic or metaheuristic approaches. In this research, the load flow that is implemented, is the backward-forward sweep method and we intend to use IEEE 33-bus, IEEE 69-bus, 136-bus, and 415-bus systems. Therefore, we consider the simulation of all the systems according to the network layout and proper placement of DGs in the network using the whale optimization algorithm (WOA). The objective function is to reduce power losses by the DNR and the optimal location and size of DG units, but the voltage profile also improves in this problem. Due to the nonlinear, nonconvex and large nature of the problem, the WOA is used to optimize the problem under MATLAB software. The results indicate that the WOA algorithm performs better in terms of power loss reduction and voltage profile improvement when compared with other metaheuristics shown in the chapter of the tests and results.

Keywords: whale optimization algorithm; distribution network; reconfiguration; power losses; distributed generation; MATLAB.

RESUMO

Devido ao interesse econômico da redução das perdas de potência e aos requisitos regulatórios referentes aos níveis de tensão em regime permanente, este trabalho propõe uma metodologia computacional para auxiliar na otimização das perdas de potência e perfil de tensão em regime permanente através da reconfiguração da rede de distribuição (RRD) e Gerações Distribuídas (GDs). A execução do fluxo de potência e os métodos de otimização sofisticados são capazes de investigar os grandes problemas combinatórias necessários para estudar o RRD. O tipo de procedimento de otimização utilizado na rede de distribuição é determinado com base no tamanho da rede. Abordagens que são caras em termos de computação ou proibitivas incluem abordagens diretas, mas abordagens que têm resultados aceitáveis com menor gasto computacional incluem abordagens heurísticas ou metaheurísticas. Nesta pesquisa, o fluxo de carga implementado é o método backward-forward e são usados os dados dos sistemas de IEEE 33 barras, IEEE 69 barras, 136 barras e 415 barras. Portanto, consideramos a simulação de todos os sistemas de acordo com o tipo de rede e o posicionamento adequado dos GDs na rede usando o algoritmo de otimização de baleias (AOB). A função objetivo é minimizar a perdas de potência pelo RRD e a localização e tamanho ideais das unidades GD, mas o perfil de tensão também melhora neste problema. Devido à natureza não linear, não convexa e grande porte do problema, o AOB é usado para otimizar o problema usando o software MATLAB. Os resultados indicam que o algoritmo AOB apresenta melhor desempenho em termos de redução de perdas de potência e melhora do perfil de tensão quando comparado com outras metaheurísticas mostradas no capítulo de testes e resultados.

Palavras-chave: algoritmo de otimização de baleias; rede de distribuição; reconfiguração; perdas de potência; geração distribuída; MATLAB.

LIST OF FIGURES

LIST OF TABLES

LIST OF ABBREVIATIONS

AACO	Adaptive Ant Colony Optimization
ACSA	Adaptive Cuckoo Search Algorithm
APS	Adaptive Protection System
ALO	Antlion Optimizer
ABRADEE	Associação Brasileira de Distribuidores de Energia Elétrica
DERs	Distributed Energy Resources
DGs	Distributed Generations
DMS	Distribution Management Systems
DNR	Distribution Network Reconfiguration
DNRP	Distribution Network Reconfiguration Problem
EEDS	Electrical Energy Distribution System
ESSs	Energy Storage Systems
EMPA	Enhanced Marine Predators Algorithm
EP	Evolutionary Programming
FCL	Fault Current Limiter
FA	Firefly Algorithm
FWA	Fireworks Algorithm
FACTS	Flexible Alternating Current Transmission Systems
FLs	Fundamental Loops
GA	Genetic Algorithm
GWO	Grey Wolf Optimization
HS	Harmonic Search

IEOA	Improved Equilibrium Optimization Algorithm
IEEE	Institute of Electrical and Electronics Engineers
LP	Linear Programming
LSF	Loss Sensitivity
MDP	Markov Decision Process
MATLAB	MATrix LABoratory
MBGWO	Modified Binary Gray Wolf Optimization
MPGSA	Modified Plant Growth Simulation Algorithm
NR	Newton Raphson
NC	Normally Closed Switches
NO	Normally Open Switches
OPF	Optimal Power Flow
PSO	Particle Swarm Optimization
PSOGSA	Particle Swarm Optimization and Gravitational Search Algorithm
PV	Photovoltaic
PVSI	Photovoltaic Smart Inverter
PLI	Power Loss Index
PVQ	Bus Voltage Control considering the Supply of Variable Reactive Power at P Bus
QOCNNA	Quasi-Oppositional Chaotic Neural Network Algorithm
QRSMA	Quasi-Reflection-Based Slime Mould Algorithm
RDN	Radial Distribution Networks
RDS	Radial Distribution System

SSA	Salp Swarm Algorithm
SHS	Self-Healing System
SNR-DG	Simultaneous Network Reconfiguration and Location of Distributed Generations
S-matrix	State-Matrix
SFS	Stochastic Fractal Search
SMDGs	Synchronous Machine-Based Distributed Generations
TMS	Time Multiplier Settings
TLMS	Transformer Load Management Systems
UVDA	Uniform Voltage Distribution-Based Constructive Reconfiguration Algorithm
VSF	Voltage Sensitivity Factors
VSI	Voltage Stability Index
VVC	Volt-Var Control
WOA	Whale Optimization Algorithm

LIST OF SYMBOLS

P_{losses} Power losses

R Electrical resistance of conductor

I Current intensity

V_q Module of voltage

Z Conductor impedance module

ZIP Constant power (P), constant current (I) and constant impedance (Z)

P_m Active power losses in line m

R_m Resistance of line m

I_m Current module in line m

$P_m[n]$ Active power losses in line m in interval n

$I_m[n]$ Module of current in line m in time interval n

N Time intervals

T Time sampling period

E_m Active energy losses in line m in a planning period

E_{total} Active energy losses in primary distribution network

ϕ Set of primary lines of network

$V_i[n]$ Nodal voltage at bus i in instant n

$V_j[n]$ Nodal voltage at bus j in instant n

v_{min} Minimum observed voltage

v_{max} Maximum observed voltage

V_{ref} Network nominal voltage

Ω_b Set of all buses of system

X Vector of states of primary network section switches

P Considered planning period

$E_{total}(X)$ Dissipated energy by primary distribution network for state X

$A_v(X)$ Result of aggregation function for maximum and minimum voltages of state X

P_{loss} Total power losses of network

P_G Total active power injection at the substation and DGs

P_D Total active power load

F Objective function of problem

V_i Voltage magnitude at bus i

$V_{\min}$ Minimum acceptable bus voltage magnitude

$V_{\max}$ Maximum acceptable bus voltage magnitude

N_{bus} Total number of buses in network

$P_{DG,i}$ Active power output of DG unit i

$Q_{DG,i}$ Reactive power output of DG unit i

$P_{DG\min,i}$ Minimum size of DG unit i

$P_{DG\max,i}$ Maximum size of the DG unit i

N_{DG} Number of DG units

$\vec{X}$ Location vector

$\vec{X}^*$ Location vector of the best solution

t Current iteration

$\vec{A}$, $\vec{C}$ Coefficient vectors

$\vec{a}$ Vector with decreasing values from 2 to 0

$\vec{r}$ Random vector

$\vec{D}'$, $\vec{D}$ Distance between a whale and prey

b Constant value

l, p Random numbers

$\vec{X}_{rand}$ Random whales in current iteration

X_i Initial population

SW_i Status of switch i

N_{Tie} Number of tie-switches

N_p Number of solutions in population

$it\,max$ Maximum number of iterations

SUMMARY

1 INTRODUCTION

As smart grid technologies mature and deploy, the gap for developing efficient operations methods is created (COMMISSION, 2017). In electric power distribution systems, it is desirable to take advantage of computational intelligence and automation provided by the Smart Grid technologies which in a unified fashion create an efficient, reliable, clean, secure, and sustainable electric power supply (GHARAVI; GHAFURIAN, 2011). Some of the inconveniences in distribution systems are system overloading at different periods of the day and load capacity increase; these inconveniences cause excessive power losses and voltage levels variations beyond standard operational levels, consequently lowering power quality or even interrupting the power supply. Reduction of power losses and improvement of voltage profile in power distribution networks has been often approached by methodologies such as distribution network reconfiguration (DNR), capacitor bank placement and Volt/Var control (GUTIÉRREZ-ALCARAZ; TOVAR-HERNÁNDEZ, 2017; LOHIA et al., 2016). Recently, optimal allocation of distributed generation (DG) has been taken into consideration as a method for grid support due to its attributions towards frequency drop stabilization (EL-ELA et al., 2010), power loss reduction and voltage profile improvement (CRUZ et al., 2017; IMRAN et al., 2014; KHAIRUDDIN; CIPCIGAN, 2016; MOHAMMADI; FARAMARZI, 2012; RAKESH et al., 2017; REKOWSKI et al., 2017; TOLBA et al., 2017; VIRAL; KHATOD, 2012). Combination of multiple methodologies such as distribution reconfiguration and optimal allocation of DGs have been proposed to increase the benefits; however, the practical complexity of implementing such combination of methodologies increases significantly.

Radial distribution networks often feature sectionalizing switches and tie switches mainly used for fault isolation, power supply recovery and system reconfiguration. These switches allow for reconfiguring the topology of the network, with the objectives being reduction of power losses, load balancing, voltage profile improvement and increasing reliability of the system. Reference Ma et al. (2017) present a comprehensive overview of reconfiguration benefits and some optimization algorithms applied to the DNR problem. A large search space resulting from all possible switch configurations make the network reconfiguration task a complex non-linear combinatorial problem, with the complexity dramatically increasing with the number of loops, i.e., both the network size and the number of switches. Due to the nature of the DNR problem, artificial intelligence and metaheuristic optimization techniques are often applied. In Jakus et al. (2017) the authors implement an algorithm for network reconfiguration for a realistic distribution network based on a genetic algorithm (GA), taking as objective power loss minimization and load balancing index. In Nguyen and Truong (2015), an optimization algorithm based on the parasitic behaviour of the Cuckoo bird is proposed and applied to 33-bus, 69-bus and 119-bus test networks taking as objective function active power loss minimization and voltage profile improvement; the results are then compared with other methods applied to the same networks. In Patel et al. (2017), the authors propose a method for solving the DNR problem based on the Hopfield neural network, having as objective power loss reduction and reliability improvement.

Although the majority of modern DNR solution methods exploit population-based algorithms, sequential stochastic methods such as simulated annealing (ALREFAEI; DIABAT, 2009) may also be potentially advantageous. In Boicea (2017), a feasible approach to DNR with multiple feeding points is introduced; The approach adopts a hybrid optimization method involving simulated annealing and the Tabu search to avoid solution unfeasibility; DNR is implemented on a small distribution network consisting on 3 power nodes and 16 load nodes.

Incentivized by factors such as liberalization of the energy market, environmental concerns, and technology development, incorporation of DG to the power systems has recently been increasing (FRASER, 2002; PEPERMANS et al., 2005), particularly at the distribution level (RAKESH et al., 2017). DG interconnections may bring multiple technical benefits, i.e., active/reactive power loss reduction, voltage profile improvement, reliability enhancement as well as overall power delivery efficiency. However, if misallocated, DG can actually lead to degradation of the network performance (in particular, an increase of the power losses, and increase of the voltage levels above the operational standards) and contribute to instability (VIRAL; KHATOD, 2012). Consequently, it is important to consider optimal sitting and sizing of DG sources. Several optimization methods have been proposed for solving the optimal DG allocation problem. In Mohammadi and Faramarzi (2012), a Particle Swarm Optimization (PSO) algorithm has been applied to the optimum sitting and sizing of two DGs on a 13-bus network, however, the basis for selecting the optimum location of DG is not provided. In Rakesh et al. (2017), the authors determine optimal location of DG based on the Power Loss Index (PLI) and sizing is performed using the GA taking into account three objective functions, power loss reduction, voltage profile improvement and voltage stability index (VSI). In Tolba et al. (2017), the authors determine candidate buses for DG allocation based on the loss sensitivity (LSF) and voltage sensitivity factors (VSF); the optimum DG size is then determined with a hybrid PSOGSA optimization algorithm, which is the combination of Particle Swarm Optimization (PSO) and Gravitational Search Algorithm (GSA). While DNR and optimal allocation of DG can be performed individually, their benefits can be further enhanced when performed collectively. In Imran et al. (2014), DNR and optimum sitting and sizing of DG based on the fireworks algorithm (FWA) under three different loading scenarios has been proposed. The buses with the lowest VSI are selected as candidate buses followed by optimal DG sizing determined by the FWA; when both methods are performed simultaneously, losses are reduced by up to 84 percent. In Cruz et al. (2017), the authors apply GA to a 16-bus network taking as objective minimization of power costs; here, all buses are candidate for DG placement and DG sizes are generated randomly.

Although all methods mentioned above solve the reconfiguration and optimal DG allocation problem, no statistical data is presented, which is essential for measuring quality of results obtained by the algorithm. Also, in majority of cases, very small networks are considered, which does not permit conclusive assessment of the proposed methodologies in terms of their prospective performance when applied to more realistic cases.

1.1 PROBLEM STATEMENT

The distribution system is the part of the power system that receives energy from generation and delivers it to consumers. Despite the simplicity of distribution networks, a large share of investments in the network is allocated to this sector. The reason for this can be considered the extent of this part, i.e., distribution system compared to other parts, i.e., transmission system and generation. In a simpler definition, the distribution system is the part of the power system that starts from the above distribution substations and continues to the pre-meter switches of the consumers. The designers of the distribution network development projects aim to optimize economic, ensure load growth, supply required electricity consumption, design different combinations of equipment and lines, reduce the blackouts created for individual consumers, and deliver the desired energy to them. In this regard, the type of distribution system is selected according to the improvement of energy quality and its economic evaluation (MAHINDARA et al., 2020).

Todays, the extensive changes are taking place in power systems. The presence of solar, wind farms and geothermal resources at the transmission level and small renewable energy sources such as fuel cells and solar cells at the distribution level is increasing day by day. This increasing presence of renewable resources in distribution systems has created a new network structure called micro-grids (LI et al., 2017). A micro-grid consists of several distributed generation (DG) sources that are responsible for supplying power to local loads. These distributed generation sources can be wind turbines, solar cells, micro-turbines or other sources along with energy storage devices such as batteries and energy capacitors. With the increasing use of renewable energy sources in micro-grids, the coordination of these sources with electronic power raises major concerns regarding sustainability and protection issues (LU et al., 2019). Micro-grid is a new concept that is introduced with the introduction of smart grids. The micro-grid configuration is island-like in distribution systems and near local loads, which includes a set of loads. Micro-grids are active low or medium voltage distribution networks in various sizes and shapes, which include renewable energy sources such as photovoltaic (PV), wind turbines, batteries, loads and control devices. Micro-grids can be connected to or disconnected from the main network and continue to operate independently, and when connected to the network can create two-way power exchange. The main purpose of these networks is to raise technical issues related to increasing the reliability and quality of power delivered to consumers (ZHANG; CHEN, 2014).

Figure 1 – The schematic of a micro-grid

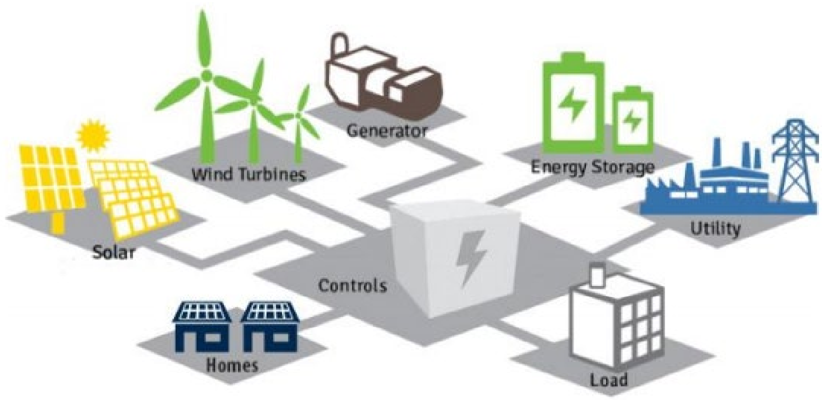

Source: Author's elaboration.

So, the implementation of DG units in distribution systems is one of the main solutions to supply the load of consumers (PANWAR et al., 2011). In fact, renewable energy sources generally require less maintenance costs than other DG technologies. Their operating costs are also low because their fuel comes from natural and available sources. In addition, the emission of greenhouse gases such as carbon dioxide with other chemical pollutants is significantly reduced by using renewable energy sources and as a result, its destructive and harmful effects on the environment are reduced. DG plays an important role in the performance of the distribution system. Deployment and size of DG units at the right time and in the distribution system is very important and challenging. Strategic deployment of DG units reduces power losses in the system and improves system voltage characteristics, reliability, voltage regulation, power quality issues, etc. (MASHAYEKH et al., 2017). Installation of DG units can have positive or negative effects (MILANOVIĆ et al., 2007). The use of DG in distributed system also reduces power system losses, but requires power electronics and telecommunications peripherals. In island grids with normal loads (active or reactive), frequency fluctuations are usually associated with controlling the losses in active converters during grid formation (GUO et al., 2020). Economic factors can be considered the most important factor among the various factors increasing the presence of DG in distributed systems. In other words, in the study of various factors in the use of DGs, the reasons and positive environmental effects have been mentioned, but economic factors have been the main reason for the increasing development of DG in distributed system (GUO et al., 2020). According to the contents and cases, some of the reasons for using DG in distributed networks can be summarized as follows:

- Issues and problems in the design of power plants, economic and environmental factors.
- Low efficiency of large power plants.
- High cost of installation, repair and maintenance of large power plants.
- Expanding and increasing demand of energy consumers.
- Reducing network outages.
- Reducing fuel consumption of power plants.
- Reducing pollution caused by power plants.

- Low investment risk (LU et al., 2019).

Distribution networks are usually designed to increase the level of reliability and reduce blackouts, but are used to reduce the level of short circuit and coordination of protection systems radially, which increases the losses in the distribution network. For this purpose, the reconfiguration of distribution feeders to reduce losses, improve reliability, etc. is performed by switching management in the distribution network. In the reconfiguration process, the arrangement of the distribution feeders is renewed according to the condition of the switches to achieve different goals. In reconfiguration, a series of restrictions must be observed, such as maintaining the radial structure of the network after reconfiguration, feeding all loads, keeping the bus voltage within a certain range, and loading the lines. The reconfiguration problem of distribution feeders is a nonlinear and nonconvex problem. Therefore, mathematical methods are not suitable due to the limitations of objective functions and constraints of this problem such as discontinuity and derivation (AZIZIVAHED et al., 2017).

Smart distributed systems are a kind of distribution which have ability to reduce power consumption on the load side during peak hours, called load side management, enabling distributed generation sources (such as photovoltaic cells, small wind turbines, or even simultaneous generation of electricity and heat in buildings) to connect to the grid, using grid energy savers to balance the load on distributed generation resources, eliminating faults such as burst faults in the power grid and automatic reconfiguration. Increased efficiency and increased reliability of the smart grid are expected to save consumers costs and reduce carbon dioxide emissions. Due to the growing focus of governments on energy security, investing in smart grids can be useful in reducing dependence on non-household energy sources (VIJAYAPRIYA; KOTHARI, 2011). Smart distributed system technologies are used to perform a specific set of applications and functions of electrical power systems. A number of smart grid technologies can be used for each function, which can be categorized into five switch areas. The focus of this study is limited to technologies of smart grids that are used to improve the reliability of electrical power delivered to individual consumers in the power distribution system (SRIKANTHA; KUNDUR, 2019).

In discussing the reliability of production, transmission and distribution systems, each of these systems is studied in several subsystems. Production system includes production unit and production post, transmission system including transmission lines, switching stations, transmission substations, and sub-transmission system, as well as distribution system including substations, distribution feeder circuits, switches, protective equipment, primary circuits, distribution transformers, and services. The last step in supplying electricity is the delivery of power from the feeders to individual consumers, which is the main purpose of the distribution system. The reliability of the service delivered to individual consumers can be changed by faults inside and outside the operating area of the power distribution system. These faults are called internal and external faults. Irrespective of the location of the fault, the effects that occur for individual consumers due to voltage changes are blackouts, voltage drops and minor changes in the supply voltage. The effects of external faults are more pronounced in the form of voltage drops, and this is the main reason for the network formation of the transmission and sub-transmission system, which can be supplied electrically to the distribution system. As a result, the power disorders experienced by individual consumers and caused by external factors are less than the interruptions affected by internal factors. In contrast, internal faults lead to voltage interruptions and voltage losses. Therefore, the share of internal faults in the total interruptions and voltage losses is greater than external faults (PEYGHAMI et al., 2020).

The configuration and operation modes of area-focused protection systems are markedly different from a traditional protection system. Therefore, to evaluate the reliability of intelligent distribution networks, the method of assessing the reliability of area-focused protection systems is proposed as a basic idea. Traditional protection systems such as fuses, old electromechanical reclosers and electromechanical relays cannot fully protect the network because they do not have directional features in critical situations. All traditional protective devices cannot be replaced by directional protective devices because the reconstruction of all traditional protective devices is expensive for a company (NDAHEPELE; CHOWDHURY, 2020).

In order for a distribution network to perform a secure protection operation, the protection system must be able to perform the following factors (NDAHEPELE; CHOWDHURY, 2020):

- If the operation of distribution network and power source (such as DG) is a failure in parallel mode, the protection system must be able to operate.
- All power sources (such as DGs) connected to the grid must be protected against problems experienced due to grid disturbances such as automatic

reclosing. The greater the disruption in the network, the more damage the network will endure.

- Protection system should be designed taking into account the short-circuit current level and the additional current level.

Therefore, in this study, we seek to use the optimal approach in the placement and size of distributed generation resources in distribution network, which has the ability to reconfigure properly. In other words, in this study, an attempt is made to reduce the power losses of the distribution network as much as possible through the reconfiguration of the distribution network and the optimal allocation and size of the distributed energy resources, and subsequently, the voltage profile is improved.

1.2 LITERATURE REVIEW

Nick et al. (2017) provide a method for optimal planning, location and optimal size of energy storage systems (ESSs) that are directly controlled by active distribution network operators. The main purpose of the proposed planning is to reconfigure the network. For this purpose, the exact conditional convex optimal flow (OPF) has been used as the core of the optimization model, which includes both technical and economic goals. Sub-objectives of this research include minimizing voltage deviations, congestion of feeders / lines, load supply costs and ESS-related investment costs. In this model, the randomness of loads and renewable products are also considered. The results show the effectiveness of the proposed method.

Chabanloo et al. (2018) examined the comprehensive coordination of radial distribution network protection in the presence of distributed generation sources while using the fault current limiter. In this paper, a reconfiguration algorithm to modify the time multiplier settings (TMS) and regulate the current of protective devices, such as overcurrent relays, reclosers and fuses, to overcome common synchronous machine-based distributed generations (SMDGs) installation problems, such as interrupts and fuse burns, it has been suggested. The proposed algorithm uses the fault current limiter (FCL) as well as the resynchronization algorithm to restore the coordination of protection systems in high-penetration radial distribution networks of SMDGs. For this purpose, a multi-objective optimization algorithm is used to determine the minimum FCL size and optimal adjustment of the protection system. This algorithm is formulated based on the combined genetic algorithm (GA) and linear programming method (LP) to reduce the computation time. The results show that the proposed method provides more practical and effective solutions for optimal coordination reconstruction and minimizes FCL size.

Hariri et al. (2020) presented an analytical method for assessing the reliability of smart grids, including distributed renewable and non-renewable generations and plug-in hybrid electric vehicles. The main contribution of this paper is to propose a new state-matrix method (S-matrix) including a new model for examining intelligent network reconfiguration performance modes using the concepts of segmentation and graph theory. The proposed method is applied to the standard 33-bus network. Comparison of test results and methods based on smart micro-grids as well as other existing analytical methods shows the accuracy of the proposed method. The results of sensitivity analysis show that the proposed method does not have a negative effect due to changes in various parameters.

Alam et al. (2020) presented a protection plan in adjustable radial distribution networks in the presence of distributed generation sources. In this paper, a new scheme of fuse and recloser coordination for adjustable radial distribution networks (RDN) with distributed generation sources (DG) is introduced. In addition, a new graph theory-based approach is proposed to achieve all possible topologies in radial distribution networks. Also, a new constraint reduction strategy is proposed in order to remove a large number of constraints in the formulation due to different topologies. An internal point analysis method has been adopted to solve the fuse-collector coordination problem, and to determine the best fuse. The developed strategy has been used to obtain the most optimal settings in IEEE standard 33 and 69 bus radial networks with the ability to reset in the presence of DGs. The obtained settings are compared with the usual settings and as a result, the effectiveness of the proposed design is proven.

Sampaio et al. (2020) investigated a multi-factor integrated self-healing system (SHS) and adaptive protection system (APS) for power distribution systems with distributed generation sources. The proposed method in this paper is to minimize the adverse effects of network reconstruction on distribution network protection systems that include distributed generation (DG) sources. SHS uses communication between agents to maximize the number of recovered loads, while APS agents recover protection settings after changes in network topology and DG status. APS is able to change the current configuration group and, if necessary, calculate new settings that can be sent to the relays to ensure the exact coordination of the protection systems. Proposed designs are evaluated using commercial digital relays in a variety of scenarios, including DG intrusion levels and network topology changes. The results clearly show that this strategy is quite fast and reliable when strengthening and providing strength through self-healing method.

Shi et al. (2021) proposed a new scheme of network reconfiguration and distributed energy resource scheduling for improved distribution system resilience. In this paper, an outage management strategy is proposed to enhance distribution system resilience through network reconfiguration and distributed energy resources (DERs) scheduling. After a line fault, the proposed algorithm can identify radial network topology based on the rank of the incidence matrix. The reconfiguration is implemented by switching tie lines and sectionalizing lines. With the new network topology, an optimal DER scheduling problem is solved to minimize the accumulative cost for dispatchable DER operation and load reduction. Finally, the optimal topology that minimizes the accumulative cost is selected from all radial topologies. The computational workload is relatively low because only linear programming needs to be solved. Using the case studies of the IEEE 69-bus and IEEE 123-bus systems, we consider the worst-case scenarios in which faults occur in the upstream feeder. The simulation results demonstrate that the proposed strategy allows for a relatively high percentage of the load to remain in service after line faults. Furthermore, compared with microgrid-formation approaches, the proposed strategy has advantages when applied to the distribution systems with several normally-open tie lines and low DER penetration.

Shaheen, A. M. et al. (2021) used an improved equilibrium optimization (IEOA) algorithm to investigate network restructuring and locate DG resources in distribution networks. In this research, standard 33 and 69 bus networks have been used to investigate three different loading levels. These diuretic simulations ultimately show the increase in performance, quality and reliability of the distribution system by the proposed method. Also, a multi-objective function has been used considering the total active power and the total voltage increase in compliance with the system constraints. The proposed algorithm is compared with other algorithms such as harmonic search (HS), genetics algorithm (GA), fireworks and firefly optimization, which confirms the results, effectiveness and robustness of the proposed method compared to competing algorithms.

Sambaiah and Jayabarathi (2021) proposed a method for network reconfiguration and allocation of DG resources in electrical distribution networks in order to reduce power losses and voltage deviations using the Salp Swarm algorithm (SSA). To evaluate the performance of SSA, it uses five different scenarios such as only reconfiguration, only DG allocation, DG allocation after reconfiguration, reconfiguration after DG allocation and simultaneous reconfiguration and DG allocation. The proposed SSA algorithm has been tested on 33 and 69 distribution systems, and the simulation results show the performance of the proposed algorithm compared to other optimization algorithms.

In Wang et al. (2020), a reconfigurable approach of consecutive system based on state is developed through a Markov decision process (MDP) pattern, which aims to minimize renewable DG curtailment and load shedding under operating restrictions. Existing DG power outputs and the network configuration in each time of decision are shown as the states of Markov. Two systems are used to validate the proposed model. Real-time reconfiguration strategies based on the observed system states can be implemented.

This paper demonstrates a strategy that simultaneously emphasizes the optimum placement and size of capacitor banks, DGs, and reconfiguration of radial distribution system (RDS). The proposed algorithm is the maiden application of the proposed quasi-reflection-based slime mould algorithm (QRSMA), which is tested in three systems (BISWAL et al., 2021).

Barnwal et al. (2022) present a new strategy that enhances the stability of voltage, minimizes the power losses, and maintains the fine voltage profile of RDS using the optimal placement of DG, DNR, and PVQ bus voltage control considering the supply of variable reactive power at P bus. The purpose of this approach is to increase maximum network loading and minimize system loss. Thus, a multi-objective function is defined. The suggested algorithm is the grey wolf optimization (GWO) technique.

Tran et al. (2021) deal with simultaneous network reconfiguration and location of distributed generations (SNR-DG) of radial systems using a new quasi-oppositional chaotic neural network algorithm (QOCNNA) and aims to reduce active power losses and make voltage more stable in distribution systems such as 33-, 69- and 118-bus.

As a result, excellent SNR-DG solutions are found by QOCNNA, which converge quickly and have a slight criterion deviation.

Shaheen, Abdullah M. et al. (2021) develop an Enhanced Marine Predators Algorithm (EMPA) to simultaneously reconfigure the distribution network and distributed generators. A multi-objective pattern is managed by EMPA for the power loss reduction and the index enhancement of the voltage stability at the levels of various loading. The tests are conducted using three systems.

Rahim et al. (2019) propose a reconfigurable distribution system procedure combined with distributed generation, which includes protective devices. This study optimally reconfigures the network and calculates the size of DG to minimize power losses and guarantee proper operation of protection devices under conditions of normality and fault. Three systems such as IEEE 33-bus, 69-bus, and 118-bus are tested by the firefly algorithm (FA) and evolutionary programming (EP) algorithm. It can be concluded that FA is better than EP as an optimization tool to find the optimal result in this proposed method.

Ghasemi et al. (2021) propose a new approach to plan the flexible distribution network with line hardening and allocate distributed generation according to two-step random optimization to decrease the load shedding expenses against the disasters of the nature. The second step coordinates the resources located in each microgrid using the master-slave control strategy. The expenses of load shedding can be reduced by 63% in the course of strong storms by forming the microgrid and reconfiguring the system.

Moghaddam et al. (2020) proposed a new model for reconfiguration and distributed generation (DG) allocation in the distribution network by considering network loss reduction and power quality improvement by using the new antlion optimizer (ALO) algorithm. As a result, the suggested method decreases the amount of power quality indicators and the power losses in the studied systems.

Conventional volt-var control (VVC) instruments, a distribution network reconfiguration (DNR), and a photovoltaic smart inverter (PVSI) operate coordinately and effectively to save energy. The proposed algorithm is a modified binary gray wolf optimization (MBGWO) method implemented on the systems of balanced and unbalanced distribution (PAMSHETTI et al., 2020).

1.3 MOTIVATION

Modern and industrial civilization in recent years has done a lot of work in the field of energy extraction using fossil fuels. Energy production using fossil fuels has led to the production of greenhouse gases such as carbon dioxide, methane, etc., which will lead to climate change. Reducing the use of fossil fuels is essential to prevent irreparable damage from severe climate change. For this purpose, in the field of electricity generation, the fuel used as well as the production technology must undergo fundamental changes. The use of renewable energy as well as nuclear energy can effectively influence the methods of generating electricity. From the perspective of some energy experts, the use of renewable energy can save, reduce costs, and improve system performance and satisfaction.

The use of renewable energy and facing issues such as responding to demand poses major challenges to electricity supply networks. Conventional and traditional power supply networks are designed for situations where the amount of output power is under control and the demand is often one-way. In traditional networks, the uncertainty in production has been merely the exit of the generating units. Because demand is often indefinite, but it has statistically predictable behaviour. The existing network has not been built for renewable production and demand response and other uncertainties, including hybrid electric vehicles. As a result, a smart electricity distribution network is necessary to adapt to the proposed changes.

As mentioned, breakdowns and malfunctions of the distribution network that occur in blackouts are often caused by accidents and accidental factors. If these events occur as a result of deliberate and disruptive activities, actions are taken to increase the reliability of the distribution network. In other words, one of the most up-to-date issues in the electricity industry in electricity distribution networks is to have more reliability and reduce the rate of redistributed energy.

The configuration of a power distribution system is radial. However, as mentioned earlier, due to the numerous problems of the radial structure in the use of large distributed generation resources, it is necessary to upgrade the primary feeders. In the current distribution system, the primary feeders have switches that open normally. By closing the two-way switches, the radial distribution structure can be turned into a meshed structure without installing additional power lines. Therefore, investing to upgrade a radial to meshed network using a smart grid in distribution networks not only does not impose a cost on the distributors, but also reduces the cost of network losses, causing the return of this investment and the total cost. It will reduce and ultimately increase the profitability and revenue of power distribution companies.

Therefore, reconfiguration of the distribution network along with distributed generation (DG) sources can reduce power losses and increase network reliability and voltage profile. However, moving the distribution network towards intelligence (equipment and controls that are installed on the distribution network) can change the reconfiguration of the distribution network and the amount of losses caused by it. As a result, it is necessary to study the issue of rearrangement of the distribution network in the presence of intelligent equipment of this network.

1.4 PROBLEMS

Power losses is one of the basic problems of distribution systems, which causes the amount of electricity produced to not reach the consumer completely due to the loss of energy in transformers, measuring devices, connections, capacitor banks, voltage regulators, etc. As a result, in this research, we are trying to reduce power losses through the reconfiguration of the distribution network and the optimal allocation of distributed generation with the right capacity by the whale optimization algorithm (WOA).

1.5 INNOVATIONS

In this study the reconfiguration of distribution networks along with the optimal location and size of DGs will be described in order to reduce power losses and improve the voltage profile. Therefore, in this research, we will optimize the proposed model using the Whale Optimization Algorithm (WOA), which will show the innovation of this study compared to other methods shown in the chapter of the tests and results.

1.6 OBJECTIVES

1- The whale optimization algorithm (WOA) is implemented for the power losses reduction and the voltage profile improvement through the reconfiguration with the simultaneous allocation of distributed generations (DGs).

2- Tests have been conducted using the IEEE 33-bus, IEEE 69-bus, 136-bus, and 415-bus distribution networks in different cases using the WOA.
3- The obtained results are compared with the solutions provided by other techniques.

1.7 ASSUMPTION

1- Reconfiguration of the distribution network will significantly reduce the power losses and improve the voltage profile.
2- Optimal placement and size of DG units will minimize the power losses and enhance the voltage profile in the distribution network.
3- The WOA outperforms other methods such as the adaptive cuckoo search algorithm (ACSA) in Nguyen et al. (2016), uniform voltage distribution-based constructive reconfiguration algorithm (UVDA) in Bayat et al. (2016), modified plant growth simulation algorithm (MPGSA) in Rajaram et al. (2015), stochastic fractal search (SFS) algorithm in Tran et al. (2020), and adaptive ant colony optimization (AACO) in Swarnkar et al. (2011).

2 ELECTRICAL ENERGY DISTRIBUTION

Electrical energy consumption in 2022, according to data from the Statistical Yearbook of Electrical Energy, was 509 TWh (EPE., 2023). This level of energy demand requires that a complex and extensive infrastructure be kept in constant operation. To facilitate its operation and coordination, such an infrastructure is composed of smaller subsystems that perform specific functions. Such subsystems are classified into three types: generation; transmission; and distribution.

The energy generation subsystem supplies all energetic demand through the conversion of a primary energy source in electricity. The systems of the conventional generation and large-scale, normally, are formed by large plants of located generation in remote regions from the consumption centres. However, the concept of Distributed Generation presents changes in this scenario, to propose that small generation units are located near to the consumption centres (PEPERMANS et al., 2005).

Due to the long distances between the generation units and the consumption centres, there is the necessity of an infrastructure to transport, with efficient manner, the generated energy. This infrastructure consists of the energy transmission system, which is basically composed of transmission lines and substations. The generated energy is transported by the transmission lines, which operate with voltages above 230 kV. Voltage levels are high, thus it is possible to transport large amounts of energy in long distances of efficient manner (SCHERER; VASSELL, 1985). Thus, the substations are used to adapt the voltage levels for the transmission. Raising the voltage next to the generation units and lowering it, subsequently, for the sub-transmission.

Sub-transmission lines operate with inferior voltage levels than transmission lines. Normally, the operation voltage varies between 34.5 kV until 138 kV. Its function includes the transfer of energy from the step-down substations of the transmission to the distribution substations and large-scale consumers. Therefore, accomplishing the transition between the energy transmission and distribution systems.

The initiation of the energy distribution is characterized by located step-down substations near to the consumption centres and fed by the sub-transmission lines. At that point, a distribution circuit begins, whose range of energy supply is restricted to a geographical area that can correspond, for example, to a city or a set of neighbourhoods.

2.1 ELECTRICAL ENERGY DISTRIBUTION SYSTEM

In Brazil, the electrical energy consumers are classified into three types: the free consumer, that has a minimum demand of 3 MW at any voltage level, and therefore can negotiate directly in the free contracting environment; the special consumer, that has a minimum demand of 500 kW and can negotiate in the free market, since the acquired electrical energy is from incentive sources, such as wind and biomass; and the captive consumer (ABRADEE, 2013b). The captive consumers are restricted to an energy distribution concessionaire. This category includes the connected consumers to low voltage and a good part of the medium voltage consumers (ABRADEE, 2013b).

The concessionaires operate as mediators between the energy producers and the small and medium-scale consumers. Attending a delimited geographic region, called the concession area. According to the Brazilian Association of Electrical Energy Distributors (Associação Brasileira de Distribuidores de Energia Elétrica (ABRADEE)) there are 64 electrical energy distributors with capital that varies between private and public operating in Brazilian territory (ABRADEE, 2012).

The managed infrastructure by the energy concessionaires consists of an Electrical Energy Distribution System (EEDS). It is through the EEDS that the transmitted energy by the transmission system or produced in small generation systems is conditioned and delivered to captive consumers. The infrastructure of a distribution system is typically segmented into: distribution substation; primary network; distribution transformers; and secondary network. In Figure 2, the typical relation between the distribution segments and the installations of medium and low voltage consumers is illustrated by means of a simple EEDS.

Figure 2 – Diagram of a typical distribution system and the relations of its segments

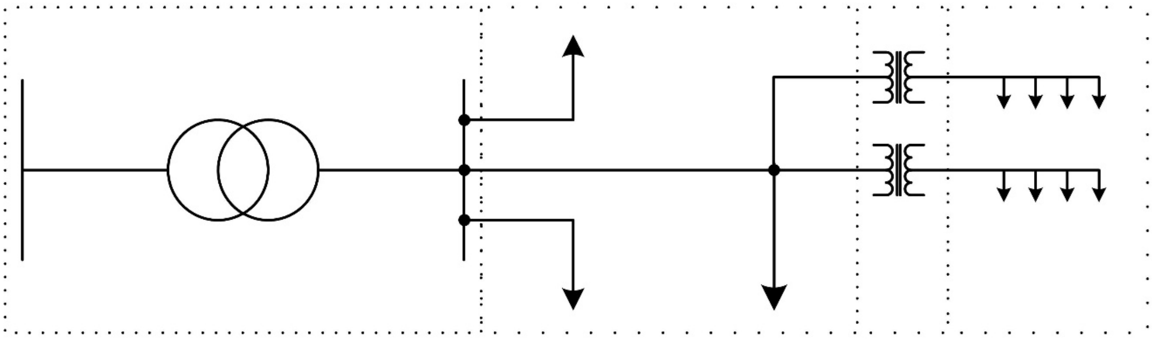

Source: Tavares (2018).

The distribution substations are usually connected to sub-transmission lines. Its characteristic function is to reduce the sub-transmission voltage to primary distribution levels, which can vary between 13.8 kV until 34.5 kV. For this, power transformers are used, which consist of the main equipment of the substation. As a crucial infrastructure in the operation of a distribution system, a substation has several measurement, control and protection equipment.

From the distribution substations are derived the primary distribution networks, which supply the medium voltage consumers and the distribution transformers. Throughout the primary network is possible to find equipment such as capacitor banks and voltage regulators, which are installed in order to correct anomalies in the distribution system (ABRADEE, 2013a).

The primary distribution networks can be aerial or underground, the aerial ones are the most used to present a lower relative cost (KAGAN et al., 2005). The aerial networks are normally operated with radial topology, that is, there is only one linking path any point of the primary network to the substation. This feature is due to the simplicity of the operation and the protection of the systems with this type of topology.

It is common the insertion of the disconnecting switches at the strategic points of the network. They are used to isolate load blocks to perform preventive and corrective maintenance in the distribution networks (KAGAN et al., 2005). Some disconnecting switches are installed by interconnecting different feeders and operate with a normally open state, are used to transfer load blocks between different circuits.

In Figure 3, the diagram of an operating network with a radial topology is illustrated, equipped with normally closed switches (NC) and normally open switches (NO), which enable the transfer and the isolation of the load blocks.

Figure 3 – Example of an equipped distribution system with disconnecting switches in NC and NO state

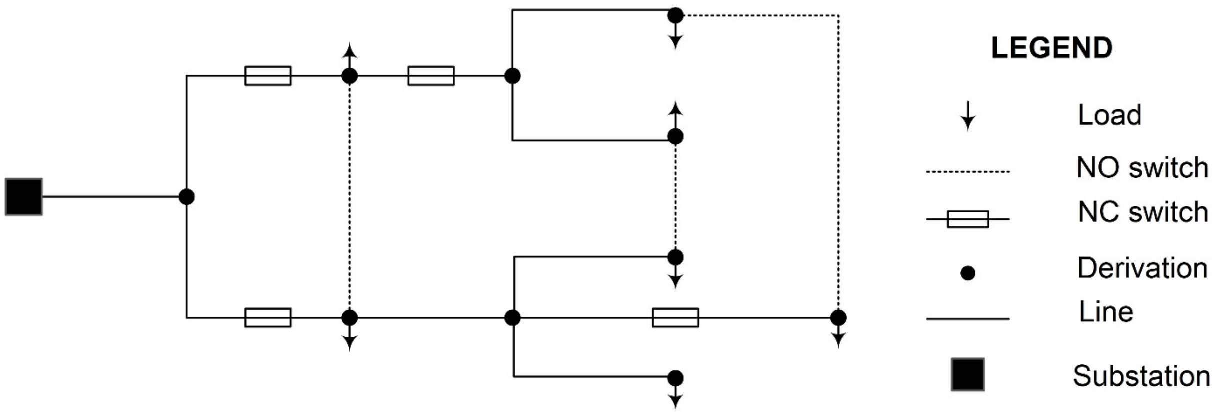

Source: Tavares (2018).

Connected to the primary distribution networks, the distribution transformers are responsible by the reduction of the primary voltage to secondary distribution voltage levels, which can vary according to the concession area between 127V / 220V and 220V / 380V. Usually, three-phase transformers are used utilizing the grounded delta-star connection scheme. Normally, a surge arrestor is installed next to this equipment for protection of overvoltages and a fuse link for protection of overcurrents (KAGAN et al., 2005). In aerial networks, the transformers are installed on distribution poles. In regions where the distribution network is underground, these devices can be installed in underground cabins or at ground level.

The secondary networks, that have origin of the distribution transformers, are responsible for electrical energy distribution to the low voltage consumers. This distribution segment is characterized by the number and diversity of connections, which single-phase, two-phase and three-phase branches can be derived. Attending the residences and small commerce and industries. Its operation topology can vary between radial or mesh.

2.2 ELECTRICAL LOSSES IN THE ELECTRICAL ENERGY DISTRIBUTION

To assess the amount of delivered electrical energy to the final consumers, is usually found that it is less than the amount of acquired energy by the concessionaire. Similar something would occur to compare the injected instantaneous power at the beginning of the distribution system with the summation of the demanded powers for each consumer. Such difference consists of the global losses of the distribution.

The global losses are composed of two types of losses, which are classified, according to their origin, into: non-technical or commercial losses; and technical losses. According to data from ABRADEE in 2015, the percentage of global energy losses in 63 Brazilian distributors was 13.54%. From the presented data in Figure 4, it is concluded that the average percentage of global energy losses in the distribution between 2005 and 2015 was 13.91%.

The non-technical or commercial losses represent the portion of energy or demand that is not invoiced on account of frauds, administrative faults or technical faults. Thus, they are characterized as sources of commercial losses: the energy thefts, popularly known as "hotwire power supply"; perusal faults; unregistered connections in the billing system; and technical defects in the energy gauges, which are not provoked by the consumer (OLIVEIRA, 2009).

Figure 4 – Percentage of energy commercial and technical losses in 63 Brazilian distributors between the 2005 and 2015 years

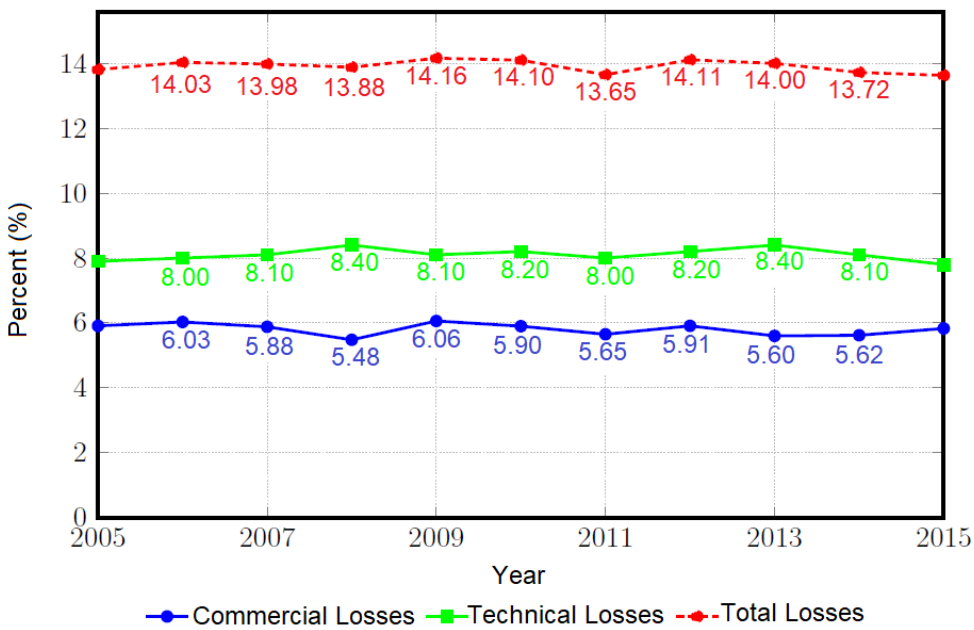

Source: Abradee (2015).

The technical losses are equivalent to the amount of energy or lost demand naturally due to the distribution process for the final consumers. The presented data in Figure 4 indicate that between 2005 and 2015, the percentage of technical losses, considering the global system of 63 Brazilian distributors, was higher than the index of commercial losses. However, depending on the concession area, the percentage of commercial losses can considerably overcome the index of technical losses due to the large number of frauds.

Technical losses occur in all segments of the electrical energy distribution. In the transformers, for example, there are the losses in the winding, provoked by the Joule effect, and in the nucleus, occasioned by eddy currents and by hysteresis. On the other hand, in the distribution lines, technical losses are occasioned principally by the Joule effect.

In Méffe (2001), an estimate is presented that indicates the expected percentage range of technical losses per segment, as is presented in Table 1. The expected percentage ranges of technical losses are indicated per segment in relation to the total of dissipated energy naturally (technical losses) and in percentage of the total of required energy by the system.

It is worth noting that the described segment as Others in Table 1 refers to the occasioned losses per: connections; capacitors bank; voltage regulators; leakage currents in the insulators and lightning arresters; and corona effect (MÉFFE, 2001).

Table 1 – Expected technical losses per segment

Segment	Expected Range (%)	
	The total of technical losses	The total of energy
Distribution Substation	9.00 – 17.00	0.50 – 1.00
Primary Network	15.00 – 30.00	0.50 – 2.50
Distribution Transformer	15.00 – 55.00	1.00 – 2.00
Secondary Network	3.00 – 30.00	0.10 – 2.00
Branch of Link	0.50 – 6.00	0.05 – 0.20
Energy Meter	3.00 – 7.00	0.20 – 0.40
Others	5.00 – 11.00	0.20 – 0.80

Source: Méffe (2001).

2.2.1 Reduction methods of the technical losses

From the presented values in Table 1, the segments with the greatest emphasis on the contribution for the increase of the technical losses are the primary and secondary networks and the distribution transformers. Thus, it is possible to substantially reduce the indexes of the technical losses of a distribution system, simply concentrating on these three segments.

2.2.1.1 Transformers

The technical losses in the transformers are composed of iron losses and in the windings, or copper. The iron losses are electromagnetic origin and are occasioned, basically, by hysteresis and eddy currents, or Foucault's currents. On the other hand, the copper losses occur due to the Joule effect.

In the iron losses, the dissipated power is proportional to the square of the density of flow or voltage (KOSOW, 1982). The proportionality constant depends on constructive aspects and the electrical operating frequency. In the distribution system, supposing that there are not significant variations in the frequency of the system and in the supply voltage of the transformer is considered, therefore, that the iron losses are fixed.

In the copper, the losses are proportional to the square of the load current. Thus, they are considered variables, for being dependents of the loading of the transformer. In Figure 5, the yield of a transformer is illustrated a set of presenting curves in the percentage function of the supply load in relation to the nominal power of the equipment. It is noted that the load power and its power factor significantly influence on the efficiency of a transformer. A transformer operates with maximum yield when the copper losses are equal to the iron losses, which is equivalent the operation with load, approximately, 50% of the nominal power (KOSOW, 1982). However, according to the curves in Figure 5, the equipment has an acceptable yield up to the nominal load.

Figure 5 – Yield curves of a transformer in the loading function

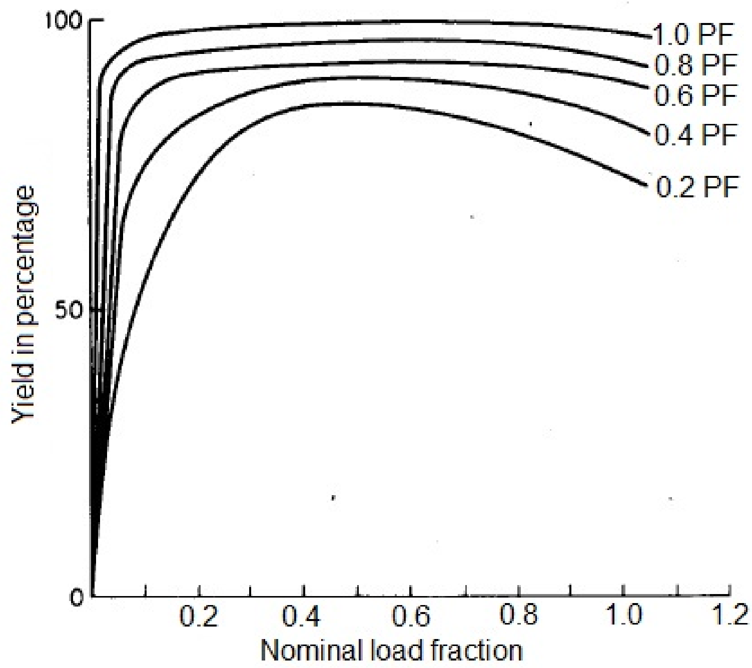

Source: Kosow (1982).

In view of the nature of the technical losses of the transformers and their operation conditions in the distribution, it appears, therefore, that the constructive characteristics of the equipment and its loading are preponderant aspects in the definition of strategies of technical losses reduction. Among the methods commonly cited in the literature to reduce the provoked technical losses by transformers in the distribution of energy, the replacement of the equipment stands out (AGUERO, 2012; OLIVEIRA, 2009) and the management of the loading (AGUERO, 2012; QUEIROZ, 2010; SARFI et al., 1995).

The replacement of the aimed transformers returns in the short-term, in some cases, may not be interesting. What is evidenced in a realized numerical study in Oliveira (2009), which it concluded not to be financially viable, considering a period of one year, to apply the replacement of the transformers in the evaluated scenario. However, they are equipment with a long life cycle, of approximately 20 years, the analysis of the financial return considering longer terms may indicate gains (AGUERO, 2012). Thus, it becomes interesting, when opting for the replacement of transformers, to realize a technical-financial study establishing returns in the long-term.

As previously mentioned, the loading so that a transformer has an acceptable yield varies between 50% to 100% of its nominal power. In operation conditions out of that range, the equipment's yield tends to fall. In view of this characteristic, the management of the loading consists of the task to periodically evaluate the loading of the transformer in order to maintain the operating equipment with an acceptable yield. In large-scale systems without communication infrastructure, the realization of this management is a defiant task, since it becomes necessary to realize measurements to know the loading of a transformer. In this case, it arises as an alternative the utilization of Transformer Load Management Systems (TLMS) that perform loading estimates, as presented in Leal et al. (2002).

2.2.1.2 Primary and secondary network

In the energy distribution networks, the Joule effect is the main agent that causes technical losses. This phenomenon occurs when there is a flow of electrons passing through an electrical conductor that offers resistance to the passage of electric current, resulting in heat production. Thus, the part of the electrical energy that would produce effective work is dissipated in the form of the heat.

The dissipated power due to the Joule effect is proportional to the product of the electrical resistance of the conductor with the square of the intensity of the electrical current. Thus, the dissipated power due to the Joule effect on a conductor can be expressed by the following equation:

$$P_{\mathrm{losses}} = R \, . I^2 \tag{1}$$

Where P_{losses} is the dissipated power due to the Joule effect; R is the electrical resistance of the conductor; and I is the current intensity that travels through the conductor.

From Equation (1), which mathematically expresses the physical concept of the occasioned technical losses by the Joule effect, it appears that it is possible to reduce the dissipated power by changing two parameters of an electrical circuit: the electrical resistances; or the currents. Even in complex circuits such as the energy distribution networks, the utilized methods to reduce the technical losses have as the direct or indirect alteration principle at least one of the two previously cited parameters.

Among the proposed methods in the literature to reduce the technical losses in the distribution networks, can stand out:

Load Balancing – In Ochoa (2003), a study is presented, which showed by means of computational simulations, the ability of the load imbalance to increase the percentage of technical losses. This occurs mainly due to the increase of the current in the neutral conductor (AGUERO, 2012). A viable solution for cases where the load imbalance is found in the distribution of the loads between the phases, either manual or automatic mode.

Reactive Compensation – The reduction of the currents in the distribution lines implies the reduction of the technical losses. One manner to reduce the current magnitude is to insert equipment to compensate for the reactive power of the inserted loads in the system. In the distribution, there is usually a demand of reactive power due to the inductive reactance of the lines and the characteristic of the loads. Thus, banks of fixed or switched capacitors are commonly used in the reactive compensation. However, with advances in power electronics and management and the control of the energy distribution, the Flexible Alternating Current Transmission Systems (FACTS) are used in the distribution systems. Among the benefits of application of the FACTS in distribution, the versatility of the equipment in the control of reactive power stands out (YU, 2014).

Distributed Generation (DG) – The insertion of small generation units in the distribution system presents benefits and challenges to be overcome (PEPERMANS et al., 2005). One of these benefits is its ability, under determined conditions, to considerably reduce the indexes of technical losses. Among the parameters that affect this ability of technical losses reduction, can stand out: the ratio between the amount of injected generated energy into the network by means of the ability of the lines conduction, a parameter known as the DG penetration index; the type of used technology for the generation; the location of the generators and how they are dispersed in the network; and the control of the reactive power (QUEZADA et al., 2006). In Chiradeja and Ramakumar (2004), the performed studies led to the conclusion that increase the DG penetration index in the distribution system is not a guarantee of technical losses reduction.

What is evidenced in Quezada et al. (2006), which showed by means of simulations that the percentage of technical losses tends to reduce with low penetration indexes until reaching an optimum point. To increase the DG penetration index beyond this optimum point, the losses index tends to grow considerably. Acting as a reactive power controller, the distributed generators proved to be effective in the reduction of the technical losses (CHIRADEJA; RAMAKUMAR, 2004; QUEZADA et al., 2006).

Reconditioning of lines – The reconditioning of the lines consists of the replacement of the used cables by conductors of bigger cross section. Thus, the resistance of the distribution line will be smaller, resulting in the reduction of the line technical losses. Under financial aspect, this method can present prohibitive values and it normally is recommended for old networks that operate near to the maximum loading (SARFI et al., 1995).

Network reconfiguration – The network reconfiguration consists of the modification of the system topology by alternating the state of the located section elements in the primary network. In the distribution, this action can be applied in order to, for example, restore a distribution network after the occurrence of faults (PERALTA, 2015; SANCHES, 2013). Its application in the reduction of the technical losses is viable due to the possibility to have a capable topology to attend the inserted loads in the system by paths whose losses index will be reduced. Thus, the reconfiguration would be equivalent to redistribute the loads between primary feeders, avoiding overload conditions.

2.3 VOLTAGE LEVELS IN STEADY STATE

In Brazil, standardized voltages in the primary networks can vary between 13.8 kV to 34.5 kV and in the secondary networks between 127V / 220V and 220V / 380V (KAGAN et al., 2005). However, depending on the operation conditions and characteristics of the EEDS, the medium and low voltage consumers receive at the entrance branches of its installation voltage levels lower than the established nominal values for the network. This type of variation in the nominal voltage of the system is called a voltage drop.

The voltage drops are classified according to time duration, in: short duration; and long duration. The short duration voltage drops are also known as *sags*, are usually related with the actuation of large loads with high departure currents or yet with short circuits at some point of the system (DUGAN et al., 2003). On the other hand, the long duration falls are caused by overloads in the network.

The voltage drops occur due to the resistance to the passage of caused alternating electrical current by the impedance of the conductors. By Ohm's law, the intensity of the voltage drop in a conductor can be determined by means of the equation:

$$V_q = Z \,.\, I \qquad (2)$$

Where V_q is the module of the voltage drop; I is the intensity of the alternating current; and Z is the conductor impedance module. By means of Equation (2), it is noted that keeping the constant resistance and increasing the current, the voltage drop grows from proportional mode.

Per they have originated in phenomena that depend on the characteristics of the electrical conductors and the intensity of the current, there is an elevated degree of correlation between the indexes of the technical losses of a distribution system and the voltage levels at the terminals of the loads. Thus, the used methods to reduce technical losses are effective and usually recommended to attenuate long duration voltage drops.

3 NETWORK RECONFIGURATION

The network reconfiguration is the modification of the topology of the primary distribution network by means of the alteration of the state of the located section switches along the network. According to Ferdavani et al. (2011) is a method that can be applied in the distribution system to: increase the reliability (BROWN, 2001); restore after the occurrence of faults (PERALTA, 2015); balance the load imbalance (BARAN; WU, 1989b); improve the voltage stability (ARUN; ARAVINDHABABU, 2009); and reduce the technical losses (MERLIN; BACK, 1975).

The search for the capable operation topology to optimize pre-selected parameters is called the Distribution Network Reconfiguration Problem (DNRP). The applied DNRP solution to reduce the technical losses was initially presented in Merlin and Back (1975), who presented two approaches to solve the problem: an exact one validates for small-scale networks and a heuristic one which begins with a topology in mesh and based on the power flow of the branches opens sequentially the cycles until a radial topology is achieved. The publication of Merlin and Back (1975) was followed by diverse works that contributed to the evolution of the DNRP solution methods, among which can stand out Civanlar et al. (1988), Baran and Wu (1989a) and Nara et al. (1992).

Lee and Brooks (1988) were the pioneers to consider the variation of the demand in the DNRP, proposing a dynamic reconfiguration, this is, the alteration of the network topology for each considerable variation of the loads. In Chen and Cho (1993) was developed an approach for the execution of the reconfiguration each season of the year, which resulted in a reduction of the switching number and, consequently, in financial gains. Bueno (2005) developed a capable methodology to determine a fixed optimization topology considering the variation of loads for a planning period. Queiroz and Lyra (2009) developed a hybrid evolutionary algorithm to solve the DNRP, keeping the fixed optimization topology along a planning period.

In the bibliographic research, it was observed that there is a small number of works that apply the network reconfiguration, specifically, for the optimization of the network voltages. The explanation may be related to the fact that the applied reconfiguration to optimize the losses naturally improves the voltage levels and usually not only the optimization of the voltage profiles. In addition, many works impose restrictions on the voltage levels in the formulation of the applied reconfiguration problem to losses, which provides satisfactory results for voltages in the buses.

The found works in the literature that use the applied reconfiguration in the voltage optimization, employ two types of evaluation parameters: voltage stability indexes; and the maximum found voltage deviation. The approaches based on stability indexes provide solutions whose voltage levels are more robust to load variations. On the other hand, the formulations based on the maximum voltage deviation have a relatively simple mathematical formulation. Among the works that use stability indexes stands out Kashem et al. (2000), Sahoo and Prasad (2006) and Arun and Aravindhababu (2009). Among those ones that are based on the maximum voltage deviation can stand out Nguyen and Truong (2015) and Imran and Kowsalya (2014).

The motivation to investigate approaches to solve the applied DNRP in the reduction of the technical losses is related to the good benefit cost of the reconfiguration when compared with other methods, for example, allocation of capacitor banks and reconditioning (SARFI et al., 1995), in addition to be an effective method in improvement of the voltage levels. In automated systems, its execution is a quick task and presents a low operational cost. On the other hand, in cases whose execution is manual, the critical switches can be prioritized, partially executing until achieve the optimal operation topology (BUENO, 2005).

3.1 MODELLING OF THE RECONFIGURATION PROBLEM

3.1.1 Equation simplifications

The modelling of the reconfiguration problem was developed in view of some considerations about the distribution network model, which simplified in the equation of the problem. As a consequence, the estimate of the technical losses index became less accurate. Among the performed considerations stand out:

Primary Distribution Network – Only the portion of dissipated energy in the lines of the primary distribution network was considered. Disregarding, therefore, other important segments, such as the secondary network and the distribution transformers. In the realized estimate by Méffe (2001), the dissipated energy in the medium voltage segment is equivalent between 15% to 30% of the total technical losses.

Balanced System – This simplification ignores the load imbalance, common in distribution. However, the distribution network can be represented as a single-phase system, therefore simplifying the calculation of the power flow. However, the occasioned technical losses by the imbalance between the phases are disregarded.

Radial Network – The consideration of the networks with radial topology does not affect the accuracy which the technical losses index is estimated. However, the study only restricts to radial networks.

Loads of Constant Power Type – There are four types of mathematical models that are commonly employed to represent the present loads in the distribution: Constant Power (P); Constant Current (I); Constant Impedance (Z); and a combination of the three mentioned models, denominated ZIP. The dynamics of the power demand of the electrical equipment that compose a load is the main criterion in the model attribution. What can affect the estimation of the technical losses, as is shown in Rossoni et al. (2013). However, in this work, all loads were modelled as constant power, since the data of the studied test systems do not present information about the characteristics of the loads.

3.1.2 Evaluation parameter of the technical losses

A primary distribution line can be represented, generically, by a series impedance and by *shunt* admittances, as illustrated in Figure 6. For being short distance lines, it is common to disregard the *shunt* impedance in aerial lines (KERSTING, 2001). Thus, the dissipated active power in the line is considered due to series impedance and is expressed mathematically by the following equation:

$$P_m = \mathrm{Re}\left\{(R_m + jX_m)\,.\,\dot{I}_m\,.\,\dot{I}_m^*\right\} = R_m\,.\,I_m^2 \tag{3}$$

Where P_m is dissipated active power in the line m; R_m is resistance of the line m; and I_m is the current module in the line m.

Figure 6 – Generic model of a primary distribution line

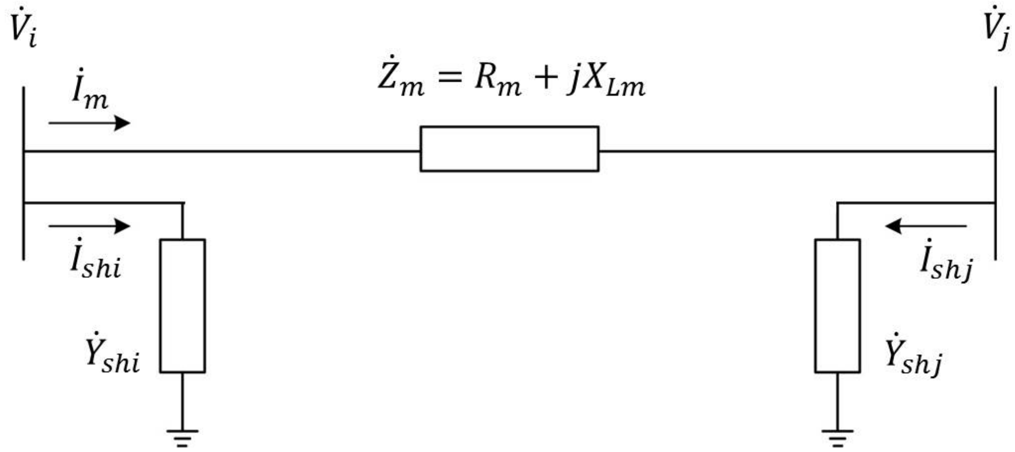

Source: Tavares (2018).

The discrete variation of the loads over time implies the alteration of the steady state currents in time. Consequently, the dissipated active power becomes a discrete time-dependent variable, represented by the following expression:

$$P_m[n] = R_m \,.\, I_m^2[n] \tag{4}$$

Where $P_m[n]$ is dissipated active power in the line m in the interval n; and $I_m[n]$ is the module of the current in the line m in time interval n. Knowing that a planning period is discretized in N time intervals with sampling period T, then the dissipated active energy in this time space is determined by:

$$E_m = \sum_{n=0}^{N-1} R_m \,.\, I_m^2[n] \,.\, T \tag{5}$$

Where E_m is the dissipated active energy in the line m in a planning period; and T is time sampling period. Thus, the total dissipated energy in the primary network in a given planning period is defined by the equation:

$$E_{total} = \sum_{m \in \phi} \sum_{n=0}^{N-1} R_m \, . \, I_m^2[n] \, . \, T \tag{6}$$

Where E_{total} is the dissipated active energy in the primary distribution network; and ϕ is the set of primary lines that compose the network.

3.1.3 Voltage levels evaluation parameter

Voltage levels were evaluated by means of a Gaussian function of two independent variables. These variables are the minimum and maximum observed voltages in the distribution network over the considered study period, expressed by (TAVARES, 2018):

$$\begin{cases} v_{\min} = \min\left(\dfrac{V_i[n]}{V_{ref}}\right) \\ v_{\max} = \max\left(\dfrac{V_j[n]}{V_{ref}}\right) \end{cases}, \quad n = 0, T, \ldots, (N-1) \, . \, T \, ; \quad i, j \in \Omega_b \tag{7}$$

Where $V_i[n]$ and $V_j[n]$ are the nodal voltages at buses i and j in the instant n; V_{ref} is network nominal voltage; and Ω_b is the set of all buses of the system. Thus, the used function equation (or aggregation function) in the evaluation of the voltage levels is given by (TAVARES, 2018):

$$A_v = 100 \, . \, \exp\left[-\frac{(v_{\min} - 1)^2 + (v_{\max} - 1)^2}{0.005} \right] \tag{8}$$

3.1.4 Network reconfiguration problem equation

To minimize the Equation (6) results in the reduction of the technical losses of the primary distribution network. On the other hand, the maximization of Equation (8) produces an improvement in the voltage levels. Thus, the implemented formulation for the reconfiguration problem aims to minimize Equation (6) and maximize the Equation (8).

The formulation must consider the variation of the demands over time, restricting itself to a planning period. Only the radial solutions will be evaluated, which consists of a restriction on the operation topology. Thus, the problem of applied network reconfiguration in the reduction of the technical losses and in the improvement of the voltage levels is expressed by:

$$\left.\begin{array}{l} Min.: E_{total}(X) \\ Max.: A_v(X) \\ \quad s.t.: \text{Load flow restrictions for each interval n} \in \text{P} \\ \qquad X \text{ of such a mode that the network is radial} \end{array}\right\} \text{over the period P} \qquad (9)$$

Where X is a vector of states of the primary network section switches; P is the considered planning period; $E_{total}(X)$ is the dissipated energy by the primary distribution network for the state X, determined by Equation (6); $A_v(X)$ is the result of the aggregation function for the maximum and minimum voltages of the state X, determined by Equation (8).

4 POWER FLOW

The calculation of the power flow involves the study of determining the state of an electrical power system in steady state from a set of known variables. This type of study is usually performed by means of algorithms that are based on numerical methods. Power flow calculation is an essential numerical (often nonlinear) analysis needed when making power systems studies (KERSTING, 2012). The practical application of proposed methods on the improvement of the power distribution network (e.g., power loss reduction, increase in reliability levels, voltage profile improvement) (BALAMURUGAN; SRINIVASAN, 2011; REMOLINO; PAREDES, 2016) typically require many power flows analysis algorithm runs. In areas like distribution management systems (DMS), a tool for the management of the Smart Grid, distribution power flow analysis will be implemented on more frequent basis, thereupon, power flow methods must be as efficient as possible. The power flow methodologies applied to distribution systems will have to adapt to the nature of the distribution network, in strict terms, they will be demanded to include single phase and three phase unbalanced system analysis, as well as the influence of distributed generation interconnection. In Fan and Borlase (2009), two industry experts report a comprehensive review on the evolution of the distribution system, the importance of DMS and the core importance of robust power flow analysis tools. In Distribution system reconfiguration, some of the objectives are to minimize power losses and enhance voltage profile, consequently, power flow analysis becomes an essential procedure to be performed in order to obtain steady state electrical characteristics of the distribution system as consequence of reconfiguration. Among the classic algorithms for calculation of the power flow methodology applied to transmission systems is mainly comprised by the Gauss Seidel using the admittance or impedance matrix, Newton Raphson (NR), Decoupled and Fast Decoupled (CHATTERJEE; MANDAL, 2017; STOTT, 1974). However, these algorithms are usually formulated considering inherent characteristics of the transmission and sub-transmission systems, such as: low imbalance; transpositions of the lines; high X / R ratio; and considerable values for the capacitive line susceptances (OCHOA, 2003). Due to these considerations in the formulation, the application of these algorithms in the study of distribution networks presents difficulties of convergence and bad results (OCHOA, 2003).

The radial topology of the distribution networks propitiated the development of branch-oriented power flow algorithms. In Ochoa (2003) these methods are classified into three types: Ladder or Staggered; Sum of the Currents; and Sum of the Powers. These power flow methods are typically used assuming a balanced system, consequently using a single-phase representation of a three-phase system. Due to the particular characteristics of distribution systems (i.e., unbalanced loads, radial topology, often untransposed lines, distributed generation) the assumptions made in the analysis of transmission systems fail to be extrapolated to the distribution system. Thereupon, a power flow method considering three phase unbalanced networks must be considered for its application in distribution systems. Reference Balamurugan and Srinivasan (2011) presents a comprehensive review and comparative analysis of power flow methods applied to the distribution system in phase frame and sequence frame references.

The branch-oriented algorithms are formed, basically, by two steps: an inverse or *backward sweep* and the direct or *forward sweep* (SRINIVAS, 2000). In the *backward sweep* stage, the current or power flow is summed, beginning by the final buses until the substation, having the possibility to update the voltages (SRINIVAS, 2000). In the *forward sweep* stage, the voltage drops are calculated, in the sense of the substation to the final buses, having the possibility to update the current or power flow (SRINIVAS, 2000). Algorithms for the power flow calculation in distribution systems that are based on this methodology are found, for example, in Shirmohammadi et al. (1988), Baran and Wu (1989b) and Kersting (2001). In the study, the forward/ backward methods (a popular power flow method applied to distribution systems) such as the ones presented in Chang et al. (2007); Das et al. (1995); Eminoglu and Hocaoglu (2005,2008); Ghosh and Das (1999); Kersting and Mendive (1976); Liu et al. (2002) are capable of performing power flow analysis assuming unbalanced phase systems, however, it is limited to radial networks. On the other hand, Newton based methods (GARCIA et al., 2000; NGUYEN, 1997; TENG; CHANG, 2002; ZHANG; CHENG, 1997) typically can deal with any topology type (i.e., radial, weakly meshed and meshed) and can consider the influence of distributed generation, in both, phase frame and sequence frame references. As expressed by Zhang and Cheng (1997), the main attribution to the success of the modified Newton method in distribution systems is the representation of the Jacobian matrix which is created based on the nature of the network topology.

4.1 BACKWARD-FORWARD SWEEP METHOD

The algorithm proposed by Shirmohammadi et al. (1988) is basically composed of six stages:

1. **Renumbering of the Branches** – This step is performed in order to define the sense of the power flow. In this way, it is possible to establish the order which the numerical calculations of the sweep steps will be executed.

2. **Attribution of the Initial Nodal Voltages** – As it is an iterative numerical method, it is necessary to estimate an initial solution for the unknown variables of the system, which this case consists of the module of the nodal voltages and their respective phase angles. Therefore, this stage of the algorithm is established a starting point for the iterative process attributing an initial nodal voltage. It is common to define the reference voltage of the network, which in p.u. is equal to $1\angle 0^{\circ}$.

3. **Calculation of the Nodal Currents** – At this point, the injected currents into all the buses are calculated. This step is essential for the execution of the inverse sweep, since the currents that circulate in the branches are the results of the sum of the nodal currents.

4. **Inverse Sweep (Backward sweep)** – In the inverse sweep, the currents in the network branches are calculated. The calculations are performed in the sense of the final buses until the substation.

5. **Direct Sweep (Forward sweep)** – The direct sweep is done in order to update the nodal voltages every iteration. Unlike the inverse sweep, the calculations of this phase are performed in the sense of the substation until the final buses.

6. **Convergence Test** – In the convergence test, the possibility to interrupt the iterative process of the algorithm is evaluated. Usually, the number of performed iterations and a convergence parameter are monitored. Among the used

convergence parameters stand out, for example, the nodal voltages or the fault between the specified injected power and the calculated power.

Figure 7 illustrates the relation between the six steps of the power flow algorithm by means of a simplified flowchart. The first two stages form the initial stage of the algorithm, while the last four stages constitute the iterative process, which is repeated until a stop condition is satisfied. In this work, the condition of satisfied stop is the maximum number of iterations.

Figure 7 – Simplified flowchart of the proposed Backward-Forward Sweep Algorithm

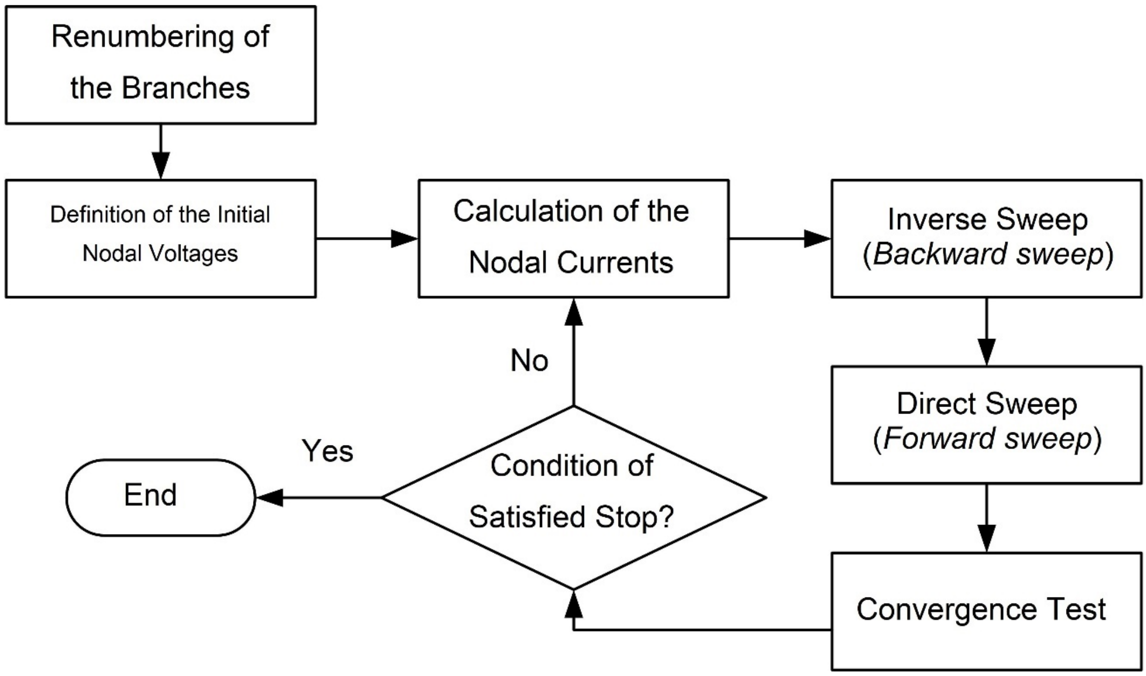

Source: Shirmohammadi et al. (1988).

5 METHODOLOGY

This work aims to minimize a distribution network's losses through the reconfiguration and allocation (locate and size) of DGs. The proposed approach to solve the problem is the WOA metaheuristic. In this context, it is not necessary to present the mathematical model of the problem. Instead, the metaheuristic generates a solution proposal, and the quality and feasibility of the proposal are verified by solving a power flow problem for radial systems. Figure 8 shows an illustrative radial distribution network (REDDY; REDDY, 2018).

Figure 8 – A sample 6-bus radial distribution system

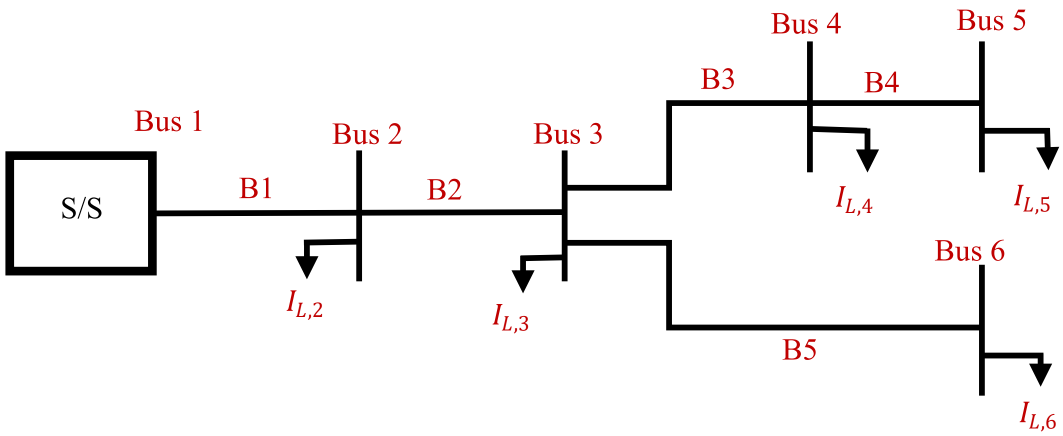

Source: Reddy and Reddy (2018).

5.1 OBJECTIVE FUNCTION

One of the main benefits of network reconfiguration with the simultaneous allocation of DGs is to minimize the power losses in the distribution network.

Equation (10) defines the total network power losses.

$$P_{loss} = P_G - P_D \tag{10}$$

Where P_{loss} is the total power losses of the network; P_G is the total active power injection at the substation and DGs; and P_D is the total active power load.

In addition, bus voltage and voltage stability are increased by installing DGs in the distribution network.

The objective function (F) of the problem is to minimize the active power losses, which is presented in (11).

$$minimize\ F = P_{loss} \tag{11}$$

5.2 CONSTRAINTS

The constraints of the problem are as follows:

1. The obtained voltage magnitudes must not exceed the permissible limits, as presented in (12).

$$V_{\min} \leq V_i \leq V_{\max}; \qquad i = 1, 2, ..., N_{bus} \tag{12}$$

Where V_i is the voltage magnitude at bus i; $V_{\min}$ is the minimum acceptable bus voltage magnitude; $V_{\max}$ is the maximum acceptable bus voltage magnitude; and N_{bus} is the total number of buses in the network.

2. The distribution network must maintain its radial topology and, after reconfiguration, must supply all loads.
3. The amount of power produced by DGs must be within the permissible limits, as shown in (13).

$$P_{DG\min,i} \leq P_{DG,i} \leq P_{DG\max,i}; \qquad i = 1, 2, ..., N_{DG} \tag{13}$$

Where $P_{DG,i}$ is the active power output of the DG unit at node i; $P_{DG\min,i}$ is the minimum size of the DG unit at node i; $P_{DG\max,i}$ is the maximum size of the DG unit at node i; and N_{DG} is the number of DG units that can be installed in the system.

4. The nonlinear equations that represent Kirchhoff's current and voltage laws, i.e., the equations of the power flow problem. The power flow analysis calculates the power losses for each topology with DGs.

5.3 DNR PROBLEM SOLVING METHOD

5.3.1 Fundamental loop

The proposal of fundamental loops (FLs) allows for building an array of matrix form, and the branches belonging to each fundamental loop appear in each row of the matrix. The number of rows of this matrix is equal to the number of fundamental loops, i.e., it is equal to the number of open branches to generate a radial topology (see illustrative examples presented in Table 2, Table 3, Table 4, and Table 5). This matrix allows the generation of radial topologies simply and efficiently.

Table 2 – Fundamental loops of the IEEE 33-bus network

FL	Switches	Length of the FL
1	2, 3, 4, 5, 6, 7, 18, 19, 20, 33	10
2	9, 10, 11, 12, 13, 14, 34	7
3	8, 9, 10, 11, 21, 33, 35	7
4	6, 7, 8, 9, 10, 11, 12, 13, 14, 15, 16, 17, 25, 26, 27, 28, 29, 30, 31, 32, 36	21
5	3, 4, 5, 22, 23, 24, 25, 26, 27, 28, 37	11

Source: Tran et al. (2020).

Table 3 – Fundamental loops of the IEEE 69-bus network

FL	Switches	Length of the FL
1	3, 4, 5, 6, 7, 8, 9, 10, 35, 36, 37, 38, 39, 40, 41, 42, 69	17
2	13, 14, 15, 16, 17, 18, 19, 20, 70	9
3	11, 12, 13, 14, 43, 44, 45, 69, 71	9
4	4, 5, 6, 7, 8, 46, 47, 48, 49, 52, 53, 54, 55, 56, 57, 58, 72	17
5	9, 10, 11, 12, 13, 14, 15, 16, 17, 18, 19, 20, 21, 22, 23, 24, 25, 26, 52, 53, 54, 55, 56, 57, 58, 59, 60, 61, 62, 63, 64, 73	32

Source: Tran et al. (2020).

Table 4 – Fundamental loops of the 136-bus network

FL	Switches	Length of the FL
1	1, 2, 3, 4, 5, 6, 7, 63, 64, 65, 66, 67, 68, 70, 73, 136	16
2	1, 2, 3, 4, 5, 6, 8, 9, 17, 18, 19, 20, 22, 24, 137	15

3	1, 2, 3, 4, 5, 6, 8, 10, 13, 15, 75, 76, 77, 78, 79, 80, 81, 83, 138	19
4	17, 18, 19, 20, 22, 24, 25, 26, 27, 28, 31, 35, 38, 121, 122, 123, 125, 127, 129, 130, 131, 132, 133, 134, 135, 139	26
5	17, 18, 19, 20, 22, 24, 25, 39, 40, 42, 43, 45, 46, 47, 48, 51, 140	17
6	39, 40, 42, 43, 45, 46, 47, 48, 49, 50, 85, 86, 88, 89, 90, 91, 92, 93, 94, 95, 96, 141	22
7	39, 40, 42, 43, 45, 46, 47, 48, 51, 52, 53, 54, 55, 85, 86, 88, 89, 90, 91, 92, 93, 97, 98, 142	24
8	39, 40, 42, 43, 45, 46, 47, 62, 99, 100, 101, 103, 104, 118, 119, 120, 143	17
9	63, 64, 65, 66, 75, 76, 77, 78, 79, 144	10
10	75, 76, 77, 78, 79, 121, 122, 123, 125, 127, 129, 130, 131, 145	14
11	75, 76, 77, 78, 79, 80, 81, 83, 84, 121, 122, 123, 125, 127, 129, 130, 131, 132, 133, 134, 135, 146	22
12	85, 86, 88, 89, 90, 91, 99, 100, 101, 103, 104, 147	12
13	85, 86, 88, 89, 90, 121, 122, 123, 125, 127, 129, 148	12
14	85, 86, 88, 89, 90, 99, 100, 101, 103, 149	10
15	85, 86, 88, 89, 90, 91, 92, 99, 100, 101, 103, 104, 150	13
16	85, 86, 88, 89, 90, 91, 92, 121, 122, 123, 125, 127, 129, 130, 131, 132, 151	17
17	85, 86, 88, 89, 90, 91, 92, 93, 94, 95, 96, 99, 100, 101, 103, 104, 118, 119, 120, 152	20
18	39, 40, 42, 43, 45, 46, 47, 99, 100, 101, 103, 104, 105, 106, 107, 110, 153	17
19	75, 76, 121, 122, 123, 125, 126, 154	8
20	75, 76, 77, 121, 122, 123, 125, 127, 128, 155	10
21	85, 86, 88, 89, 90, 91, 92, 93, 97, 98, 121, 122, 123, 125, 127, 129, 130, 131, 132, 133, 134, 135, 156	23

Source: Tran et al. (2020).

Table 5 – Fundamental loops of the 415-bus network

FL	Switches	Length of the FL
1	23, 27, 31, 244, 248	5

2	31, 35, 39, 43, 47, 51, 55, 59, 91, 99, 103, 107, 115, 236, 425, 429	16
3	91, 99, 103, 107, 111, 123, 127	7
4	111, 115, 119, 433	4
5	127, 131, 135, 151, 155, 200, 204, 220, 228, 236, 244, 248	12
6	119, 123, 147, 151, 155, 437, 441, 445, 471	9
7	131, 135, 139, 143, 147, 196, 200, 204, 208, 220, 224, 228, 445, 449	14
8	3, 7, 11, 15, 139, 143, 196, 208, 224, 280, 284, 292, 296, 300, 453, 457, 465, 469	18
9	3, 7, 11, 15, 63, 304, 308, 316, 324, 369, 373, 377, 385, 393, 397, 401, 417, 425, 429, 433, 437, 441, 449, 453, 457, 465, 469, 471	28
10	2, 21, 63, 65, 77, 81, 137, 141, 145, 149, 153, 165, 173, 177, 219, 280, 284, 292, 296, 300, 304, 308, 316, 324, 344, 348, 352	27
11	1, 21, 215, 219, 344, 348, 352	7
12	5, 211, 215, 369, 373, 377, 385, 389	8
13	13, 83, 207, 211, 389	5
14	9, 17, 40, 44, 52, 56, 60, 87, 203, 207	10
15	43, 47, 51, 55, 59, 67, 75, 83, 87, 259, 267, 393, 397, 401, 417, 447, 451, 455, 467	19
16	113, 117, 121, 125, 129, 133, 137, 141, 145, 149, 153, 165, 169	13
17	89, 93, 97, 101, 105, 109, 113, 117, 121, 125, 129, 133	12
18	2, 6, 57, 61, 69, 73, 169, 173, 177	9
19	1, 5, 9, 13, 17, 29, 33, 37, 41, 45, 49, 53, 57, 61, 65, 69	16
20	4, 10, 14, 18, 22, 26, 28, 29, 30, 33, 34, 36, 37, 41, 45, 49, 53, 58, 60, 73	20
21	14, 18, 22, 26, 30, 34, 38, 42, 46, 50, 54	11
22	10, 38, 42, 46, 50, 54, 58, 62, 66, 70, 74, 78, 82, 86, 90, 126	16
23	66, 70, 74, 78, 82, 86, 90, 130, 134, 138, 142, 146	12
24	62, 94, 126, 130, 134, 138, 142, 146, 150, 154, 158, 162, 166, 170, 174	15
25	102, 106, 110, 114, 118, 122, 154, 158, 162, 166, 170, 174	12
26	8, 12, 16, 20, 24	5

27	4, 28, 36, 40, 44, 52, 56, 75, 178, 199, 201, 203, 234, 238, 242, 246, 250, 254, 258, 263, 267	21
28	6, 64, 68, 72, 77, 81, 89, 93, 94, 97, 98, 101, 105, 109, 164, 168, 172, 176, 180, 181, 185, 189, 193, 197	24
29	112, 116, 120, 124, 164, 168, 172, 176, 180, 181, 185, 189, 193, 197	14
30	232, 252, 256	3
31	76, 80, 84, 88, 92, 96, 100, 104	8
32	128, 132, 136, 140, 144	5
33	148, 152, 156, 160	4
34	98, 102, 106, 110, 114, 116, 118, 120, 122, 124, 150, 178, 229, 233, 237, 241, 245, 253, 257	19
35	205, 209, 213, 217, 221, 238, 242, 246, 250, 254, 258	11
36	201, 205, 209, 213, 217, 221, 234, 262, 282, 286, 290, 294, 298, 302	14
37	266, 270, 274, 278, 282, 286, 290, 294, 298	9
38	225, 262, 266, 270, 274, 278, 302, 306, 310, 314, 318, 322, 330	13
39	188, 310, 314, 318, 322, 330, 354, 358	8
40	285, 289, 293, 297, 301, 305, 309, 313, 317, 321	10
41	182, 186, 190, 214, 281, 305, 309, 313, 317, 321, 325, 353, 357	13
42	182, 186, 190, 194, 214, 329, 333, 337, 341, 345, 349, 353, 357	13
43	64, 68, 72, 112, 188, 225, 229, 230, 233, 237, 241, 245, 253, 257, 277, 281, 305, 306, 309, 313, 317, 321, 325, 334, 354, 358	26
44	362, 424, 427, 431, 432, 435, 439, 443	8
45	366, 370, 408, 416, 424, 438, 442	7
46	408, 416, 432, 436, 440, 444, 448	7
47	438, 442, 446, 454, 458, 462	6
48	374, 378, 394, 402, 426	5
49	423, 427, 436, 452, 468, 472	6
50	182, 186, 190, 199, 214, 230, 259, 263, 277, 334, 353, 357, 359, 363, 367, 379, 414, 422, 427, 431, 435, 436, 439, 440, 443, 444, 446, 447, 448, 451, 454, 455, 458, 466, 467	35
51	359, 363, 367, 379, 398, 402, 410, 414, 422, 426, 462, 466	12

52	187, 383, 403, 407, 411, 415, 419	7
53	187, 387, 391, 395, 399	5
54	163, 195, 364, 399	4
55	163, 191, 364, 400, 404	5
56	175, 195, 372, 376, 403, 407, 411, 415	8
57	183, 191, 372, 396	4
58	179, 376, 380, 384	4
59	179, 183, 388, 392	4

Source: Author's elaboration.

5.3.2 Radiality constraint checking

The radial topology of the distribution network must be checked after determining the FLs. The radial structure of the network configuration is checked by the incidence matrix $\mathbb{A}$. First, the reference bus and the tie-switches, which in matrix $\mathbb{A}$ include the first column and rows related to those switches, respectively, are removed. The network configuration is a radial topology when the rest of the matrix $\mathbb{A}$ is square, and its determinant is 1 or –1 (TRAN et al., 2020).

5.4 WHALE OPTIMIZATION ALGORITHM (WOA)

5.4.1 Introduction

Population-based metaheuristic optimization algorithms share a common feature regardless of their nature. The search process is divided into two phases: exploration and exploitation. The optimizer must include operators to globally explore the search space. In this phase, movements should be randomized as largely as possible. The exploitation phase follows the exploration phase and can be defined as the process of looking over in every aspect the promising regions of the search space. Exploitation concerns to the local search capability in the promising regions of design space found in the exploration phase. Finding a good balance between exploration and exploitation is the most challenging task in the development of any metaheuristic algorithm due to the stochastic nature of the optimization process (MIRJALILI; LEWIS, 2016). Surprisingly, WOA comprises of two internal parameters to be tuned, i.e., A and C.

It is a new population dependent optimization algorithm. It has been popularized by Mirjalili and Lewis (2016). WOA mimic the unique foraging technique of humpback whales. Basically, the humpback whale used to prefer to search for small fishes in the sea. Their special hunting method makes them smarter. This foraging behaviour is known as a bubble-net hunting method. Here they whirl over to the prey and forma typical circular round shape.

The mechanism of WOA with mathematical formulation is as follows:

- Encircling the prey
- Bubble-net hunting strategy
- Search the prey

5.4.2 Encircling the prey

The area of the prey is recognized by the whale and finally encircles them. Initially, assume that the present best candidate response is the target location. Meanwhile, all other whales will readjust their spot towards the updated target area. Equations (14)–(17) represent this behaviour:

$$\vec{X}(t+1) = \vec{X}^*(t) - \vec{A} \cdot \vec{D} \tag{14}$$

$$\vec{D} = \left| \vec{C} \cdot \vec{X}^*(t) - \vec{X}(t) \right| \tag{15}$$

$$\vec{A} = 2 \cdot \vec{a} \cdot \vec{r} - \vec{a} \tag{16}$$

$$\vec{C} = 2 \cdot \vec{r} \tag{17}$$

Where $\vec{X}$ is the position vector, $\vec{X}^*$ is for best obtained position vector. 't' refers to the present iteration. $\vec{A}$ and $\vec{C}$ represent vector coefficients. In the course of iteration, $\vec{a}$ is linearly dropped from 2 to 0. The random vector $\vec{r}$ lies in [0, 1].

5.4.3 Bubble-net hunting strategy

The mathematical modelling of bubble-net behaviour is presented in the following.

5.4.3.1 Shrinking encircling mechanism

It is obtained by lessening the numerical value of $\vec{a}$ in the Equation (16). Here $\vec{A}$ refers to an arbitrary value in the range $[-a, a]$. The shifting of the spot from (X, Y) over (X^*, Y^*) can be obtained by $0 \le A \le 1$ in a search zone as shown in Figure 9.

Figure 9 – Shrinking encircling mechanism

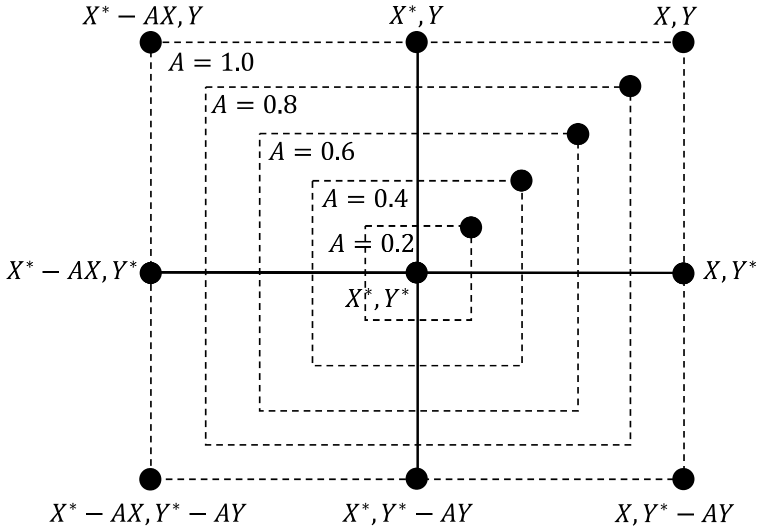

Source: Mirjalili and Lewis (2016).

5.4.3.2 Spiral updating

This procedure is based on the measured gap between the position of the whale (X, Y) and prey (X^*, Y^*). This behaviour is shown in Figure 10. The spiral equation to copy the helix-shaped motion of whale is (18):

$$\overrightarrow{X}(t+1) = \overrightarrow{D'} \cdot e^{bl} \cdot \cos(2\pi l) + \overrightarrow{X^*}(t) \tag{18}$$

Where $\vec{D}' = \left|\vec{X}^*(t) - \vec{X}(t)\right|$ represents the gap between the whale and prey represents constant for defining the logarithmic gyrate shape, b is equal to one, and l refers to an arbitrary value in the range [-1, 1].

Figure 10 – Bubble-net Spiral behaviour

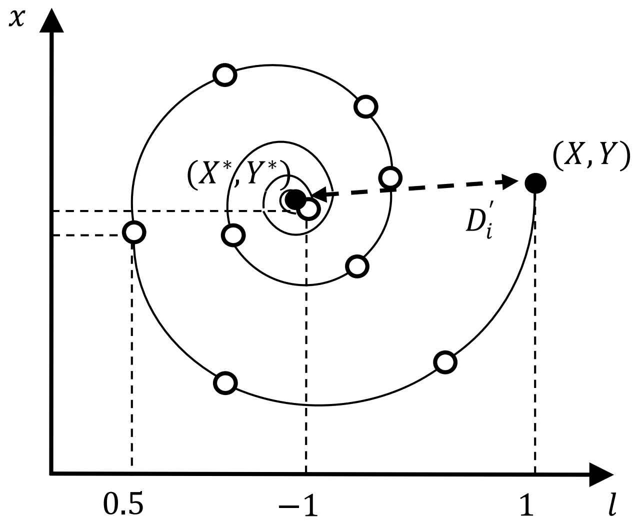

Source: Mirjalili and Lewis (2016).

Whales search for the prey simultaneously in a shrinking loop or in a spiral course. So, assume that there is a likelihood of 50% to opt either shrinking encircling behaviour or the spiral-shaped, to readjust their spot during the optimization process. It can be expressed mathematically as (19):

$$\vec{X}(t+1) = \begin{cases} \vec{X}^*(t) - \vec{A} \cdot \vec{D} & \text{if } p < 0.5 \\ \vec{D}' \cdot e^{bl} \cdot \cos(2\pi l) + \vec{X}^*(t) & \text{if } p > 0.5 \end{cases} \tag{19}$$

Where p refers to the arbitrary value in [0, 1].

5.4.4 Search the prey

In this process, the humpback whale used to randomly seeking for the prey. The global search of prey is basically used by varying the $\vec{A}$ vector. $\left|\vec{A}\right| > 1$ indicates exploration which permits WOA for the global search. Mathematically the behaviour can be expressed by (20) and (21):

$$\vec{D} = \left| \vec{C} \cdot \vec{X}_{rand} - \vec{X} \right| \tag{20}$$

$$\vec{X}(t+1) = \vec{X}_{rand} - \vec{A} \cdot \vec{D} \tag{21}$$

Where $\vec{X}_{rand}$ represents the position of random whale in the current iteration. The flow chart for the WOA is presented in Figure 11.

Figure 11 – Proposed WOA flow diagram

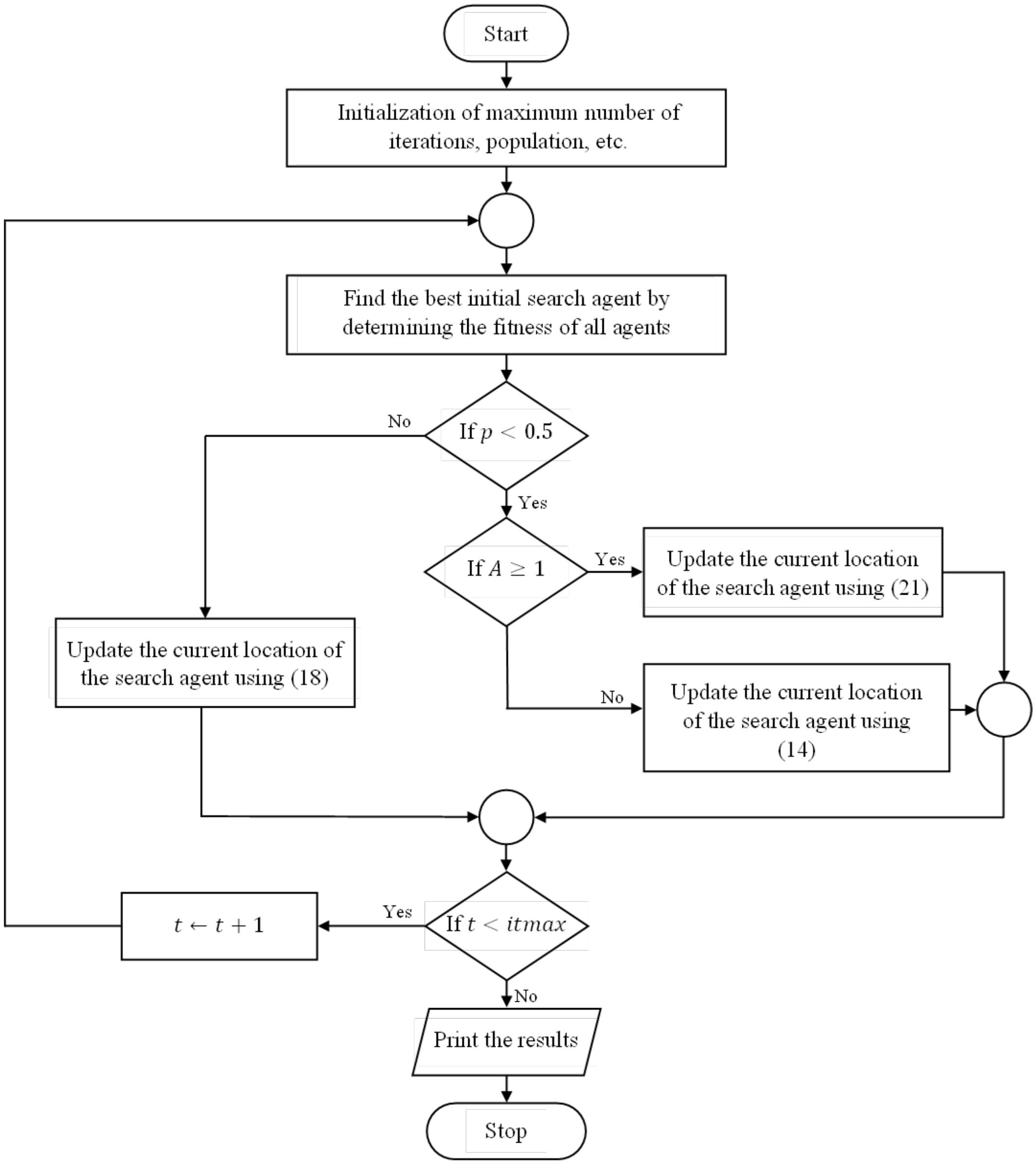

Source: Babu and Tiwari (2019).

5.5 IMPLEMENTATION OF THE WOA FOR DNR CONSIDERING THE ALLOCATION OF DG

5.5.1 Initialization

The flowchart of the WOA for the DNR problem with simultaneous DG allocation is illustrated in Figure 12. The element i, X_i, of the population represents a solution vector with three parts. The numbers of the open switches (SW_i) is considered the first part considering the fundamental loop lists. The numbers of determined buses ($x_{DG,i}$) to which the DGs are connected are represented in the second part. The number of elements in the first and second parts are integer values. The third part shows the capacity of DGs ($P_{DG,i}$). Therefore, these parts form the structure to specify the open switches, the location, and the capacities of DGs, as shown in (22).

$$X_i = [SW_1, ..., SW_{N_{Tie}}, x_{DG,1}, ..., x_{DG,N_{DG}}, P_{DG,1}, ..., P_{DG,N_{DG}}] \tag{22}$$

In the WOA, the solutions are randomly generated within the specified ranges. Thus, the variables of the initial solution proposals are generated as shown in (23)–(25).

$$SW_i = round[SW_{\min,i} + rand(0,1).(SW_{\max,i} - SW_{\min,i})] \qquad i = 1, ..., N_{Tie} \tag{23}$$

$$x_{DG,i} = round[x_{DG\min,i} + rand(0,1).(x_{DG\max,i} - x_{DG\min,i})] \qquad i = 1, ..., N_{DG} \tag{24}$$

$$P_{DG,i} = P_{DG\min,i} + rand(0,1).(P_{DG\max,i} - P_{DG\min,i}) \qquad i = 1, ..., N_{DG} \tag{25}$$

$$Q_{DG,i} = P_{DG,i} \times pf \qquad i = 1, ..., N_{DG} \tag{26}$$

Where $SW_{\min,i}$ and $SW_{\max,i}$ equals to the i^{th} fundamental loop vector length. SW_i is the sequential number of each switch in the i^{th} fundamental loop. pf is the chosen power factor, which is considered 0.9 in this work. $Q_{DG,i}$ is the reactive power output of DG unit i . N_{Tie} and N_{DG} are the number of open switches and the number of DGs, respectively.

Figure 12 – Flowchart of the proposed WOA for distribution network reconfiguration with simultaneous allocation of DGs

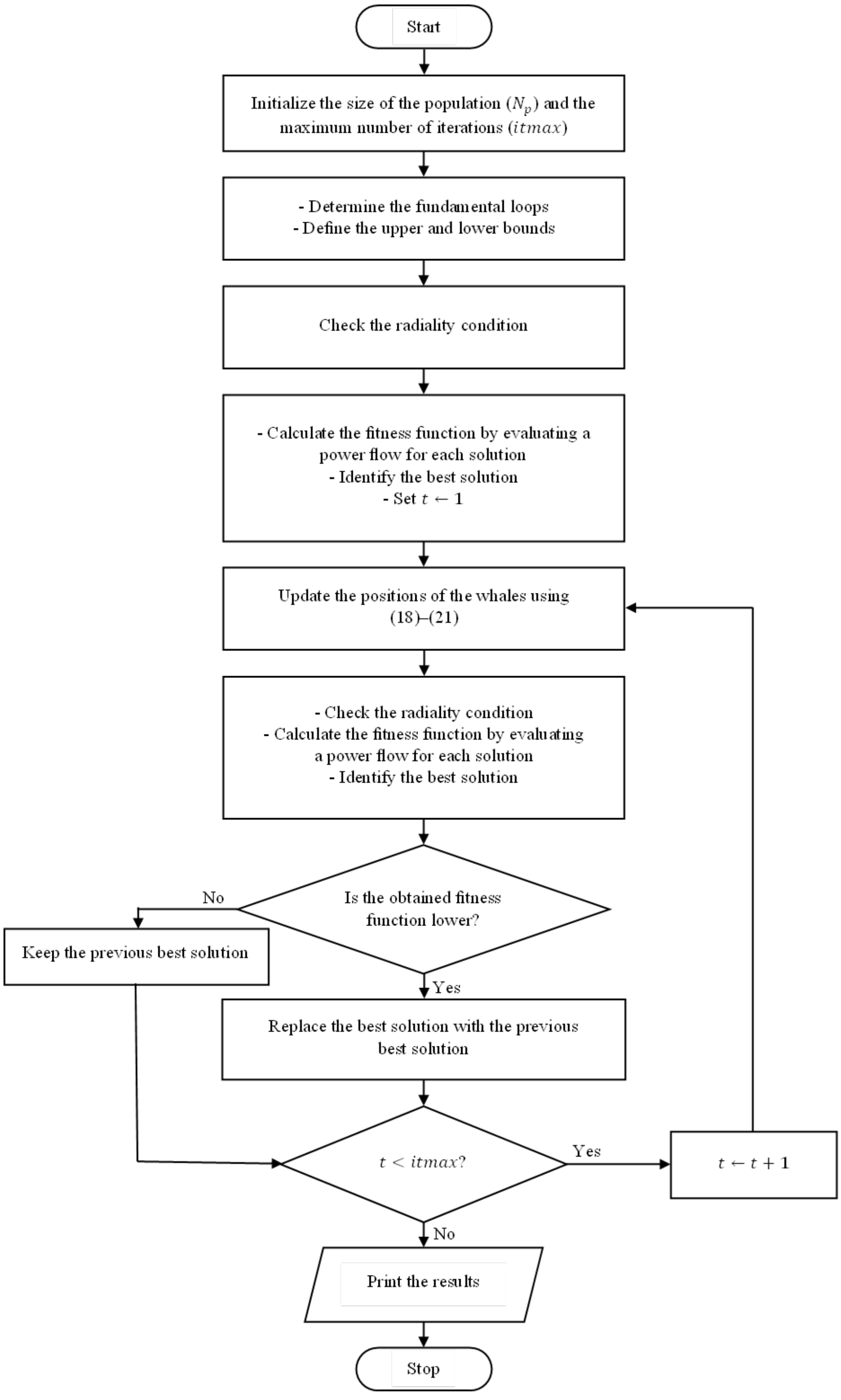

Source: Author's elaboration.

5.5.2 Overall procedure

The DNR with the simultaneous allocation of DGs is implemented using the WOA as follows:

- ***Step 1:*** Initialize population size (N_p) and the maximum number of iterations ($it\,max$).
- ***Step 2:*** Specify the fundamental loops of the distribution network (see Section 5.3.1). Determine the lower and upper limits for each loop.
- ***Step 3:*** Check the radiality condition of the solution (see Section 5.3.2) and if it is not radial, find another solution until the radial condition is met.
- ***Step 4:*** Calculate the fitness function (10) by performing power flow calculations and determine the minimum power losses. Start the iteration counter from $t \leftarrow 1$.
- ***Step 5:*** Update the position of the whales using (18)–(21).
- ***Step 6:*** Check the radiality condition (see Section 5.3.2) and if the solution is not radial, find another solution until the radial condition is met, determine the fitness function by performing power flow calculations according to (10), and determine the minimum power losses.
- ***Step 7:*** If the obtained fitness function is lower, replace the best solution with the previous best solution.
- ***Step 8:*** Let $t \leftarrow t+1$. If $t < it\,max$, increase the number of iterations and return to Step 5. If $t \geq it\,max$, print the results and stop the algorithm.

6 TESTS AND RESULTS

To evaluate the performance of the WOA, tests were conducted using the IEEE 33-bus in Soliman et al. (2020), IEEE 69-bus in Soliman et al. (2020), 136-bus in Mantovani et al. (2000), and 415-bus networks in Bernal-Agustin (1998). The algorithm was implemented in MATLAB R2018a and run on a computer with a 1.80 GHz Intel® Core™ i7-8565U processor and 16 GB of RAM. In this study, the power flow analysis was performed using the backward-forward sweep method. The population sizes for the 33-bus, 69-bus, 136-bus, and 415-bus systems were 50, 50, 70, and 100, respectively and the maximum number of iterations for the 33-bus, 69-bus, 136-bus, and 415-bus networks were equal to 300, 400, 700, and 500, respectively. As described in Section 5.3.1, the FLs were found in the mentioned networks. In addition, the voltage magnitudes at buses were limited as presented in (27).

$$0.93 \le V_i \le 1.05; \qquad i = 1, 2, ..., N_{bus} \tag{27}$$

Where the limits are in p.u.; V_i is the value of the voltage magnitude at bus i; and N_{bus} is the total number of buses.

For the optimal location and size of DGs, three DGs were considered, and the capacity range of each DG is shown in (28).

$$10 \le P_{DG,i} \le \frac{P_D}{6}; \qquad i = 1, 2, 3 \tag{28}$$

Where the limit is in kW; $P_{DG,i}$ is the size of the i^{th} DG; and P_D is the total active power demand of the system.

Four cases are considered to investigate the performance of the WOA:

- ***Case 1:*** Base case (without DNR and DGs).
- ***Case 2:*** Only reconfiguration is performed.
- ***Case 3:*** The optimal location and size of 3 DGs are performed after reconfiguration according to the result of Case 2.

- ***Case 4:*** The reconfiguration and the optimal location and size of 3 DGs are performed simultaneously.

6.1 IEEE 33-BUS NETWORK

The 33-bus system is presented in Soliman et al. (2020). It has 32 load buses, one substation bus and 37 feeders. The voltage at the substation bus is 12.66 kV and the base power of the system is 100 MVA. The total active and reactive power demands are 3715 kW and 2300 kVAr, respectively. The maximum size of each DG unit is 619.17 kW. For comparing the performance of the WOA method with other methods, ACSA in Nguyen et al. (2016), UVDA in Bayat et al. (2016), MPGSA in Rajaram et al. (2015), and SFS in Tran et al. (2020) methods are considered (see Table 9).

Figure 13 illustrates the 33-bus system with five tie switches 33, 34, 35, 36 and 37 that are initially open and illustrated by dashed lines, and the basic loops of the network are presented in Table 2. The complete data of this system are presented in Appendix A.

Figure 13 – Topology of the IEEE 33-bus network

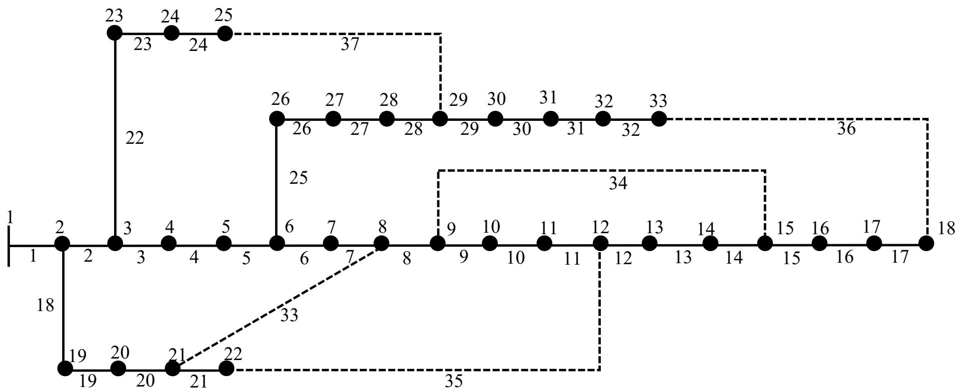

Source: Soliman et al. (2020).

6.1.1 DNR using WOA algorithm

Figure 14 illustrates voltage profiles before and after DNR on a 33-bus system. As shown in Figure 14 and Table 6, the power loss was 202.68 kW and minimum voltage was 0.9131 per-unit in base case. The power loss was reduced to 139.55 kW, thus having a reduction of 31.15 % compared to the base case. The minimum voltage was improved to 0.9378 per-unit after DNR. The tie switches which were opened after DNR, were 7, 9, 14, 32, and 37.

Figure 14 – Voltage profiles for the 33-bus network before and after DNR obtained with the WOA

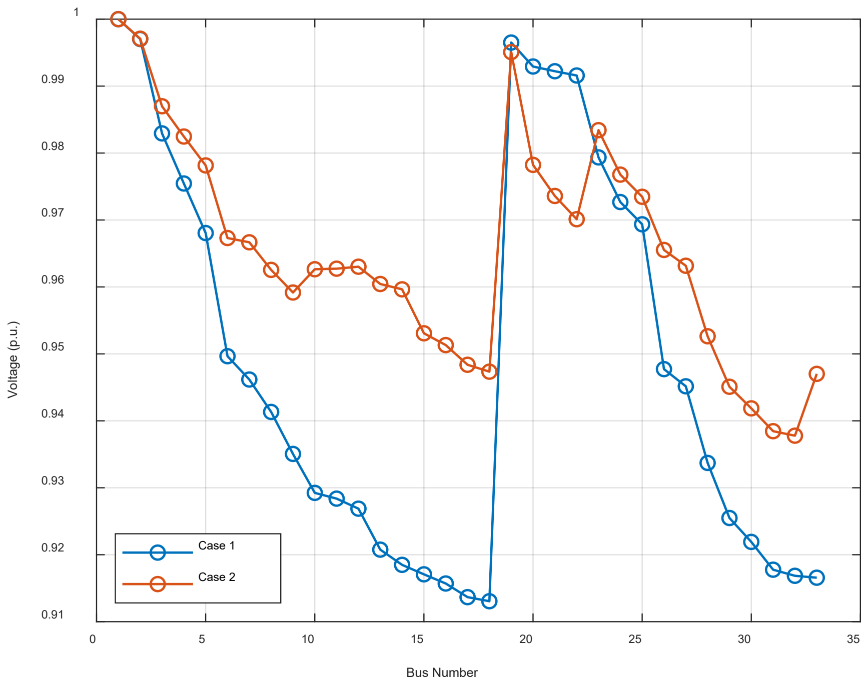

Source: Author's elaboration.

Table 6 – Simulation results for the 33-bus network before and after DNR using WOA

	Base Case	DNR
Active power loss:	202.68 kW	139.55 kW
Reactive power loss:	135.14 kVAr	102.31 kVAr
Active power loss reduction:	_	31.15 %
Tie switches:	33, 34, 35, 36, 37	7, 9, 14, 32, 37
Minimum voltage:	0.9131 p.u.	0.9378 p.u.

Source: Author's elaboration.

Figure 15 illustrates the convergence of the WOA after DNR along the iterations on a 33-bus system. In Figure 15, the fitness (optimal solution) was found around the 220th iteration.

Figure 15 – Convergence of WOA for the 33-bus network after DNR

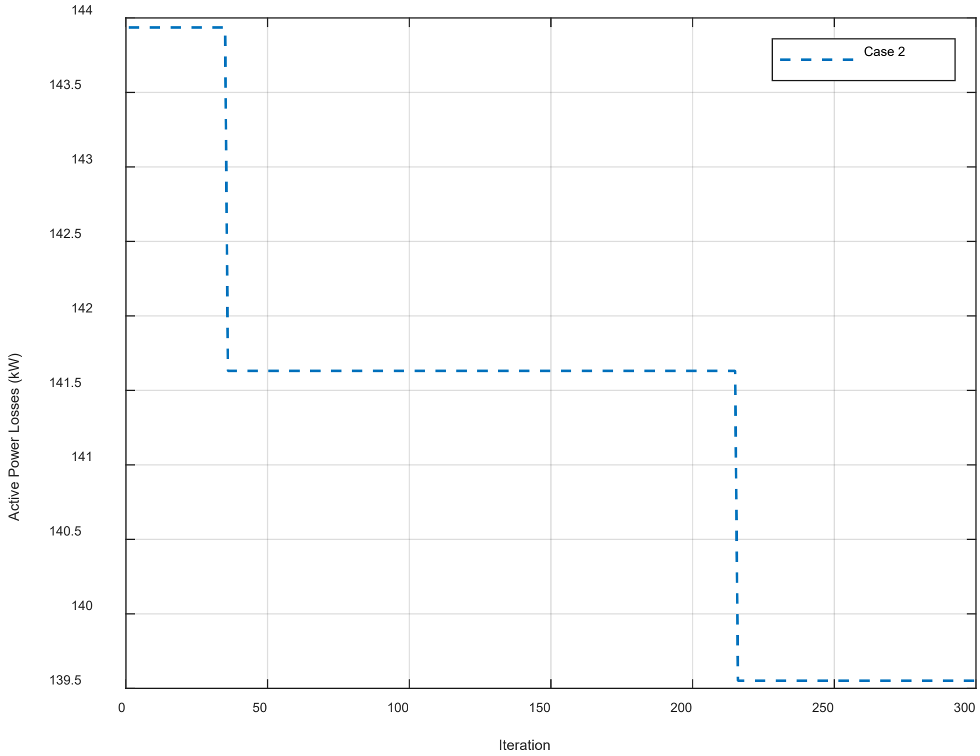

Source: Author's elaboration.

6.1.2 The optimal location and size of 3 DGs after DNR according to the result of Case 2 using WOA algorithm

The tie switches were determined after network reconfiguration in Case 2 and the opened tie switches were 7, 9, 14, 32, and 37. We assumed that these switches were open and then the optimal location and size of DG units were specified by WOA algorithm. We installed 3 DG units in this Case after DNR.

Figure 16 illustrates voltage profiles before and after 3 DGs and DNR on a 33-bus system. As shown in Figure 16 and Table 7, the power loss was 202.68 kW and minimum voltage was 0.9131 per-unit in base case. The power loss was reduced to 40.80 kW, thus having a reduction of 79.87 % compared to the base case. The minimum voltage was improved to 0.9737 per-unit after 3 DGs and DNR. Also, the WOA method determines buses 16, 29, and 31 as the best places to connect the DGs, and the three DGs operate at the limit of 619.2 kW.

Figure 16 – Voltage profiles for the 33-bus network before and after 3 DGs and DNR obtained with the WOA

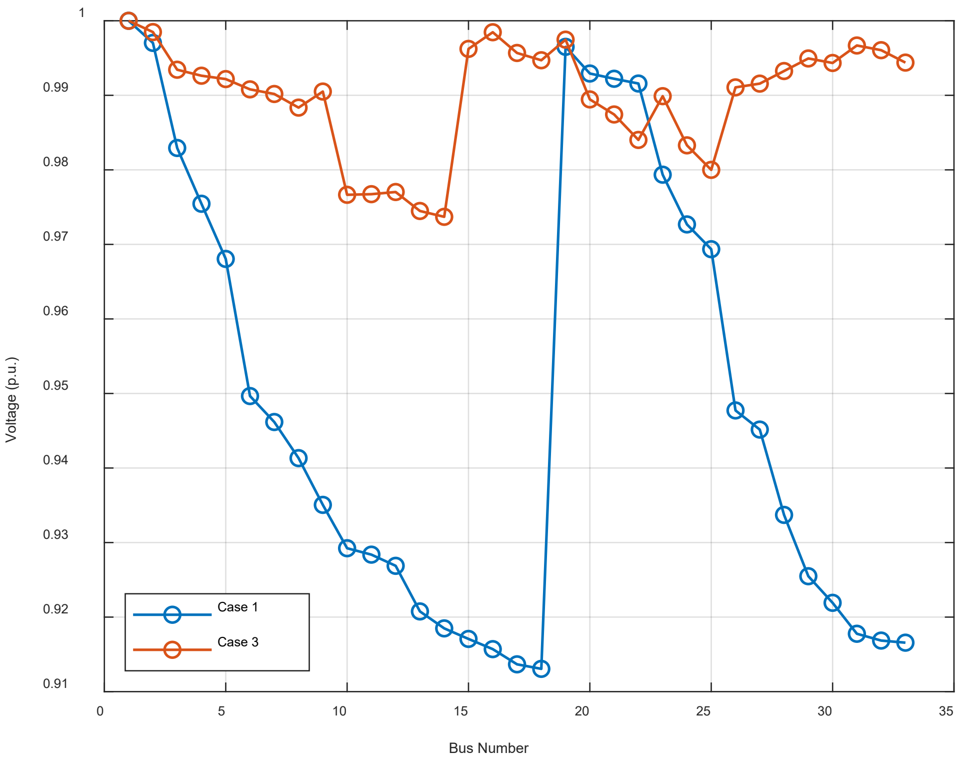

Source: Author's elaboration.

Table 7 – Simulation results for the 33-bus network before and after 3 DGs and DNR using WOA

	Base Case	3 DGs after DNR
Active power loss:	202.68 kW	40.80 kW
Reactive power loss:	135.14 kVAr	31.30 kVAr
Active power loss reduction:	_	79.87 %
Tie switches:	33, 34, 35, 36, 37	7, 9, 14, 32, 37
Optimal DG location	_	16, 29, 31
Optimal DG size P	_	619.2, 619.2, 619.2 kW
Optimal DG size Q	_	299.9, 299.9, 299.9 kVAr
Minimum voltage:	0.9131 p.u.	0.9737 p.u.

Source: Author's elaboration.

Figure 17 illustrates the convergence of the WOA after 3 DGs and DNR along the iterations on a 33-bus system. In Figure 17, the fitness (optimal solution) was found around the 25th iteration.

Figure 17 – Convergence of WOA for the 33-bus network after 3 DGs and DNR

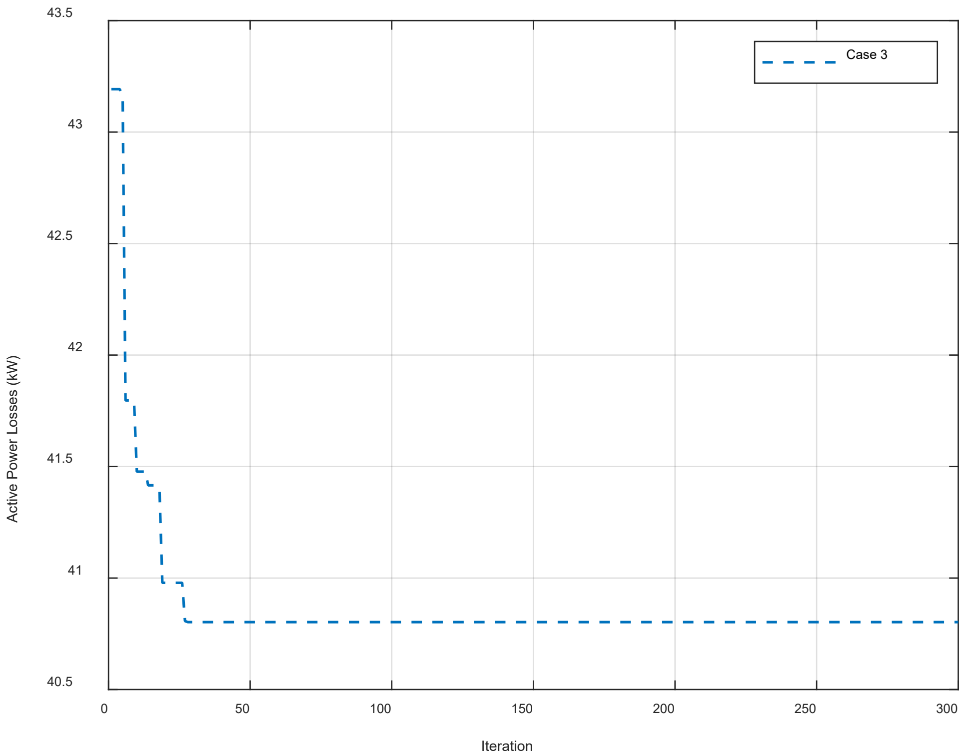

Source: Author's elaboration.

6.1.3 The simultaneous DNR and optimal location and size of 3 DGs using WOA algorithm

Figure 18 illustrates voltage profiles before and after simultaneous 3 DGs and DNR on a 33-bus system. As shown in Figure 18 and Table 8, the power loss was 202.68 kW and minimum voltage was 0.9131 per-unit in base case. The power loss was reduced to 31.17 kW, thus having a reduction of 84.62 % compared to the base case. The minimum voltage was improved to 0.9804 per-unit after simultaneous 3 DGs and DNR. Also, the optimal location and size of DGs were obtained by the WOA algorithm and 3 DG units with the capacity of 614.0 kW, 610.0 kW, and 613.0 kW were allocated in buses 13, 29, and 32. The tie switches which were opened after simultaneous 3 DGs and DNR, were 7, 8, 9, 27, and 36.

Figure 18 – Voltage profiles for the 33-bus network before and after simultaneous 3 DGs and DNR obtained with the WOA

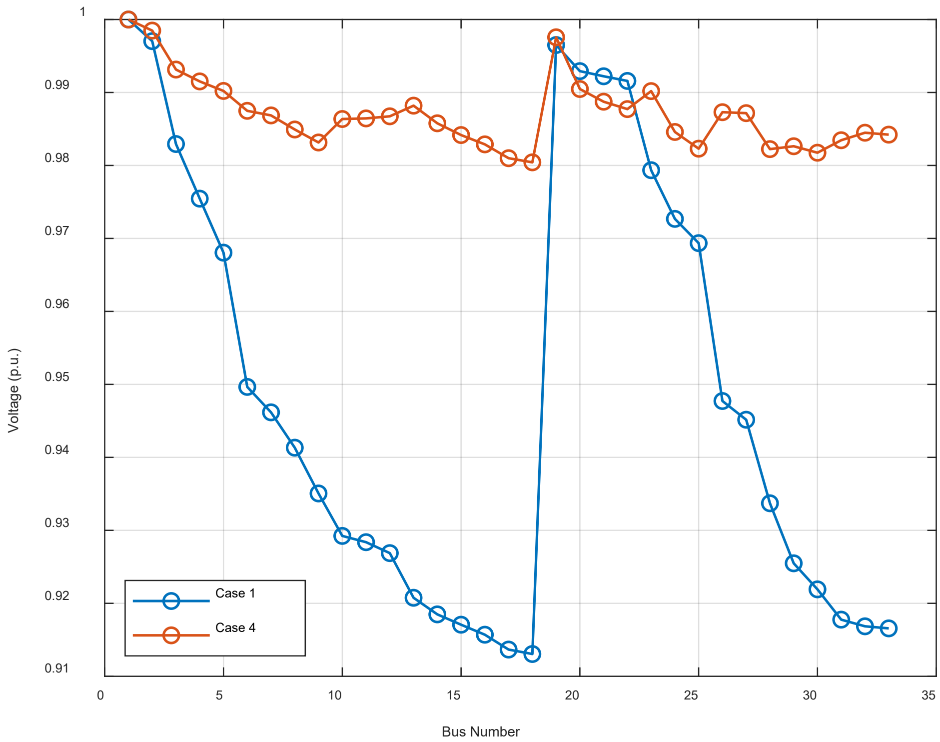

Source: Author's elaboration.

Table 8 – Simulation results for the 33-bus network before and after simultaneous 3 DGs and DNR using WOA

	Base Case	Simultaneous 3 DGs and DNR
Active power loss:	202.68 kW	31.17 kW
Reactive power loss:	135.14 kVAr	22.58 kVAr
Active power loss reduction:	_	84.62 %
Tie switches:	33, 34, 35, 36, 37	7, 8, 9, 27, 36
Optimal DG location	_	13, 29, 32
Optimal DG size P	_	614.0, 610.0, 613.0 kW
Optimal DG size Q	_	297.4, 295.4, 296.9 kVAr
Minimum voltage:	0.9131 p.u.	0.9804 p.u.

Source: Author's elaboration.

Figure 19 illustrates the convergence of the WOA after simultaneous 3 DGs and DNR along the iterations on a 33-bus system. In Figure 19, the fitness (optimal solution) was found around the 30th iteration.

Figure 19 – Convergence of WOA for the 33-bus network after simultaneous 3 DGs and DNR

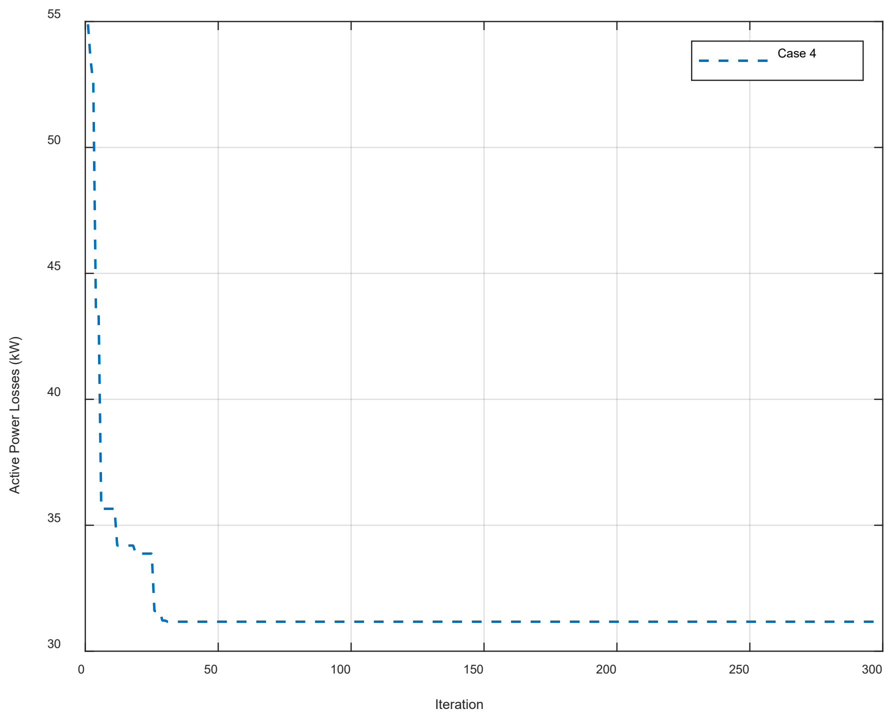

Source: Author's elaboration.

Figure 20 demonstrates the comparison of the voltage profiles of the four cases. Table 9 shows that the power losses reduction percentage and voltage profile improvement for Case 4 are more significant than for the other cases. Figure 21 presents the comparison of the evolution of the WOA for Cases 2 to 4.

The results of the WOA are compared with the solutions provided by other methods, as shown in Table 9. In Case 2, the power losses of the WOA are similar to the UVDA, MPGSA, and SFS, but the difference in the power losses of the proposed algorithm with ACSA is very insignificant. The difference between the WOA and other methods is that the power losses of Case 3 are significantly lower for the WOA. The results of Case 4 obtained by the WOA is more desirable in terms of power losses reduction compared to ACSA and SFS, but the obtained values are almost similar in terms of minimum voltage magnitude. The proposed WOA further optimizes the results of Cases 2 to 4 and provides better results for the 33-bus network.

Figure 20 – Comparison of voltage profiles for the 33-bus network obtained with the WOA

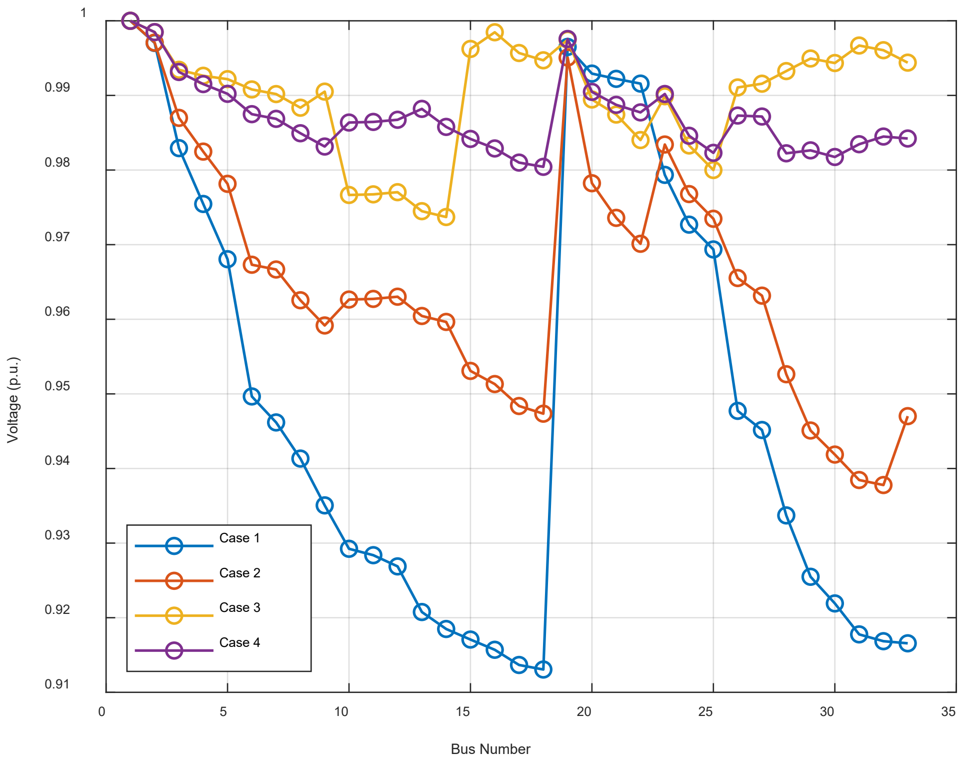

Source: Author's elaboration.

Figure 21 – Comparison of convergence of the WOA for the 33-bus network

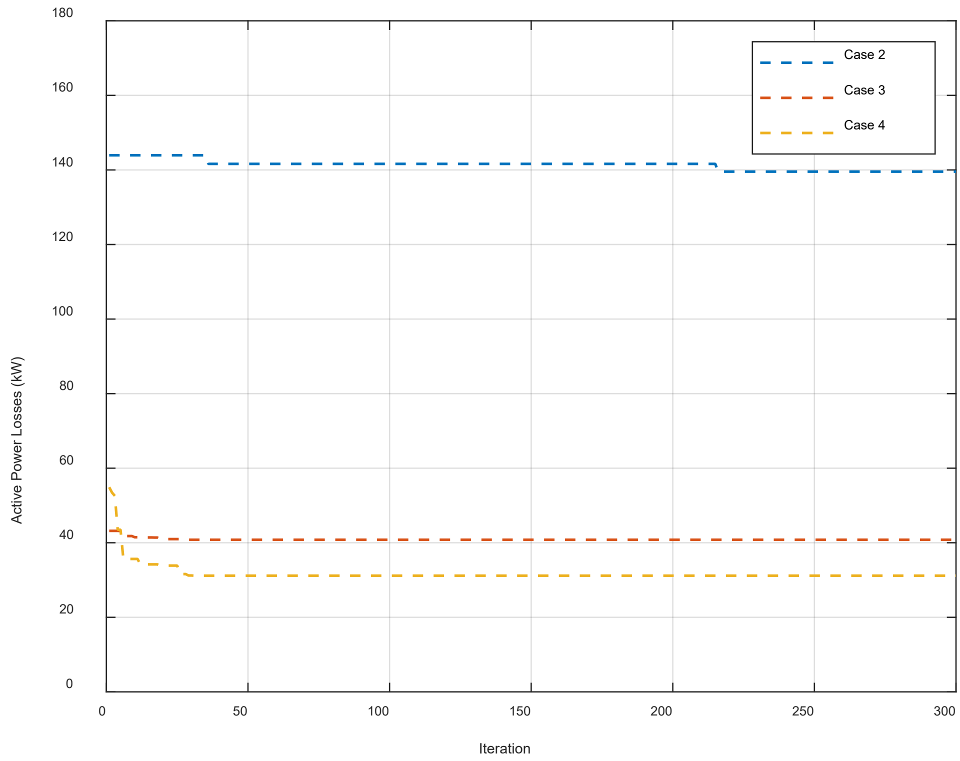

Source: Author's elaboration.

Table 9 – Summary of the results for the 33-bus network

Case	Item	ACSA (Nguyen et al., 2016)	UVDA (Bayat et al., 2016)	MPGSA (Rajaram et al., 2015)	SFS (Tran et al., 2020)	WOA
1	**Tie switches**	–	–	–	–	33-34-35-36-37
	P_L **(kW)**	–	–	–	–	202.68
	Q_L **(kVAr)**	–	–	–	–	135.14
	$V_{\min}$ **(p.u.)**	–	–	–	–	0.9131
	Time (s)	–	–	–	–	0.2
2	**Tie switches**	7-9-14-28-32	7-9-14-32-37	7-9-14-32-37	7-9-14-32-37	7-9-14-32-37
	P_L **(kW)**	139.98	139.55	139.55	139.55	139.55
	Q_L **(kVAr)**	–	–	–	–	102.31
	P_L **reduction (%)**	30.93	31.15	31.15	31.15	31.15
	$V_{\min}$ **(p.u.)**	0.9413	0.9378	0.9378	0.9378	0.9378
	Time (s)	–	–	–	–	4265.4
3	**Tie switches**	7-9-14-28-32	7-9-14-32-37	7-9-14-32-37	7-9-14-32-37	7-9-14-32-37
	P_{DG} **(kW)/(Bus)**	539.7/(12) 504.5/(16) 1753.6/(29)	526.0/(12) 592.0/(15) 1125.0/(30)	246.9/(31) 179.5/(32) 664.5/(33)	931.7/(8) 1068.2/(24) 950.3/(30)	619.2/(16) 619.2/(29) 619.2/(31)
	Q_{DG} **(kVAr)**	– – –	– – –	– – –	– – –	299.9 299.9 299.9
	P_L **(kW)**	58.79	66.60	92.87	58.88	40.80
	Q_L **(kVAr)**	–	–	–	–	31.30
	P_L **reduction (%)**	71.00	67.14	54.17	70.95	79.87
	$V_{\min}$ **(p.u.)**	0.9802	0.9758	0.9482	0.9741	0.9737
	Time (s)	–	–	–	–	3926.5
4	**Tie switches**	11-28-31-33-34	–	–	7-9-14-27-30	7-8-9-27-36

	P_{DG} **(kW)/(Bus)**	964.6/(7) 896.8/(18) 1438.1/(25)	– – –	– – –	775.3/(22) 1285.8/(25) 735.6/(33)	614.0/(13) 610.0/(29) 613.0/(32)
	Q_{DG} **(kVAr)**	– – –	– – –	– – –	– – –	297.4 295.4 296.9
	P_L **(kW)**	53.21	–	–	53.01	31.17
	Q_L **(kVAr)**	–	–	–	–	22.58
	P_L **reduction (%)**	73.75	–	–	73.85	84.62
	$V_{\min}$ **(p.u.)**	0.9806	–	–	0.9720	0.9804
	Time (s)	–	–	–	–	4764.6

Source: Author's elaboration.

6.2 IEEE 69-BUS NETWORK

The 69-bus system is presented in Soliman et al. (2020). It has 68 load buses, one substation bus and 73 feeders. The voltage at the substation bus is 12.66 kV and the base power of the system is 100 MVA. The total active and reactive power demands are 3801.9 kW and 2694.1 kVAr, respectively. The maximum size of each DG unit is 633.7 kW. For comparing the performance of the WOA method with other methods, ACSA in Nguyen et al. (2016), UVDA in Bayat et al. (2016), and SFS in Tran et al. (2020) methods are considered (see Table 13).

Figure 22 illustrates the 69-bus system with five tie switches 69, 70, 71, 72 and 73 that are initially open and illustrated by dashed lines, while the basic loops of the network are presented in Table 3. The complete data of this system are presented in Appendix B.

Figure 22 – Topology of the IEEE 69-bus network

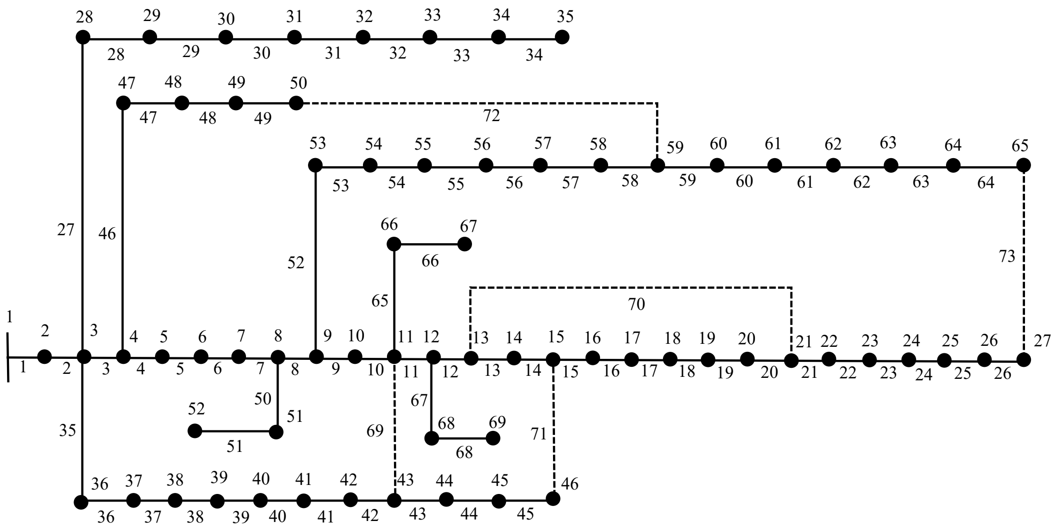

Source: Soliman et al. (2020).

6.2.1 DNR using WOA algorithm

Figure 23 illustrates voltage profiles before and after DNR on a 69-bus system. As shown in Figure 23 and Table 10, the power loss was 224.96 kW and minimum voltage was 0.9090 per-unit in base case. The power loss was reduced to 99.80 kW, thus having a reduction of 55.64 % compared to the base case. The minimum voltage was improved to 0.9427 per-unit after DNR. The tie switches which were opened after DNR, were 12, 57, 61, 69, and 70.

Figure 23 – Voltage profiles for the 69-bus network before and after DNR obtained with the WOA

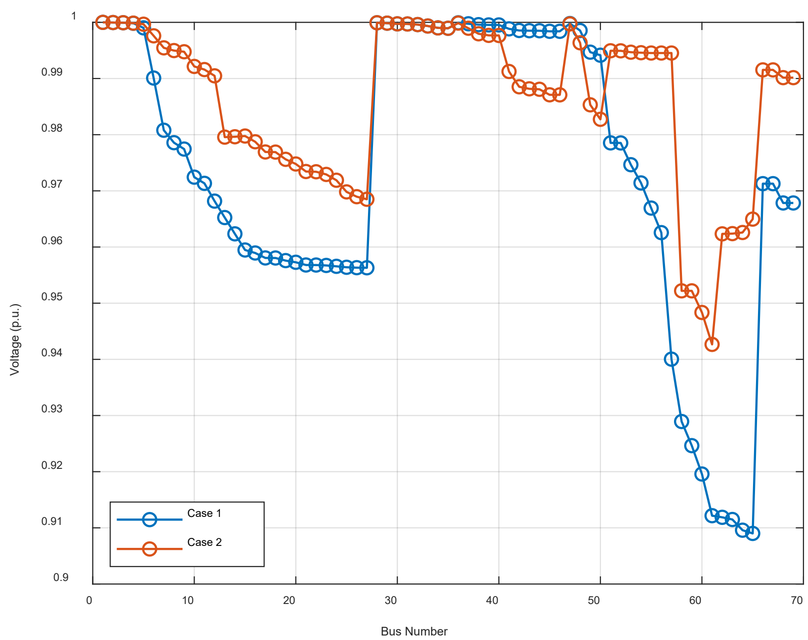

Source: Author's elaboration.

Table 10 – Simulation results for the 69-bus network before and after DNR using WOA

	Base Case	DNR
Active power loss:	224.96 kW	99.80 kW
Reactive power loss:	102.15 kVAr	115.14 kVAr
Active power loss reduction:	–	55.64 %
Tie switches:	69, 70, 71, 72, 73	12, 57, 61, 69, 70
Minimum voltage:	0.9090 p.u.	0.9427 p.u.

Source: Author's elaboration.

Figure 24 illustrates the convergence of the WOA after DNR along the iterations on a 69-bus system. In Figure 24, the fitness (optimal solution) was found around the 100th iteration.

Figure 24 – Convergence of WOA for the 69-bus network after DNR

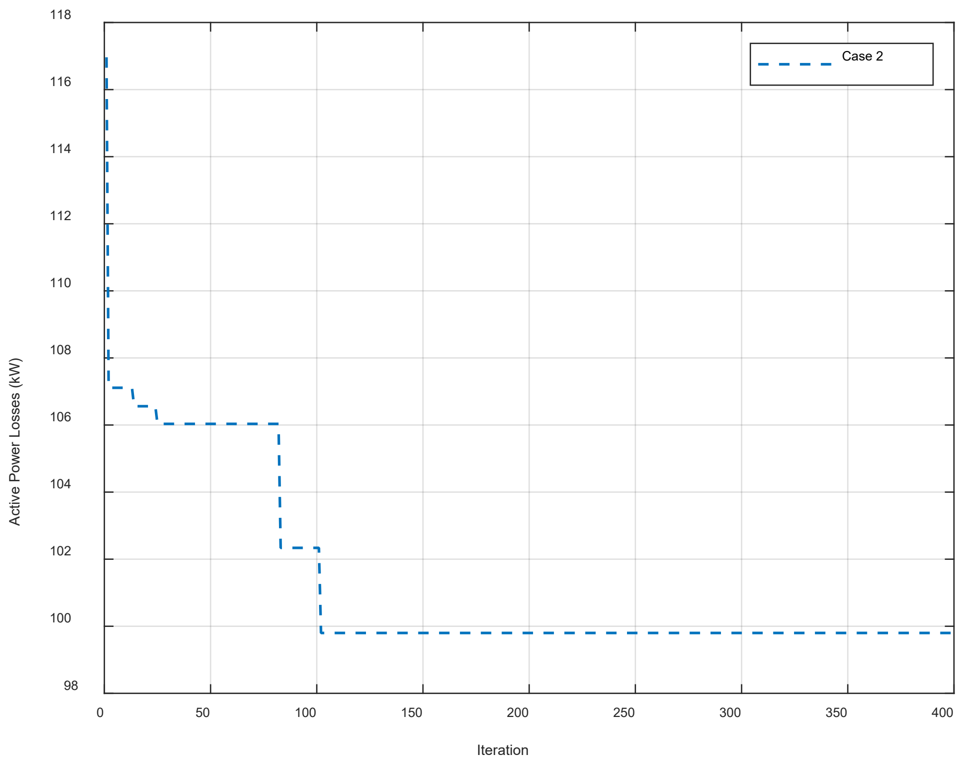

Source: Author's elaboration.

6.2.2 The optimal location and size of 3 DGs after DNR according to the result of Case 2 using WOA algorithm

The tie switches were determined after network reconfiguration in Case 2 and the opened tie switches were 12, 57, 61, 69, and 70. We assumed that these switches were open and then the optimal location and size of DG units were specified by WOA algorithm. We installed 3 DG units in this Case after DNR.

Figure 25 illustrates voltage profiles before and after 3 DGs and DNR on a 69-bus system. As shown in Figure 25 and Table 11, the power loss was 224.96 kW and minimum voltage was 0.9090 per-unit in base case. The power loss was reduced to 28.05 kW, thus having a reduction of 87.53 % compared to the base case. The minimum voltage was improved to 0.9707 per-unit after 3 DGs and DNR. Also, the WOA method determines buses 27, 60, and 61 as the best places to connect the DGs, and the three DGs operate at the limit of 572.0 kW, 205.0 kW, and 633.7 kW.

Figure 25 – Voltage profiles for the 69-bus network before and after 3 DGs and DNR obtained with the WOA

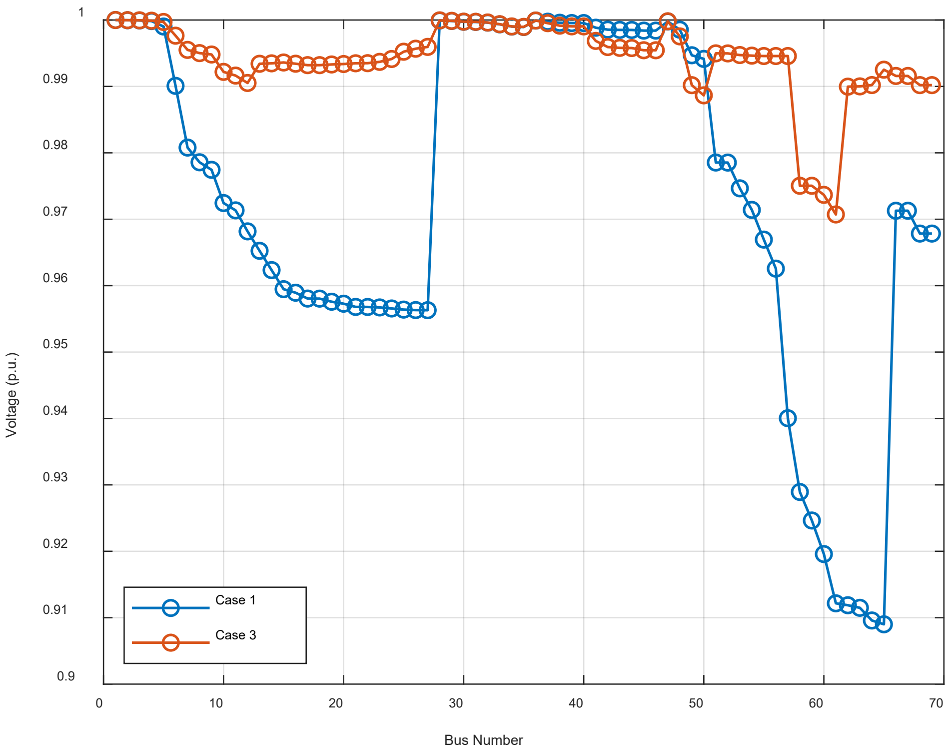

Source: Author's elaboration.

Table 11 – Simulation results for the 69-bus network before and after 3 DGs and DNR using WOA

	Base Case	3 DGs after DNR
Active power loss:	224.96 kW	28.05 kW
Reactive power loss:	102.15 kVAr	34.30 kVAr
Active power loss reduction:	_	87.53 %
Tie switches:	69, 70, 71, 72, 73	12, 57, 61, 69, 70
Optimal DG location	_	27, 60, 61
Optimal DG size P	_	572.0, 205.0, 633.7 kW
Optimal DG size Q	_	277.0, 99.3, 306.9 kVAr
Minimum voltage:	0.9090 p.u.	0.9707 p.u.

Source: Author's elaboration.

Figure 26 illustrates the convergence of the WOA after 3 DGs and DNR along the iterations on a 69-bus system. In Figure 26, the fitness (optimal solution) was found around the 80th iteration.

Figure 26 – Convergence of WOA for the 69-bus network after 3 DGs and DNR

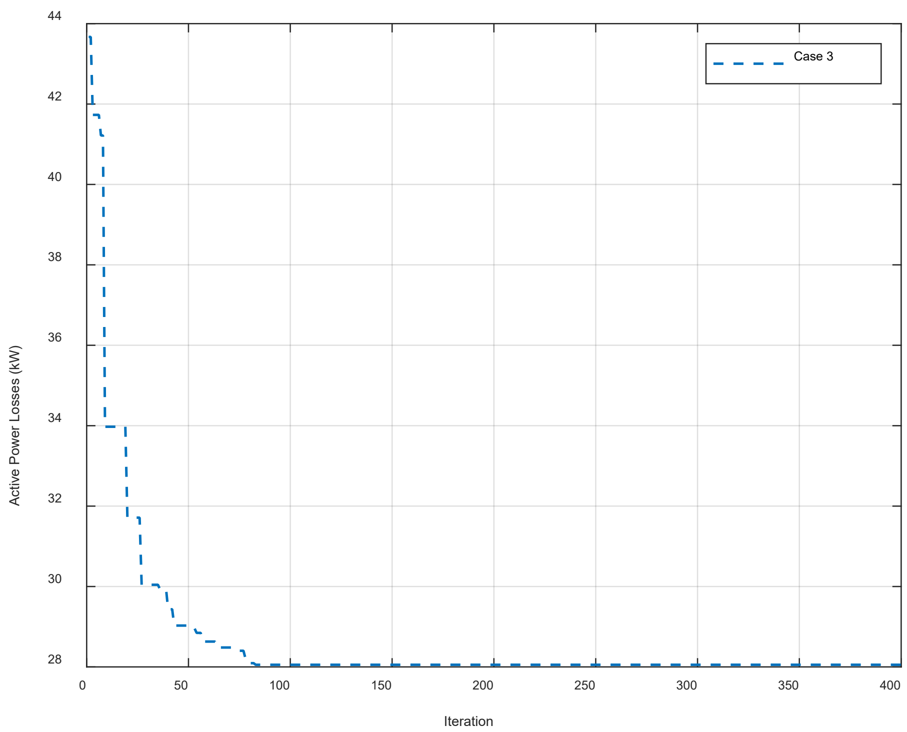

Source: Author's elaboration.

6.2.3 The simultaneous DNR and optimal location and size of 3 DGs using WOA algorithm

Figure 27 illustrates voltage profiles before and after simultaneous 3 DGs and DNR on a 69-bus system. As shown in Figure 27 and Table 12, the power loss was 224.96 kW and minimum voltage was 0.9090 per-unit in base case. The power loss was reduced to 19.49 kW, thus having a reduction of 91.34 % compared to the base case. The minimum voltage was improved to 0.9820 per-unit after simultaneous 3 DGs and DNR. Also, the optimal location and size of DGs were obtained by the WOA algorithm and 3 DG units with the capacity of 633.7 kW, 496.0 kW, and 607.0 kW were allocated in buses 62, 63, and 64. The tie switches which were opened after simultaneous 3 DGs and DNR, were 10, 12, 20, 21, and 58.

Figure 27 – Voltage profiles for the 69-bus network before and after simultaneous 3 DGs and DNR obtained with the WOA

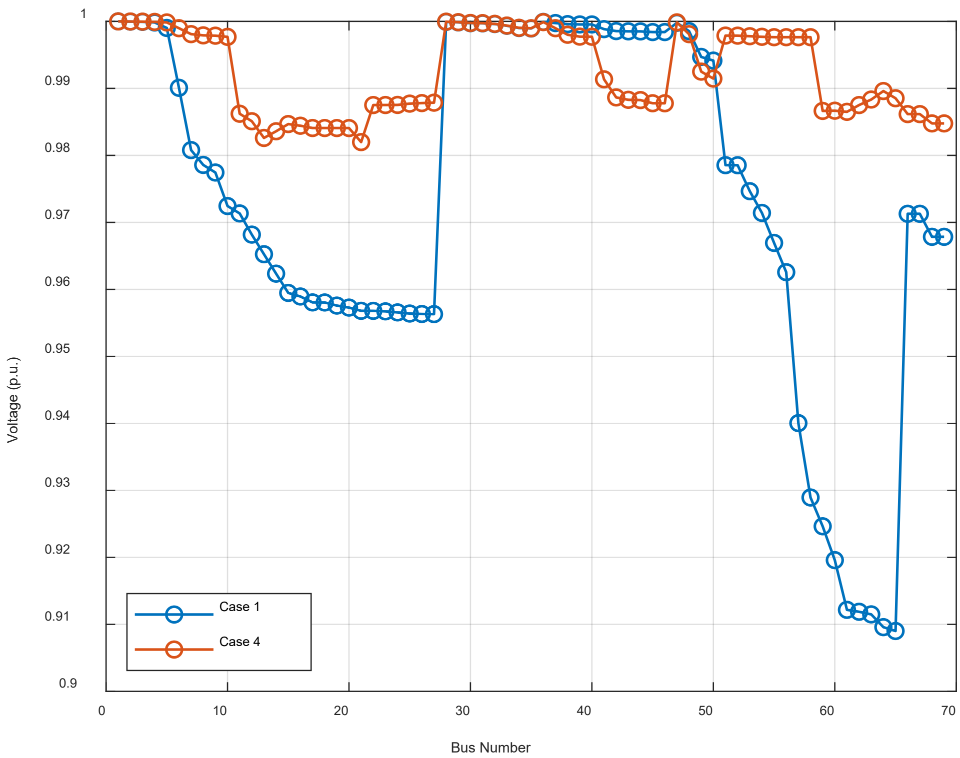

Source: Author's elaboration.

Table 12 – Simulation results for the 69-bus network before and after simultaneous 3 DGs and DNR using WOA

	Base Case	Simultaneous 3 DGs and DNR
Active power loss:	224.96 kW	19.49 kW
Reactive power loss:	102.15 kVAr	24.80 kVAr
Active power loss reduction:	_	91.34 %
Tie switches:	69, 70, 71, 72, 73	10, 12, 20, 21, 58
Optimal DG location	_	62, 63, 64
Optimal DG size P	_	633.7, 496.0, 607.0 kW
Optimal DG size Q	_	306.9, 240.2, 294.0 kVAr
Minimum voltage:	0.9090 p.u.	0.9820 p.u.

Source: Author's elaboration.

Figure 28 illustrates the convergence of the WOA after simultaneous 3 DGs and DNR along the iterations on a 69-bus system. In Figure 28, the fitness (optimal solution) was found around the 80th iteration.

Figure 28 – Convergence of WOA for the 69-bus network after simultaneous 3 DGs and DNR

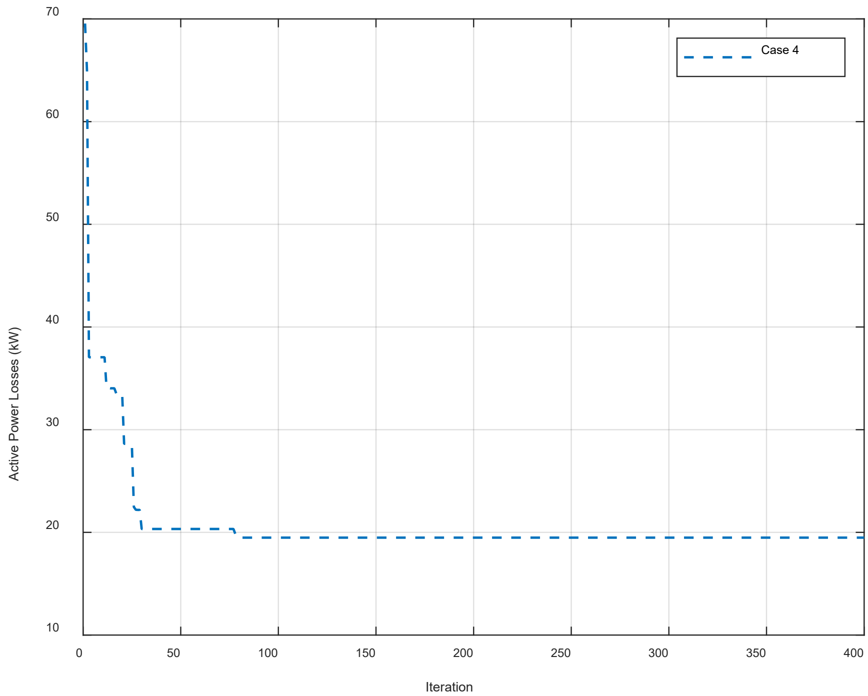

Source: Author's elaboration.

Table 13 shows that the power losses reduction percentage and voltage profile improvement for Case 4 is more significant than for the other cases. For all cases, the comparison of the voltage profiles is shown in Figure 29 and the comparison of the convergence characteristics of the proposed method is depicted in Figure 30.

The results of the WOA are compared with the solutions provided by other methods, as shown in Table 13. In Case 2, the difference in the power losses for the solution obtained by the proposed algorithm in comparison with other methods is very insignificant. The difference between the WOA and other methods is that the power losses for the solution obtained by the WOA for Case 3 are significantly lower than the results obtained by the other methods. The result of Case 4 obtained by WOA is more desirable in terms of power losses reduction when compared to ACSA and SFS, but the obtained values are almost similar in terms of minimum voltage magnitude. The proposed WOA further optimizes the results of Cases 2 to 4 and provides better results for the 69-bus network.

Figure 29 – Comparison of voltage profiles for the 69-bus network obtained with the WOA

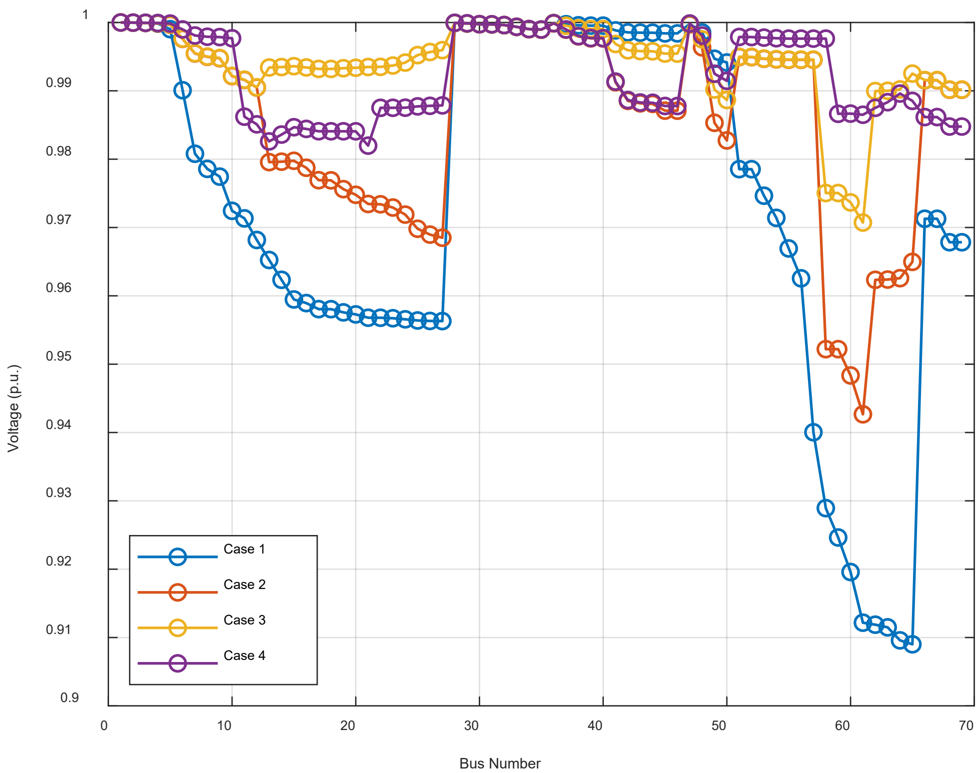

Source: Author's elaboration.

Figure 30 – Comparison of convergence of the WOA for the 69-bus network

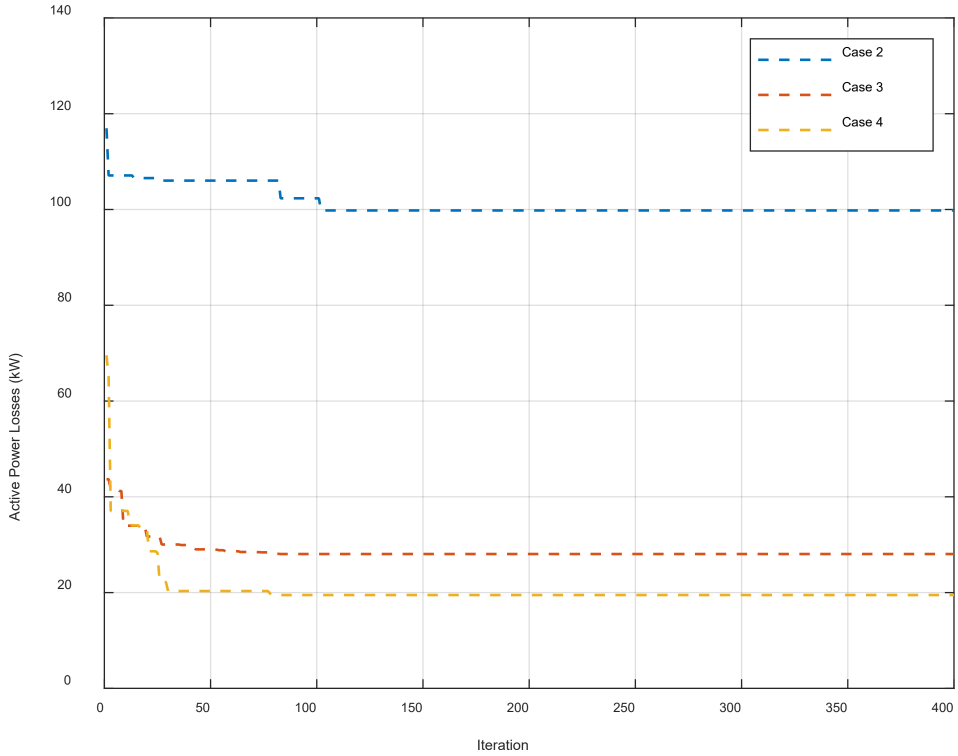

Source: Author's elaboration.

Table 13 – Summary of the results for the 69-bus network

Case	Item	ACSA (Nguyen et al., 2016)	UVDA (Bayat et al., 2016)	SFS (Tran et al., 2020)	WOA
1	Tie switches	–	–	–	69-70-71-72-73
	P_L (kW)	–	–	–	224.96
	Q_L (kVAr)	–	–	–	102.15
	$V_{\min}$ (p.u.)	–	–	–	0.9090
	Time (s)	–	–	–	0.3
2	Tie switches	14-57-61-69-70	14-58-61-69-70	14-55-61-69-70	12-57-61-69-70
	P_L (kW)	98.59	98.58	98.62	99.80
	Q_L (kVAr)	–	–	–	115.14
	P_L reduction (%)	56.16	56.19	56.17	55.64
	$V_{\min}$ (p.u.)	0.9495	0.9495	0.9495	0.9427
	Time (s)	–	–	–	27553.3
3	Tie switches	14-57-61-69-70	14-58-61-69-70	14-55-61-69-70	12-57-61-69-70

	P_{DG} **(kW)/(Bus)**	368.6/(12) 1725.4/(61) 466.6/(64)	620.0/(11) 1378.0/(61) 722.0/(64)	537.6/(11) 1434.0/(61) 490.3/(64)	572.0/(27) 205.0/(60) 633.7/(61)
	Q_{DG} **(kVAr)**	– – –	– – –	– – –	277.0 99.3 306.9
	P_L **(kW)**	37.23	37.84	35.17	28.05
	Q_L **(kVAr)**	–	–	–	34.30
	P_L **reduction (%)**	83.45	83.18	84.37	87.53
	$V_{\min}$ **(p.u.)**	0.9870	0.9801	0.9813	0.9707
	Time (s)	–	–	–	14310.7
4	**Tie switches**	14-58-61-69-70	–	14-56-61-69-70	10-12-20-21-58
	P_{DG} **(kW)/(Bus)**	541.3/(11) 1724.0/(61) 553.6/(65)	– – –	537.6/(11) 1434.0/(61) 490.3/(64)	633.7/(62) 496.0/(63) 607.0/(64)
	Q_{DG} **(kVAr)**	– – –	– – –	– – –	306.9 240.2 294.0
	P_L **(kW)**	37.02	–	35.16	19.49
	Q_L **(kVAr)**	–	–	–	24.80
	P_L **reduction (%)**	83.54	–	84.37	91.34
	$V_{\min}$ **(p.u.)**	0.9869	–	0.9810	0.9820
	Time (s)	–	–	–	27902.1

Source: Author's elaboration.

6.3 136-BUS NETWORK

The 136-bus system is presented in Mantovani et al. (2000). It has 135 load buses, one substation bus and 156 feeders. The voltage at the substation bus is 13.80 kV and the base power of the system is 100 MVA. The total active and reactive power demands are 18313.810 kW and 7932.534 kVAr, respectively. The maximum size of each DG unit is 3052.30 kW. For comparing the performance of the WOA method with other methods, UVDA in Bayat et al. (2016), SFS in Tran et al. (2020), and AACO in Swarnkar et al. (2011) methods are considered (see Table 16).

Figure 31 illustrates the 136-bus system with 21 tie switches 136, 137, 138, 139, 140, 141, 142, 143, 144, 145, 146, 147, 148, 149, 150, 151, 152, 153, 154, 155, and 156 that are initially open and illustrated by dashed lines, while the basic loops of the network are presented in Table 4. The complete data of this system are presented in Appendix C.

Figure 31 – Topology of the 136-bus network

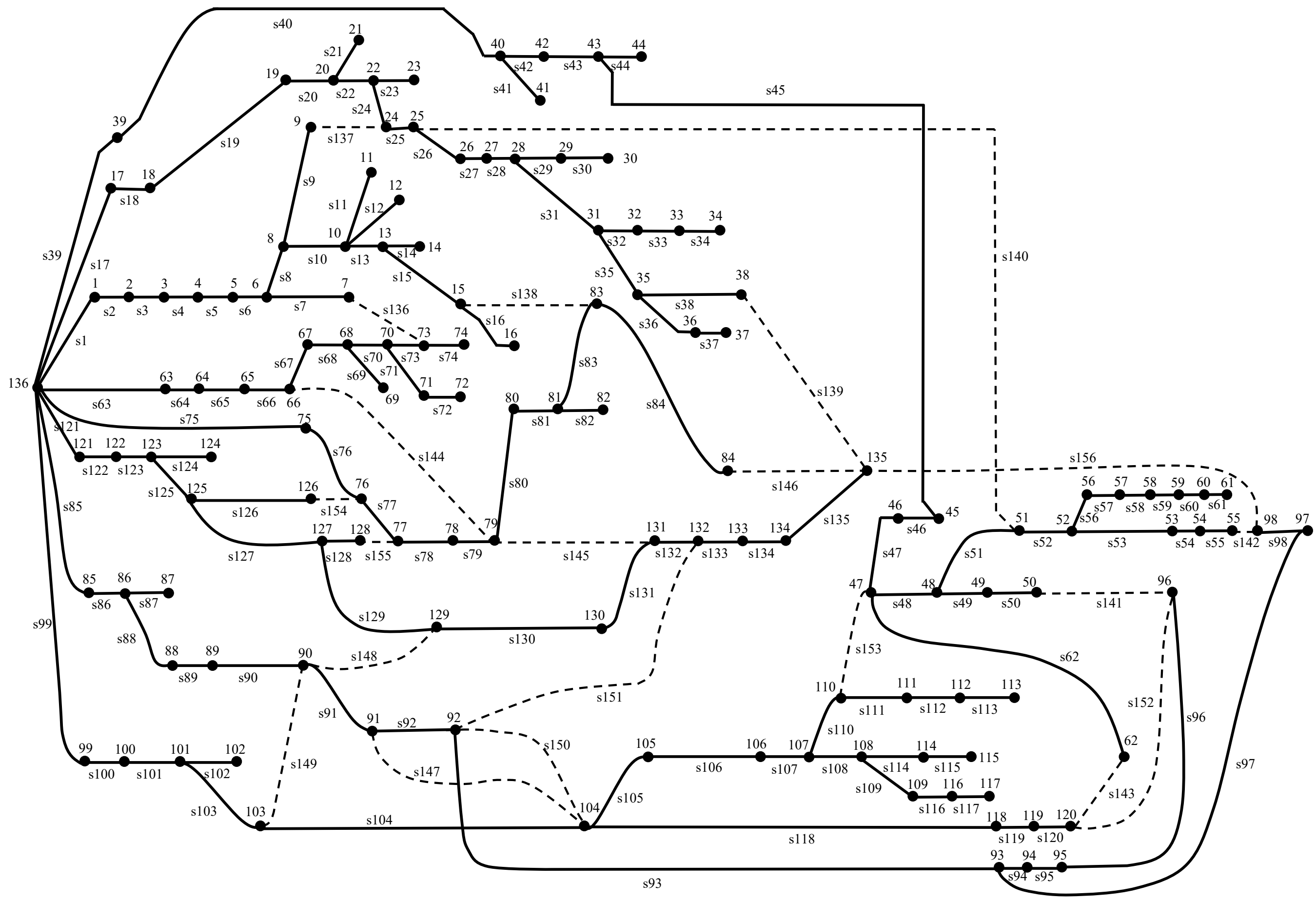

Source: Mantovani et al. (2000).

6.3.1 DNR using WOA algorithm

Figure 32 illustrates voltage profiles before and after DNR on a 136-bus system. As shown in Figure 32 and Table 14, the power loss was 320.37 kW and minimum voltage was 0.9290 per-unit in base case. The power loss was reduced to 283.63 kW, thus having a reduction of 11.47 % compared to the base case. The minimum voltage was improved to 0.9655 per-unit after DNR. The tie switches which were opened after DNR, were 7, 9, 51, 53, 84, 96, 106, 119, 128, 138, 139, 144, 145, 147, 148, 149, 150, 151, 152, 154, and 156.

Figure 32 – Voltage profiles for the 136-bus network before and after DNR obtained with the WOA

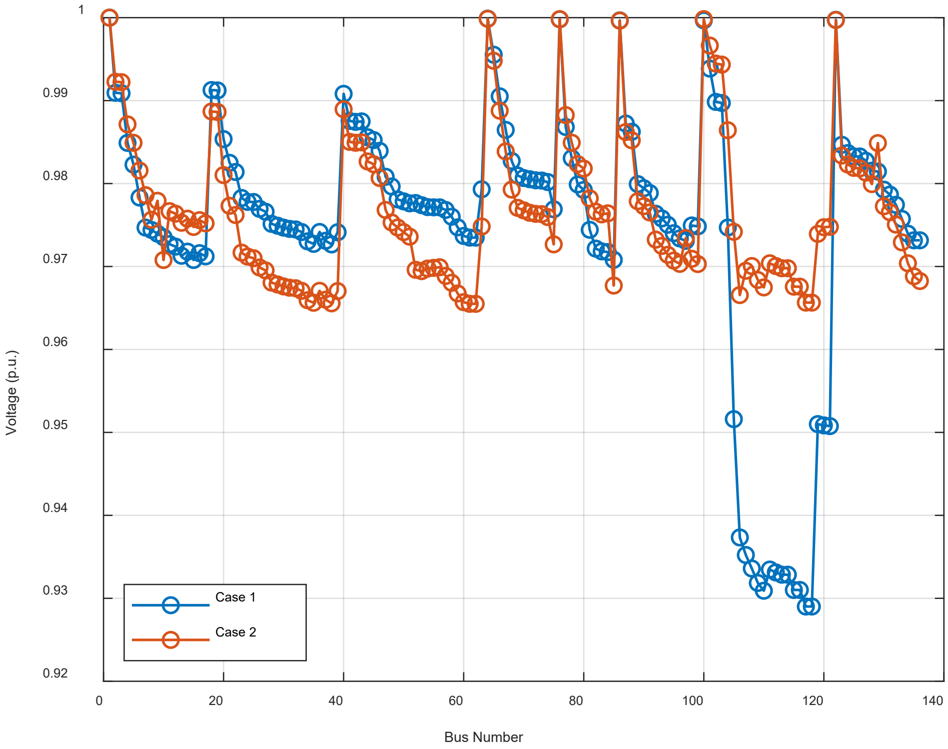

Source: Author's elaboration.

Table 14 – Simulation results for the 136-bus network before and after DNR using WOA

	Base Case	DNR
Active power loss:	320.37 kW	283.63 kW
Reactive power loss:	702.95 kVAr	618.11 kVAr
Active power loss reduction:	–	11.47 %
Tie switches:	136, 137, 138, 139, 140, 141, 142, 143, 144, 145, 146, 147, 148, 149, 150, 151, 152, 153, 154, 155, 156	7, 9, 51, 53, 84, 96, 106, 119, 128, 138, 139, 144, 145, 147, 148, 149, 150, 151, 152, 154, 156
Minimum voltage:	0.9290 p.u.	0.9655 p.u.

Source: Author's elaboration.

Figure 33 illustrates the convergence of the WOA after DNR along the iterations on a 136-bus system. In Figure 33, the fitness (optimal solution) was found around the 360th iteration.

Figure 33 – Convergence of WOA for the 136-bus network after DNR

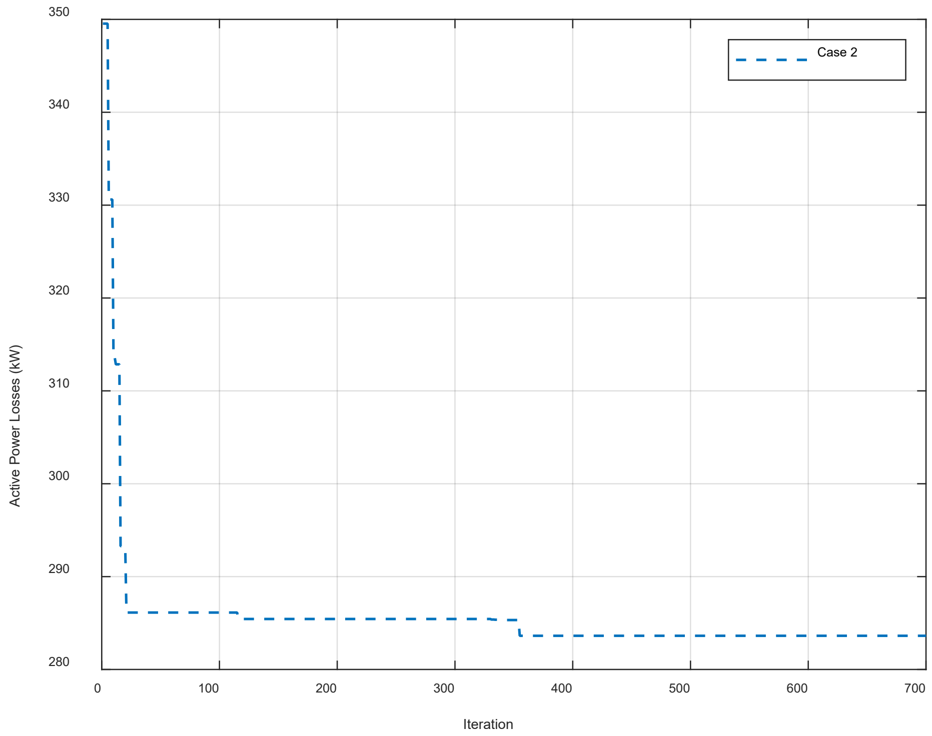

Source: Author's elaboration.

6.3.2 The optimal location and size of 3 DGs after DNR according to the result of Case 2 using WOA algorithm

The tie switches were determined after network reconfiguration in Case 2 and the opened tie switches were 7, 9, 51, 53, 84, 96, 106, 119, 128, 138, 139, 144, 145, 147, 148, 149, 150, 151, 152, 154, and 156. We assumed that these switches were open and then the optimal location and size of DG units were specified by WOA algorithm. We installed 3 DG units in this Case after DNR.

Figure 34 illustrates voltage profiles before and after 3 DGs and DNR on a 136-bus system. As shown in Figure 34 and Table 15, the power loss was 320.37 kW and minimum voltage was 0.9290 per-unit in base case. The power loss was reduced to 160.99 kW, thus having a reduction of 49.75 % compared to the base case. The minimum voltage was improved to 0.9666 per-unit after 3 DGs and DNR. Also, the

WOA method determines buses 25, 91, and 110 as the best places to connect the DGs, and the three DGs operate at the limit of 3017.0 kW, 1823.0 kW, and 2191.0 kW.

Figure 34 – Voltage profiles for the 136-bus network before and after 3 DGs and DNR obtained with the WOA

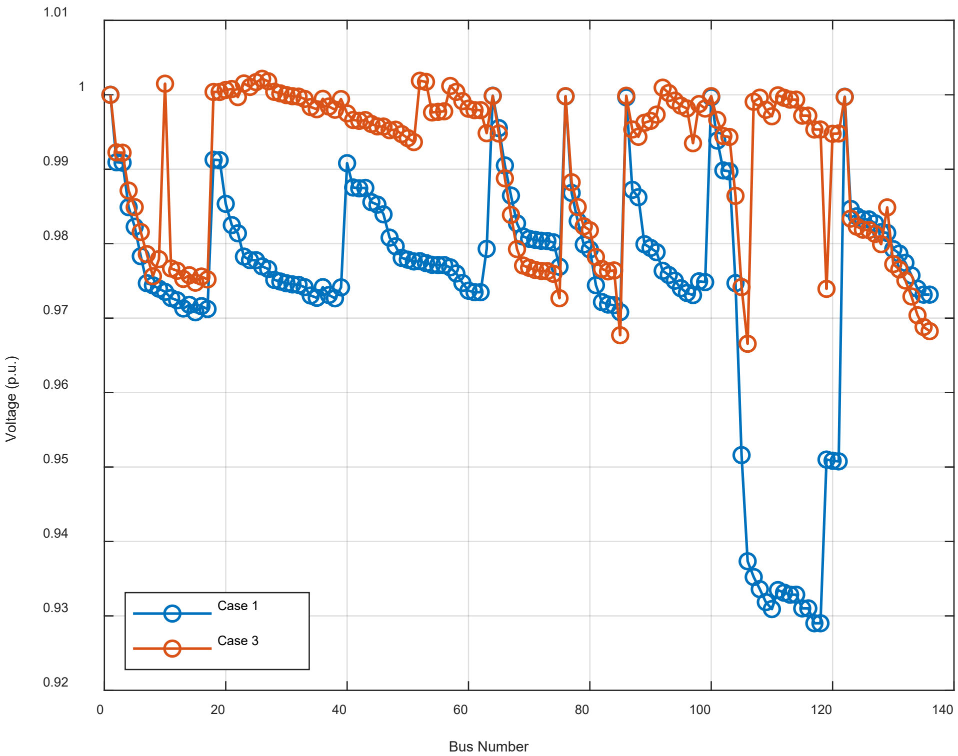

Source: Author's elaboration.

Table 15 – Simulation results for the 136-bus network before and after 3 DGs and DNR using WOA

	Base Case	3 DGs after DNR
Active power loss:	320.37 kW	160.99 kW
Reactive power loss:	702.95 kVAr	337.92 kVAr
Active power loss reduction:	_	49.75 %
Tie switches:	136, 137, 138, 139, 140, 141, 142, 143, 144, 145, 146, 147, 148, 149, 150, 151, 152, 153, 154, 155, 156	7, 9, 51, 53, 84, 96, 106, 119, 128, 138, 139, 144, 145, 147, 148, 149, 150, 151, 152, 154, 156
Optimal DG location	_	25, 91, 110

Optimal DG size P	_	3017.0, 1823.0, 2191.0 kW
Optimal DG size Q	_	1461.2, 882.9, 1061.2 kVAr
Minimum voltage:	0.9290 p.u.	0.9666 p.u.

Source: Author's elaboration.

Figure 35 illustrates the convergence of the WOA after 3 DGs and DNR along the iterations on a 136-bus system. In Figure 35, the fitness (optimal solution) was found around the 30th iteration.

Figure 35 – Convergence of WOA for the 136-bus network after 3 DGs and DNR

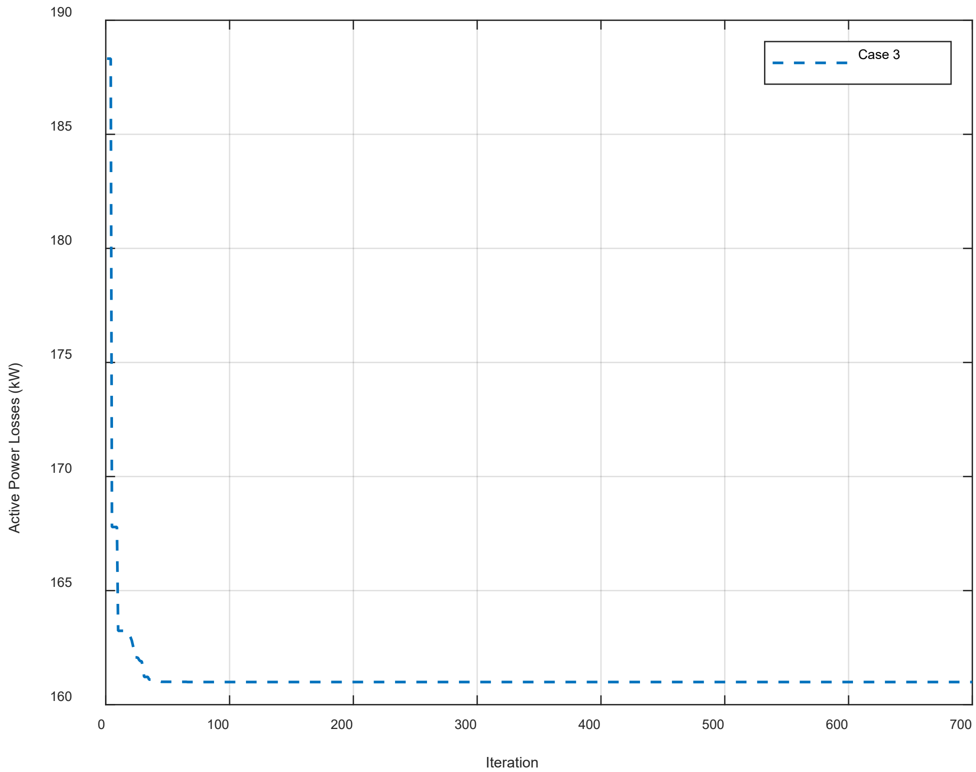

Source: Author's elaboration.

6.3.3 The simultaneous DNR and optimal location and size of 3 DGs using WOA algorithm

Figure 36 illustrates voltage profiles before and after simultaneous 3 DGs and DNR on a 136-bus system. As shown in Figure 36 and Table 16, the power loss was

320.37 kW and minimum voltage was 0.9290 per-unit in base case. The power loss was reduced to 102.10 kW, thus having a reduction of 68.13 % compared to the base case. The minimum voltage was improved to 0.9677 per-unit after simultaneous 3 DGs and DNR. Also, the optimal location and size of DGs were obtained by the WOA algorithm and 3 DG units with the capacity of 3052.0 kW, 3052.3 kW, and 3052.0 kW were allocated in buses 15, 47, and 135. The tie switches which were opened after simultaneous 3 DGs and DNR, were 9, 47, 54, 70, 79, 94, 106, 118, 126, 128, 132, 144, 145, 146, 147, 148, 149, 150, 151, 152, and 156.

Figure 36 – Voltage profiles for the 136-bus network before and after simultaneous 3 DGs and DNR obtained with the WOA

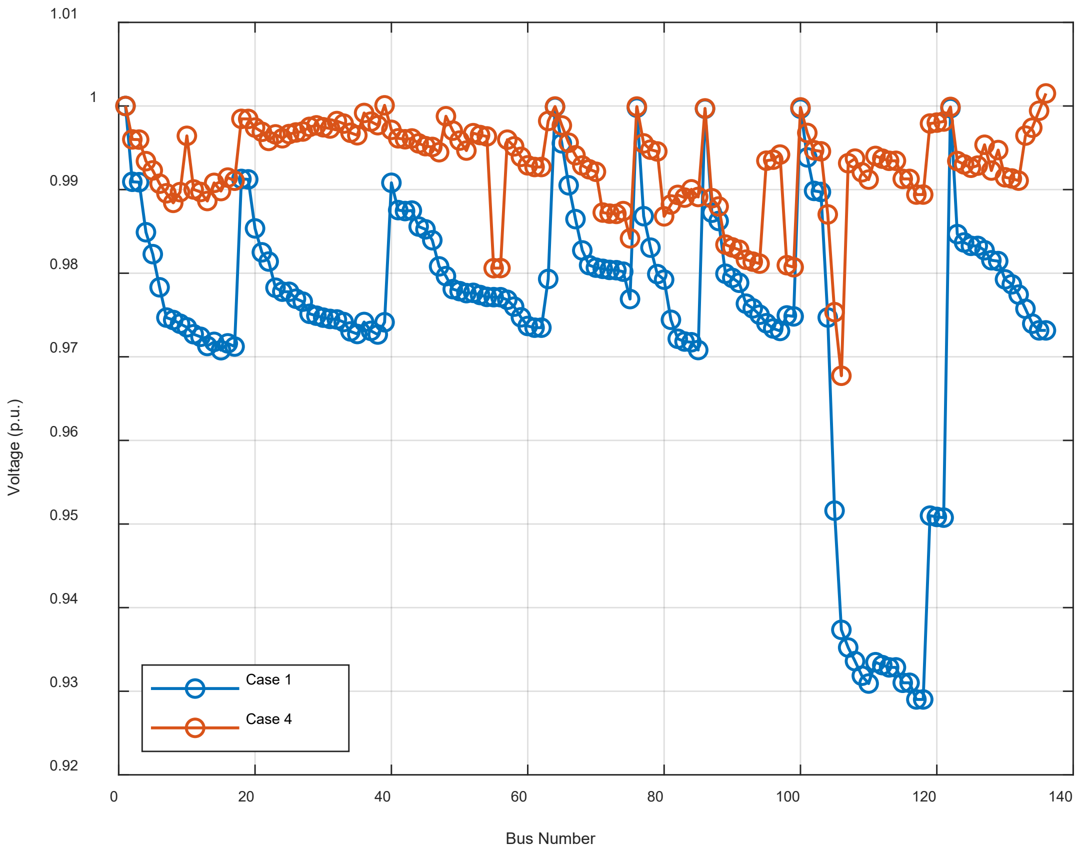

Source: Author's elaboration.

Table 16 – Simulation results for the 136-bus network before and after simultaneous 3 DGs and DNR using WOA

	Base Case	Simultaneous 3 DGs and DNR
Active power loss:	320.37 kW	102.10 kW
Reactive power loss:	702.95 kVAr	197.61 kVAr

Active power loss reduction:	_	68.13 %
Tie switches:	136, 137, 138, 139, 140, 141, 142, 143, 144, 145, 146, 147, 148, 149, 150, 151, 152, 153, 154, 155, 156	9, 47, 54, 70, 79, 94, 106, 118, 126, 128, 132, 144, 145, 146, 147, 148, 149, 150, 151, 152, 156
Optimal DG location	_	15, 47, 135
Optimal DG size P	_	3052.0, 3052.3, 3052.0 kW
Optimal DG size Q	_	1478.2, 1478.3, 1478.2 kVAr
Minimum voltage:	0.9290 p.u.	0.9677 p.u.

Source: Author's elaboration.

Figure 37 illustrates the convergence of the WOA after simultaneous 3 DGs and DNR along the iterations on a 136-bus system. In Figure 37, the fitness (optimal solution) was found around the 80th iteration.

Figure 37 – Convergence of WOA for the 136-bus network after simultaneous 3 DGs and DNR

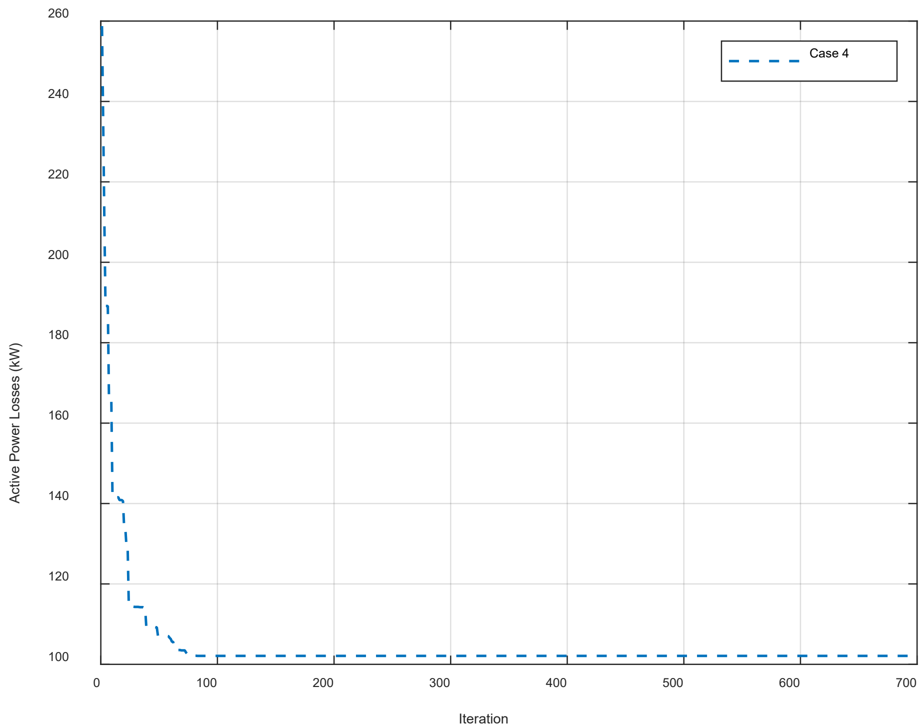

Source: Author's elaboration.

Table 17 shows that the power losses reduction percentage and voltage profile improvement for Case 4 is more significant than for the other cases. For all cases, the comparison of the voltage profiles is shown in Figure 38 and the comparison of the convergence characteristics of the proposed method is depicted in Figure 39.

The results of the WOA are compared with the solutions provided by other methods, as shown in Table 17. In Cases 2 and 3, the difference in the power losses and minimum voltage magnitude for the solution obtained by the proposed algorithm in comparison with other methods is very insignificant. The result of Case 4 obtained by WOA is more desirable in terms of power losses reduction when compared to SFS, but the obtained values are almost similar in terms of minimum voltage magnitude. The proposed WOA further optimizes the results of Cases 2 to 4 and provides better results for the 136-bus network.

Figure 38 – Comparison of voltage profiles for the 136-bus network obtained with the WOA

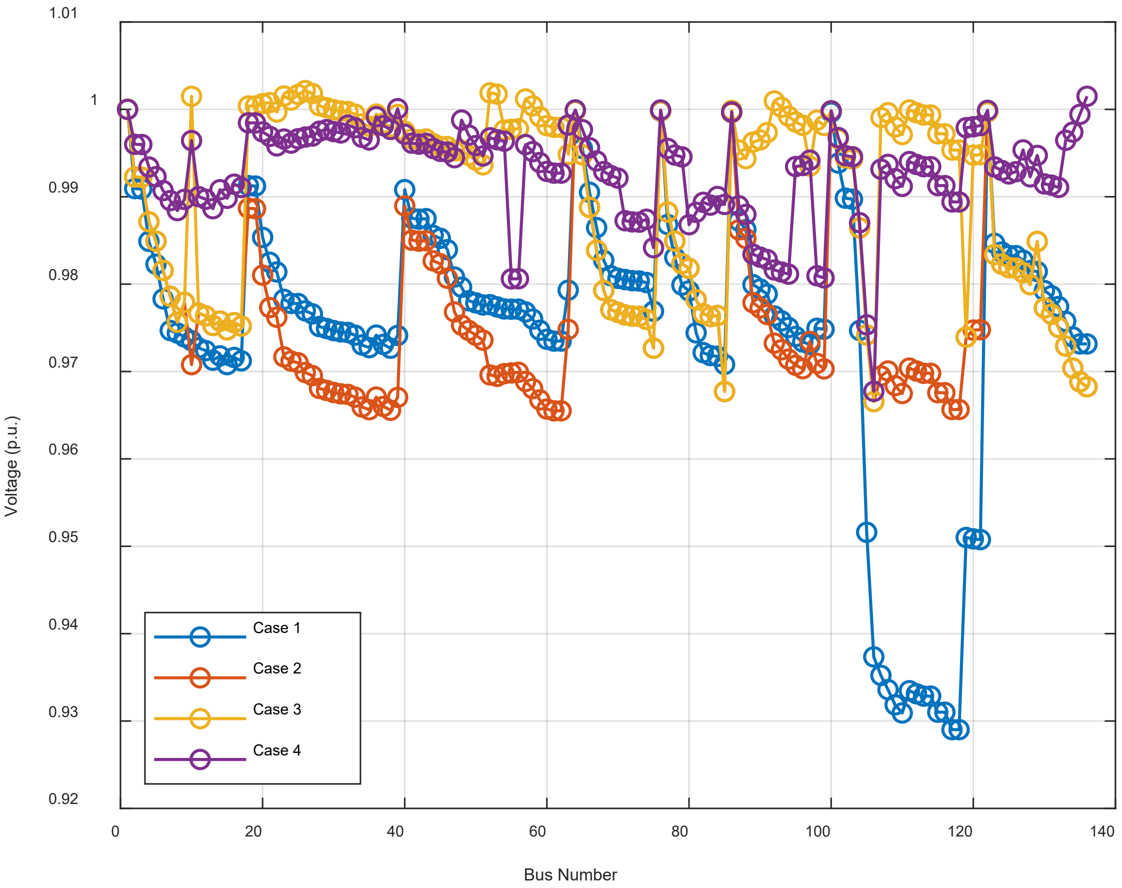

Source: Author's elaboration.

Figure 39 – Comparison of convergence of the WOA for the 136-bus network

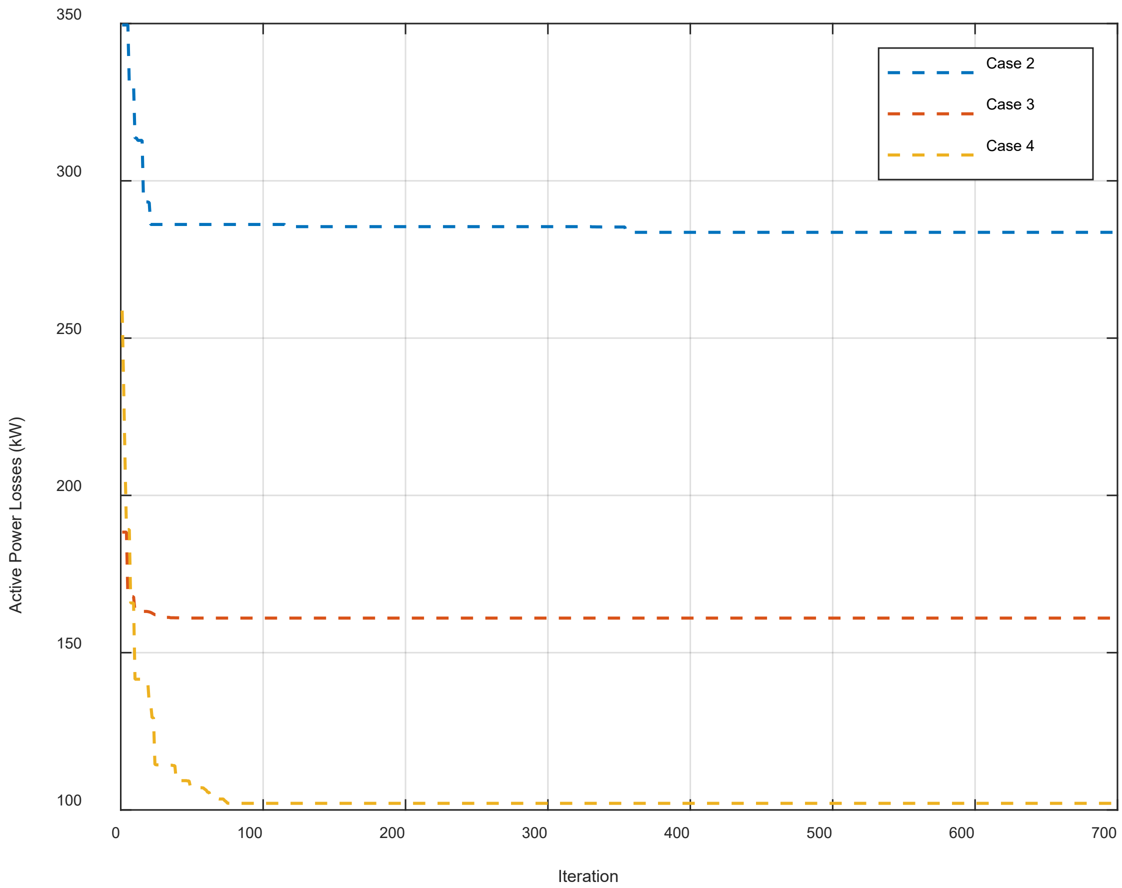

Source: Author's elaboration.

Table 17 – Summary of the results for the 136-bus network

Case	Item	UVDA (BAYAT et al., 2016)	SFS (TRAN et al., 2020)	AACO (SWARNKAR et al., 2011)	WOA
1	Tie switches	–	–	–	136-137-138-139-140-141-142-143-144-145-146-147-148-149-150-151-152-153-154-155-156
	P_L (kW)	–	–	–	320.37
	Q_L (kVAr)	–	–	–	702.95
	V_{min} (p.u.)	–	–	–	0.9290
	Time (s)	–	–	–	1.3

2	**Tie switches**	7-35-51-90-96-106-118-126-135-137-138-141-142-144-145-146-147-148-150-151-155	7-58-62-84-90-98-106-118-126-128-135-137-138-139-141-144-145-147-148-150-151	7-35- 51-90-95-106-118-126-135-137-138-141-142-144-145-146-147-148-150-151-155	7-9-51-53-84-96-106-119-128-138-139-144-145-147-148-149-150-151-152-154-156
	P_L **(kW)**	280.18	278.9	279.75	283.63
	Q_L **(kVAr)**	–	–	–	618.11
	P_L **reduction (%)**	12.55	13.03	12.68	11.47
	$V_{\min}$ **(p.u.)**	0.9589	0.9616	0.9602	0.9655
	Time (s)	–	–	–	76525.7
3	**Tie switches**	–	7-58-62-84-90-98-106-118-126-128-135-137-138-139-141-144-145-147-148-150-151	–	7-9-51-53-84-96-106-119-128-138-139-144-145-147-148-149-150-151-152-154-156
	P_{DG} **(kW)/(Bus)**	– – –	2490.7/(28) 2233.4/(48) 1844.2/(106)	– – –	3017.0/(25) 1823.0/(91) 2191.0/(110)
	Q_{DG} **(kVAr)**	– – –	– – –	– – –	1461.2 882.9 1061.2
	P_L **(kW)**	–	160.45	–	160.99
	Q_L **(kVAr)**	–	–	–	337.92
	P_L **reduction (%)**	–	49.97	–	49.75
	$V_{\min}$ **(p.u.)**	–	0.9728	–	0.9666
	Time (s)	–	–	–	60924.7
4	**Tie switches**	–	35-61-73-81-89-92-95-98-104-110-130-135-137-141-144-145-146-	–	9-47-54-70-79-94-106-118-126-128-132-144-145-146-147-148-149-

			148-150-154-155		150-151-152-156
	P_{DG} (kW)/(Bus)	– – –	3445.3/(14) 4690.2/(48) 3030.5/(106)	– – –	3052.0/(15) 3052.3/(47) 3052.0/(135)
	Q_{DG} (kVAr)	– – –	– – –	– – –	1478.2 1478.3 1478.2
	P_L (kW)	–	118.73	–	102.10
	Q_L (kVAr)	–	–	–	197.61
	P_L reduction (%)	–	62.98	–	68.13
	$V_{\min}$ (p.u.)	–	0.9662	–	0.9677
	Time (s)	–	–	–	95566.8

Source: Author's elaboration.

6.4 415-BUS NETWORK

The 415-bus system is presented in Bernal-Agustin (1998). It has 414 load buses, one substation bus and 473 feeders. The voltage at the substation bus is 10.00 kV and the base power of the system is 100 MVA. The total active and reactive power demands are 27372.40 kW and 13237.00 kVAr, respectively. The maximum size of each DG unit is 4562.06 kW.

Figure 40 illustrates the 415-bus system with 59 tie switches 1, 5, 15, 16, 26, 31, 53, 54, 55, 75, 82, 94, 96, 97, 106, 107, 119, 136, 138, 154, 155, 156, 168, 169, 177, 179, 194, 195, 201, 207, 211, 214, 219, 241, 256, 258, 282, 297, 302, 314, 321, 354, 359, 362, 364, 385, 388, 395, 396, 404, 407, 423, 424, 426, 431, 436, 445, 446 and 449 that are initially open and illustrated by dashed lines, while the basic loops of the network are presented in Table 5. The complete data of this system are presented in Appendix D.

Figure 40 – Topology of the 415-bus network

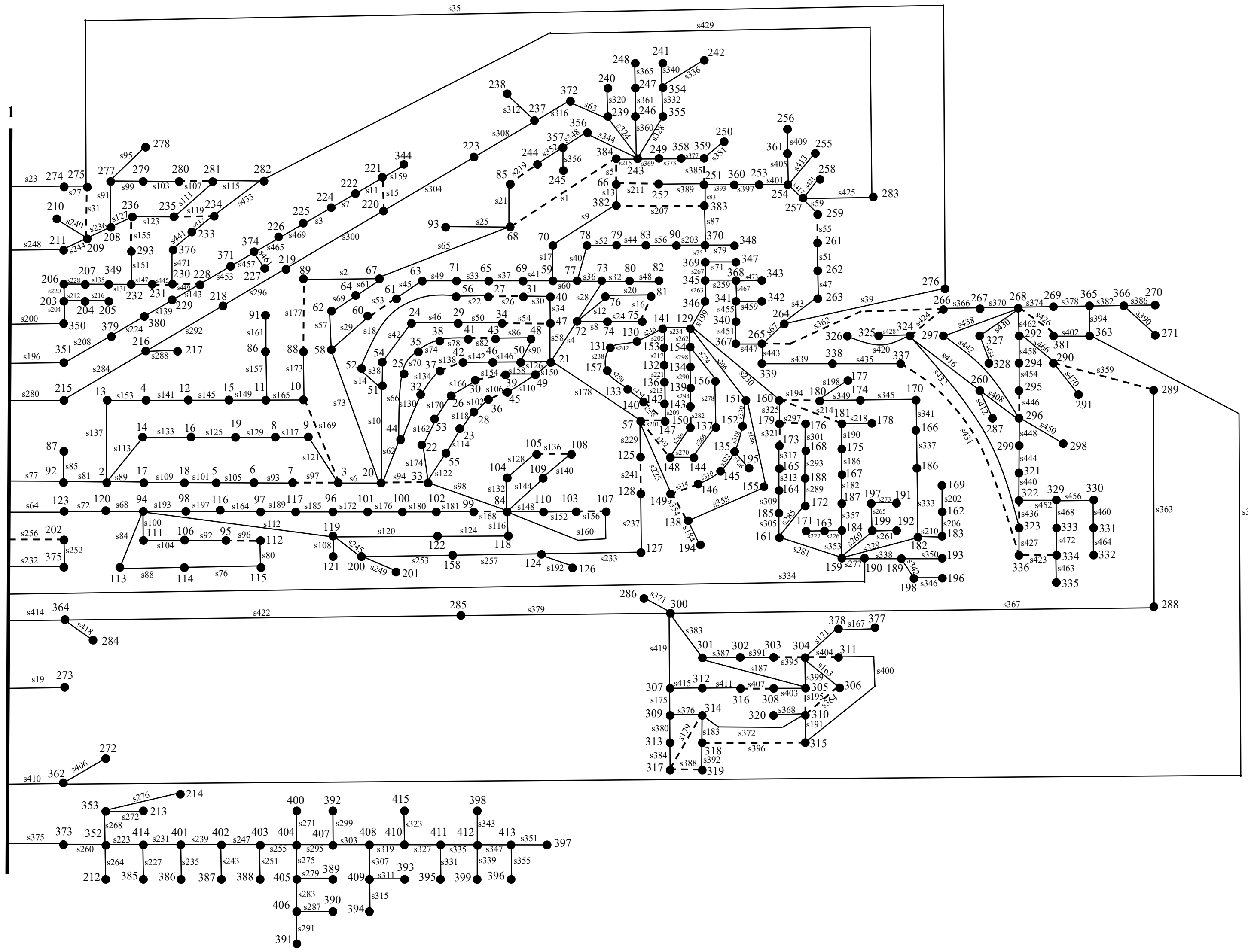

Source: Author's elaboration.

6.4.1 DNR using WOA algorithm

Figure 41 illustrates voltage profiles before and after DNR on a 415-bus system. As shown in Figure 41 and Table 18, the power loss was 708.94 kW and minimum voltage was 0.9300 per-unit in base case. The power loss was reduced to 652.72 kW, thus having a reduction of 7.93 % compared to the base case. The minimum voltage was improved to 0.9400 per-unit after DNR. The tie switches which were opened after DNR, were 5, 7, 16, 18, 21, 31, 46, 47, 53, 60, 61, 78, 87, 93, 94, 96, 99, 111, 131, 136, 146, 150, 154, 155, 156, 168, 169, 177, 178, 179, 188, 199, 209, 211, 242, 256, 266, 297, 298, 314, 325, 357, 359, 362, 364, 372, 377, 387, 388, 402, 403, 404, 408, 419, 432, 435, 437, 454, and 472.

Figure 41 – Voltage profiles for the 415-bus network before and after DNR obtained with the WOA

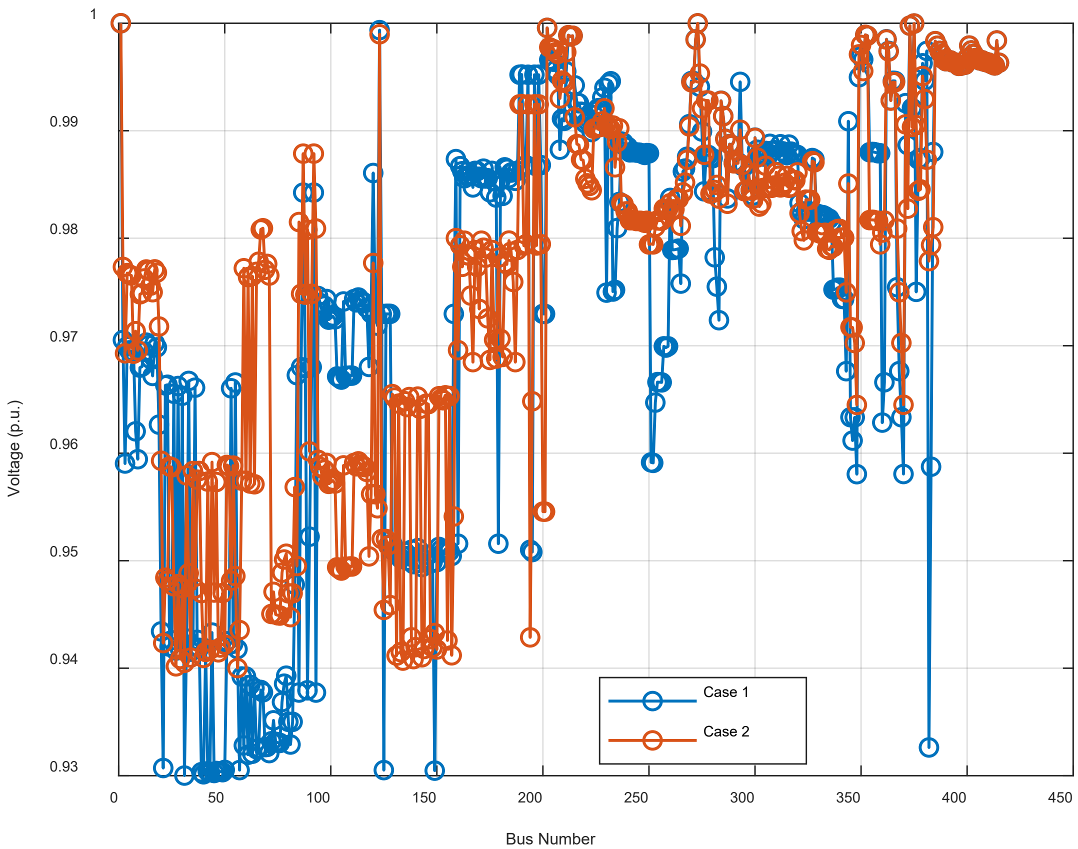

Source: Author's elaboration.

Table 18 – Simulation results for the 415-bus network before and after DNR using WOA

	Base Case	DNR
Active power loss:	708.94 kW	652.72 kW
Reactive power loss:	538.48 kVAr	551.13 kVAr
Active power loss reduction:	–	7.93 %
Tie switches:	1, 5, 15, 16, 26, 31, 53, 54, 55, 75, 82, 94, 96, 97, 106, 107, 119, 136, 138, 154, 155, 156, 168, 169, 177, 179, 194, 195, 201, 207, 211, 214, 219, 241, 256, 258, 282, 297, 302,	5, 7, 16, 18, 21, 31, 46, 47, 53, 60, 61, 78, 87, 93, 94, 96, 99, 111, 131, 136, 146, 150, 154, 155, 156, 168, 169, 177, 178, 179, 188, 199, 209, 211, 242, 256, 266, 297, 298, 314,

	314, 321, 354, 359, 362, 364, 385, 388, 395, 396, 404, 407, 423, 424, 426, 431, 436, 445, 446, 449	325, 357, 359, 362, 364, 372, 377, 387, 388, 402, 403, 404, 408, 419, 432, 435, 437, 454, 472
Minimum voltage:	0.9300 p.u.	0.9400 p.u.

Source: Author's elaboration.

Figure 42 illustrates the convergence of the WOA after DNR along the iterations on a 415-bus system. In Figure 42, the fitness (optimal solution) was found around the 150th iteration.

Figure 42 – Convergence of WOA for the 415-bus network after DNR

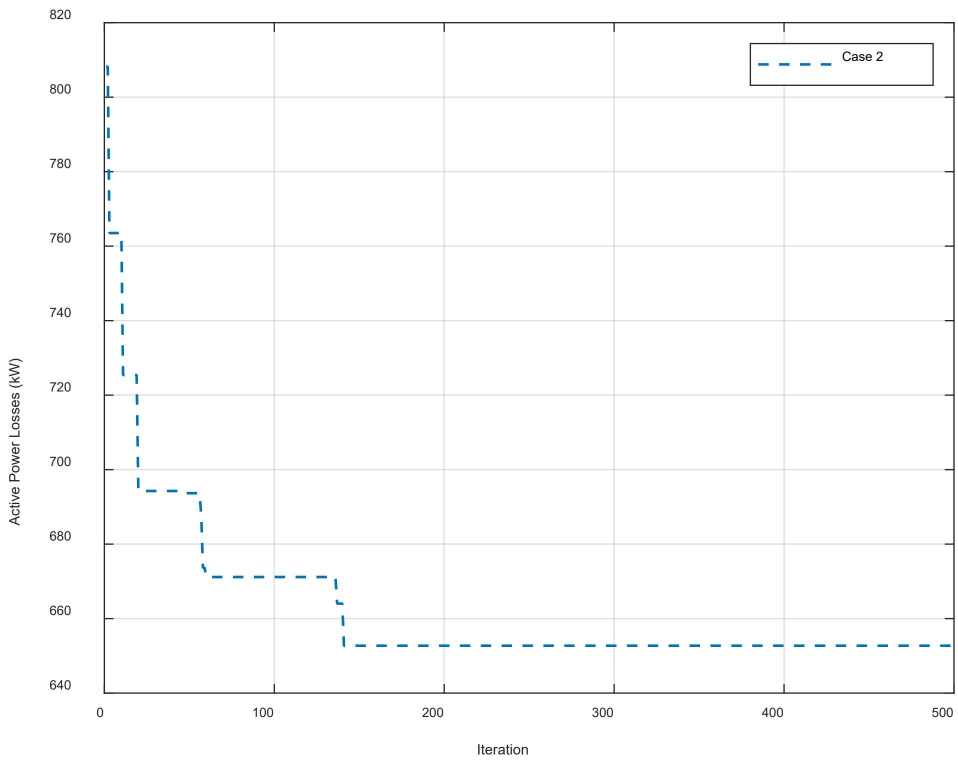

Source: Author's elaboration.

6.4.2 The optimal location and size of 3 DGs after DNR according to the result of Case 2 using WOA algorithm

The tie switches were determined after network reconfiguration in Case 2 and the opened tie switches were 5, 7, 16, 18, 21, 31, 46, 47, 53, 60, 61, 78, 87, 93, 94, 96, 99, 111, 131, 136, 146, 150, 154, 155, 156, 168, 169, 177, 178, 179, 188, 199, 209, 211, 242, 256, 266, 297, 298, 314, 325, 357, 359, 362, 364, 372, 377, 387, 388, 402, 403, 404, 408, 419, 432, 435, 437, 454, and 472. We assumed that these switches were open and then the optimal location and size of DG units were specified by WOA algorithm. We installed 3 DG units in this Case after DNR.

Figure 43 illustrates voltage profiles before and after 3 DGs and DNR on a 415-bus system. As shown in Figure 43 and Table 19, the power loss was 708.94 kW and minimum voltage was 0.9300 per-unit in base case. The power loss was reduced to 317.18 kW, thus having a reduction of 55.26 % compared to the base case. The minimum voltage was improved to 0.9641 per-unit after 3 DGs and DNR. Also, the WOA method determines buses 24, 72, and 122 as the best places to connect the DGs, and the three DGs operate at the limit of 1260.0 kW, 2361.0 kW, and 3633.0 kW.

Figure 43 – Voltage profiles for the 415-bus network before and after 3 DGs and DNR obtained with the WOA

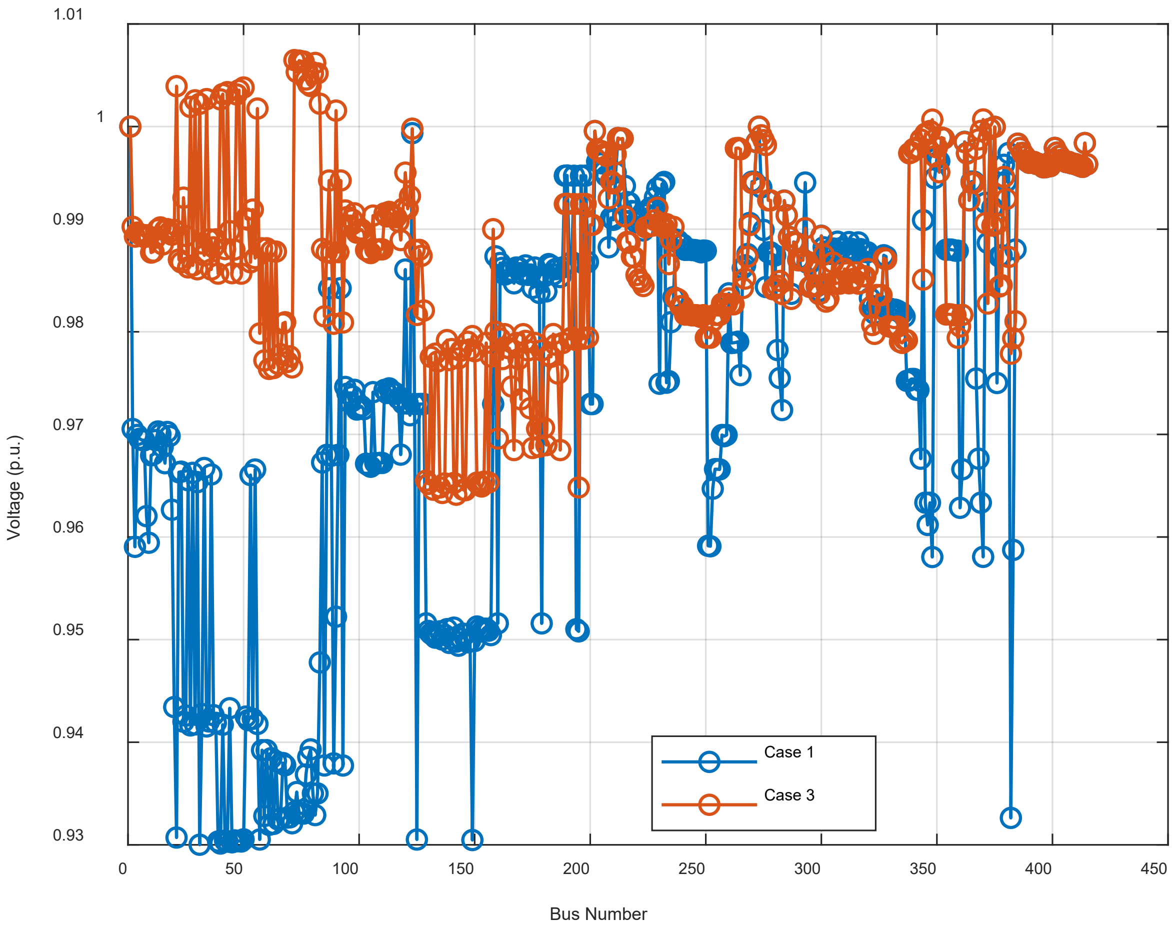

Source: Author's elaboration.

Table 19 – Simulation results for the 415-bus network before and after 3 DGs and DNR using WOA

	Base Case	3 DGs after DNR
Active power loss:	708.94 kW	317.18 kW
Reactive power loss:	538.48 kVAr	264.26 kVAr
Active power loss reduction:	_	55.26 %
Tie switches:	1, 5, 15, 16, 26, 31, 53, 54, 55, 75, 82, 94, 96, 97, 106, 107, 119, 136, 138, 154, 155, 156, 168, 169, 177, 179, 194, 195, 201, 207, 211, 214, 219, 241, 256, 258, 282, 297, 302, 314, 321, 354, 359, 362, 364, 385, 388, 395, 396, 404, 407, 423, 424, 426, 431, 436, 445, 446, 449	5, 7, 16, 18, 21, 31, 46, 47, 53, 60, 61, 78, 87, 93, 94, 96, 99, 111, 131, 136, 146, 150, 154, 155, 156, 168, 169, 177, 178, 179, 188, 199, 209, 211, 242, 256, 266, 297, 298, 314, 325, 357, 359, 362, 364, 372, 377, 387, 388, 402, 403, 404, 408, 419, 432, 435, 437, 454, 472
Optimal DG location	_	24, 72, 122
Optimal DG size P	_	1260.0, 2361.0, 3633.0 kW
Optimal DG size Q	_	610.3, 1143.5, 1759.5 kVAr
Minimum voltage:	0.9300 p.u.	0.9641 p.u.

Source: Author's elaboration.

Figure 44 illustrates the convergence of the WOA after 3 DGs and DNR along the iterations on a 415-bus system. In Figure 44, the fitness (optimal solution) was found in the 2^{th} iteration.

Figure 44 – Convergence of WOA for the 415-bus network after 3 DGs and DNR

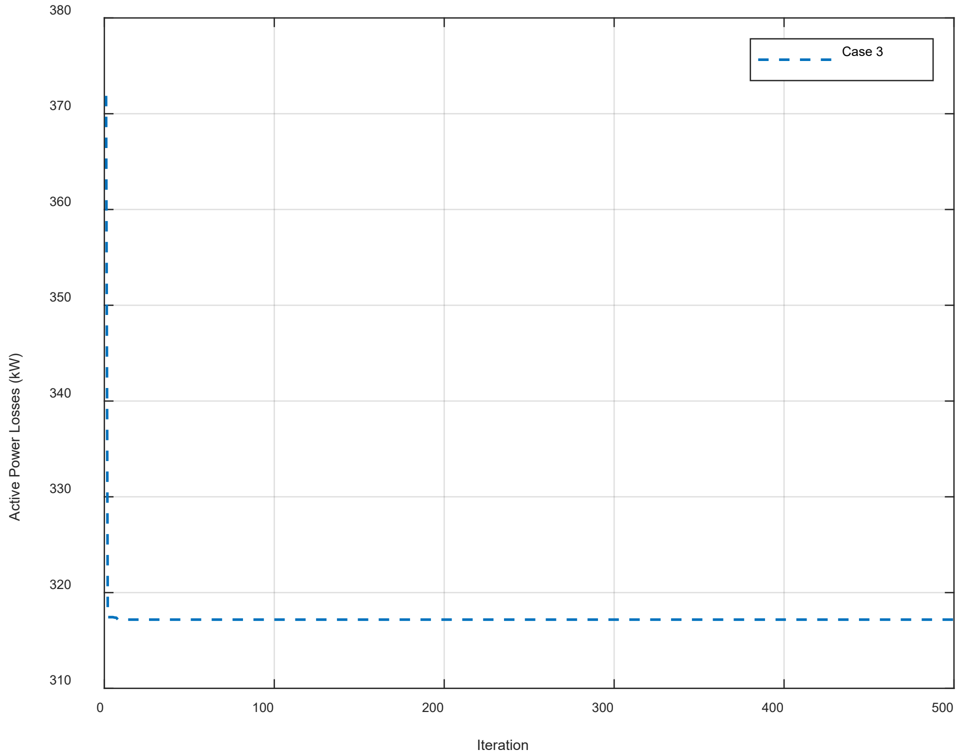

Source: Author's elaboration.

6.4.3 The simultaneous DNR and optimal location and size of 3 DGs using WOA algorithm

Figure 45 illustrates voltage profiles before and after simultaneous 3 DGs and DNR on a 415-bus system. As shown in Figure 45 and Table 20, the power loss was 708.94 kW and minimum voltage was 0.9300 per-unit in base case. The power loss was reduced to 290.57 kW, thus having a reduction of 59.01 % compared to the base case. The minimum voltage was improved to 0.9670 per-unit after simultaneous 3 DGs and DNR. Also, the optimal location and size of DGs were obtained by the WOA algorithm and 3 DG units with the capacity of 1328.0 kW, 2762.0 kW, and 4368.0 kW were allocated in buses 45, 47, and 326. The tie switches which were opened after simultaneous 3 DGs and DNR, were 2, 4, 5, 14, 15, 24, 29, 31, 43, 50, 60, 69, 70, 87, 93, 94, 100, 111, 115, 132, 138, 148, 150, 155, 162, 169, 179, 180, 183, 199, 214, 221, 242, 252, 266, 294, 301, 318, 325, 344, 358, 367, 370, 380, 385, 389, 391, 399, 400, 415, 419, 426, 436, 441, 442, 443, 445, 458, and 468.

Figure 45 – Voltage profiles for the 415-bus network before and after simultaneous 3 DGs and DNR obtained with the WOA

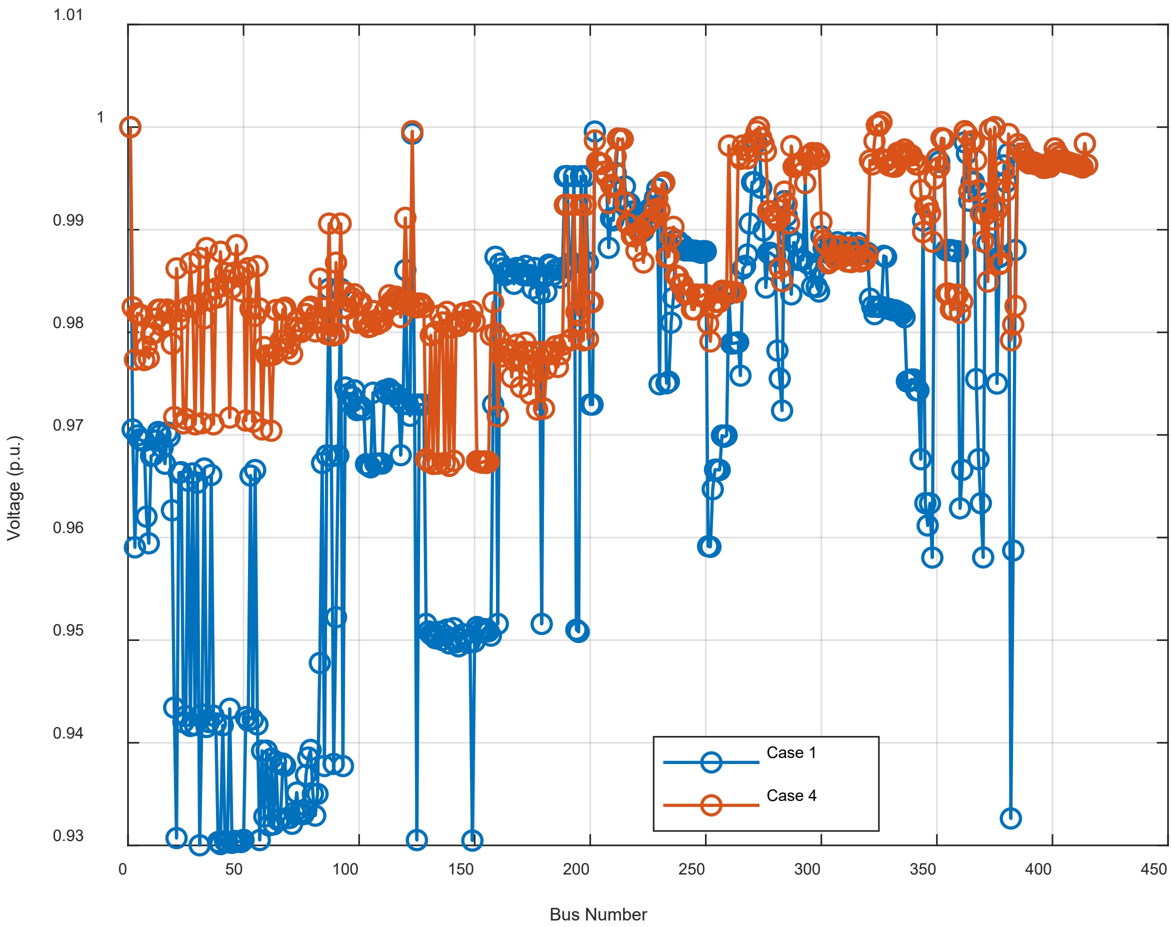

Source: Author's elaboration.

Table 20 – Simulation results for the 415-bus network before and after simultaneous 3 DGs and DNR using WOA

	Base Case	Simultaneous 3 DGs and DNR
Active power loss:	708.94 kW	290.57 kW
Reactive power loss:	538.48 kVAr	236.79 kVAr
Active power loss reduction:	–	59.01 %
Tie switches:	1, 5, 15, 16, 26, 31, 53, 54, 55, 75, 82, 94, 96, 97, 106, 107, 119, 136, 138, 154, 155, 156,	2, 4, 5, 14, 15, 24, 29, 31, 43, 50, 60, 69, 70, 87, 93, 94, 100, 111, 115, 132, 138, 148, 150, 155, 162, 169,

	168, 169, 177, 179, 194, 195, 201, 207, 211, 214, 219, 241, 256, 258, 282, 297, 302, 314, 321, 354, 359, 362, 364, 385, 388, 395, 396, 404, 407, 423, 424, 426, 431, 436, 445, 446, 449	179, 180, 183, 199, 214, 221, 242, 252, 266, 294, 301, 318, 325, 344, 358, 367, 370, 380, 385, 389, 391, 399, 400, 415, 419, 426, 436, 441, 442, 443, 445, 458, 468
Optimal DG location	_	45, 47, 326
Optimal DG size P	_	1328.0, 2762.0, 4368.0 kW
Optimal DG size Q	_	643.2, 1337.7, 2115.5 kVAr
Minimum voltage:	0.9300 p.u.	0.9670 p.u.

Source: Author's elaboration.

Figure 46 illustrates the convergence of the WOA after simultaneous 3 DGs and DNR along the iterations on a 415-bus system. In Figure 46, the fitness (optimal solution) was found around the 200th iteration.

Figure 46 – Convergence of WOA for the 415-bus network after simultaneous 3 DGs and DNR

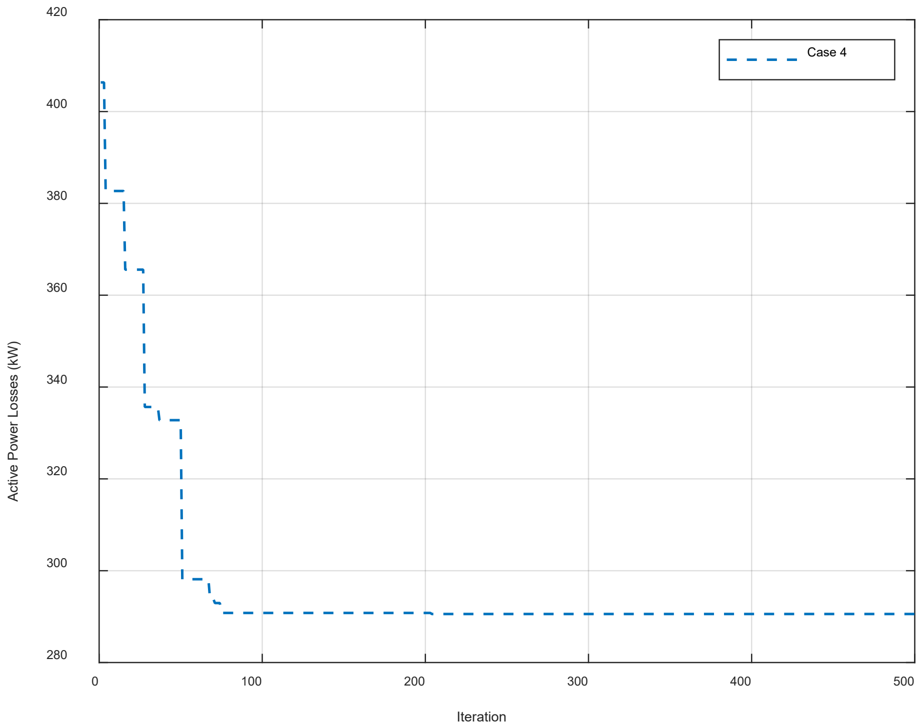

Source: Author's elaboration.

Table 21 shows that the power losses reduction percentage and voltage profile improvement for Case 4 is more significant than the other cases. For all cases, the comparison of the voltage profiles is shown in Figure 47 and the comparison of the convergence characteristics of the proposed method is depicted in Figure 48.

Figure 47 – Comparison of voltage profiles for the 415-bus network obtained with the WOA

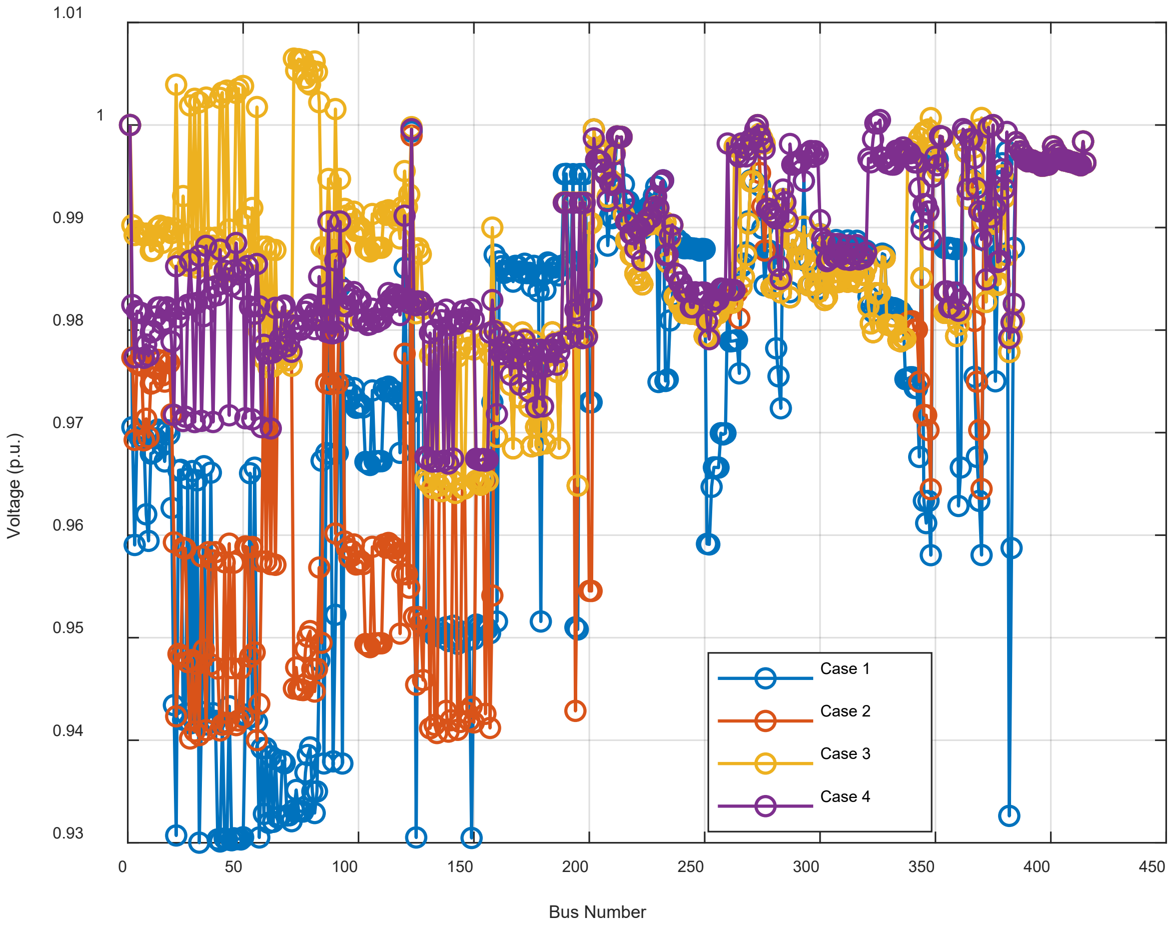

Source: Author's elaboration.

Figure 48 – Comparison of convergence of the WOA for the 415-bus network

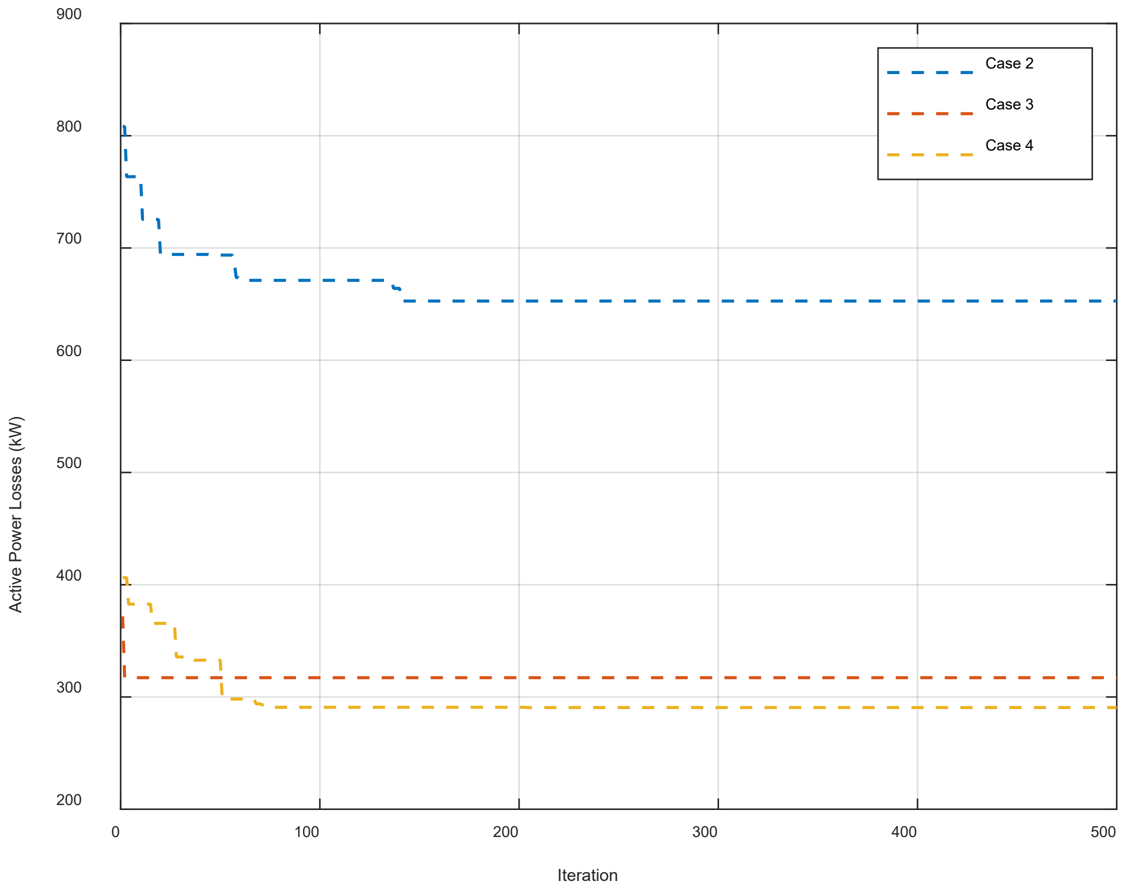

Source: Author's elaboration.

Table 21 – Summary of the results for the 415-bus network obtained with the WOA

Item	Case 1	Case 2	Case 3	Case 4
Tie switches	1-5-15-16-26-31-53-54-55-75-82-94-96-97-106-107-119-136-138-154-155-156-168-169-177-179-194-195-201-207-211-214-219-241-256-258-282-297-302-314-321-354-359-362-364-385-388-395-396-404-407-423-424-426-431-436-445-446-449	5-7-16-18-21-31-46-47-53-60-61-78-87-93-94-96-99-111-131-136-146-150-154-155-156-168-169-177-178-179-188-199-209-211-242-256-266-297-298-314-325-357-359-362-364-372-377-387-388-402-403-404-408-419-432-435-437-454-472	5-7-16-18-21-31-46-47-53-60-61-78-87-93-94-96-99-111-131-136-146-150-154-155-156-168-169-177-178-179-188-199-209-211-242-256-266-297-298-314-325-357-359-362-364-372-377-387-388-402-403-404-408-419-432-435-437-454-472	2-4-5-14-15-24-29-31-43-50-60-69-70-87-93-94-100-111-115-132-138-148-150-155-162-169-179-180-183-199-214-221-242-252-266-294-301-318-325-344-358-367-370-380-385-389-391-399-400-415-419-426-436-441-442-443-445-458-468

P_{DG} (kW)/(Bus)	– – –	– – –	1260.0/(24) 2361.0/(72) 3633.0/(122)	1328.0/(45) 2762.0/(47) 4368.0/(326)
Q_{DG} (kVAr)	– – –	– – –	610.3 1143.5 1759.5	643.2 1337.7 2115.5
P_L (kW)	708.94	652.72	317.18	290.57
Q_L (kVAr)	538.48	551.13	264.26	236.79
P_L reduction (%)	–	7.93	55.26	59.01
$V_{\min}$ (p.u.)	0.9300	0.9400	0.9641	0.9670
Time (s)	21.3	1138423.4	863823.5	1472268.9

Source: Author's elaboration.

7 CONCLUSION

In this study, the whale optimization algorithm (WOA) was able to simultaneously reconfigure the distribution network and optimize the location and size of distributed generators (DGs).

Reducing active power losses in distribution networks was the primary purpose, which improved the voltage profile. There are four scenarios such as base case without DNR and DGs, only DNR, the allocation of DGs after DNR, and simultaneous DNR and the allocation of DGs. The WOA was an efficient and robust metaheuristic procedure that rapidly converged in all considered cases.

The proposed algorithm was tested using the 33-bus, 69-bus, 136-bus, and 415-bus networks. The best active power loss reduction acquired with the WOA was 84.62 %, 91.34 %, 68.13 %, and 59.01 % in the 33-bus, 69-bus, 136-bus, and 415-bus networks, respectively, corresponding to Case 4 (simultaneous DNR and the allocation of DGs). The superiority and efficiency of the WOA method in all cases, when compared to other methods, was evident. Therefore, the WOA is an effective method for performing network reconfiguration with the simultaneous allocation of DGs.

Future research could be the integration of a battery energy storage system considering grid reliability, annual operation cost, and voltage deviation. It could also be an issue of protection and power quality in the reconfiguration of distribution systems, the improvement of the WOA algorithm, and the use of the photovoltaic systems and wind turbines.

REFERENCES

ASSOCIAÇÃO BRASILEIRA DE DISTRIBUIDORES DE ENERGIA ELÉTRICA - ABRADEE*:* Distribuidoras e Origem de Capital. Brasília, 2012. Availabe: https://www.abradee.org.br/setor-de-distribuicao/distribuidoras-e%20origem-de-capital/. Accessed on: 02 June 2017.

INSTITUTO ABRADEE DE ENERGIA - iABRADEE*:* Entenda a Indústria de Energia Elétrica - Módulo 5: Distribuição. Brasília, 2013a. Availabe: http://www.abradee.com.br/escolha-abradee-para voce/cartilha/category/8-livro-5. Accessed on: 02 June 2017.

Entenda a Indústria de Energia Elétrica - Módulo 6*:* O Mercado de Energia Elétrica. Brasília, 2013b. Availabe: https://www.abradee.org.br/escolha-abradee-para-voce/%20cartilha/category/9-livro-6. Accessed on: 02 June 2017.

Furto e Fraude de Energia. Brasília, 2015. Availabe: https://www.abradee.org.br/%20setor-de-distribuicao/perdas/furto-e-fraude-de-energia. Accessed on: 15 May 2017.

AGUERO, J. R. Improving the efficiency of power distribution systems through technical and non-technical losses reduction. *PES T&D 2012*, Orlando, p. 1-8, 2012. ISSN: 2160-8555.

ALAM, M. N.; DAS, B.; PANT, V. Protection scheme for reconfigurable radial distribution networks in presence of distributed generation. *Electric Power Systems Research*, Amsterdam, 106973, 2020.

ALREFAEI, M. H.; DIABAT, A. H. A simulated annealing technique for multi-objective simulation optimization. *Applied Mathematics and Computation*, New York, v. 215, n. 8, p. 3029-3035, 2009. DOI: https://doi.org/10.1016/j.amc.2009.09.051. ISSN: 0096-3003.

ARUN, M.; ARAVINDHABABU, P. A new reconfiguration scheme for voltage stability enhancement of radial distribution systems. *Energy Conversion and Management*, Amsterdam, v. 50, n. 9, p. 2148-2151, 2009. ISSN: 0196-8904.

AZIZIVAHED, A.; NARIMANI, H.; NADERI, E.; FATHI, M.; NARIMANI, M. R. A hybrid evolutionary algorithm for secure multi-objective distribution feeder reconfiguration. *Energy*, Oxford, v. 138, p. 355-373, 2017.

BABU, P. R.; TIWARI, R. K. RECONFIGURATION OF A RADIAL DISTRIBUTION NETWORK THROUGH WHALE OPTIMIZATION ALGORITHM. *ARPN Journal of Engineering and Applied Sciences*, Lahore, v. 14, n. 14, p. 2556-2562, July 2019. ISSN: 1819-6608.

BALAMURUGAN, K.; SRINIVASAN, D. Review of power flow studies on distribution network with distributed generation. In: *2011 IEEE Ninth International Conference on Power Electronics and Drive Systems*. Singapore, 2011, 411-417.

BARAN, M.; WU, F. F. Network reconfiguration in distribution systems for loss reduction and load balancing. *IEEE Transactions on Power Delivery*, New York, v. 4, n. 2, p. 1401-1407, Apr 1989a. ISSN: 0885-8977.

BARAN, M.; WU, F. F. Optimal sizing of capacitors placed on a radial distribution system. *IEEE Transactions on Power Delivery*, New York, v. 4, n. 1, p. 735-743, Jan 1989b. ISSN: 0885-8977.

BARNWAL, A. K.; YADAV, L. K.; VERMA, M. K. A multi-objective approach for voltage stability enhancement and loss reduction under PQV and P buses through reconfiguration and distributed generation allocation. *IEEE Access*, New York, v. 10, p. 16609-16623, 2022.

BAYAT, A.; BAGHERI, A.; NOROOZIAN, R. Optimal siting and sizing of distributed generation accompanied by reconfiguration of distribution networks for maximum loss reduction by using a new UVDA-based heuristic method. *International Journal of Electrical Power & Energy Systems*, Oxford, v. 77, p. 360-371, 2016.

BERNAL-AGUSTIN, J. L. *Application of genetic algorithms to the optimal design of power distribution systems*. 1998. 346 f. Thesis (Doctorate in Electrical Engineering) - University of Zaragoza, Zaragoza, 1998.

BISWAL, S. R.; SHANKAR, G.; ELAVARASAN, R. M.; MIHET-POPA, L. Optimal allocation/sizing of DGs/capacitors in reconfigured radial distribution system using quasi-reflected slime mould algorithm. *IEEE Access*, New York, v. 9, p. 125658-125677, 2021.

BOICEA, V. A. Distribution grid reconfiguration through simulated annealing and tabu search. In: *2017 10th International Symposium on Advanced Topics in Electrical Engineering (ATEE)*. Bucharest, 2017, 563-568.

BROWN, R. E. Distribution reliability assessment and reconfiguration optimization. In: *2001 IEEE/PES Transmission and Distribution Conference and Exposition. Developing New Perspectives (Cat.No.01CH37294)*. Atlanta, 2001, vol. 2, 994-999.

BUENO, E. A. *Redução de Perdas Técnicas através de Reconfigurações de Redes de Distribuição de Energia Elétrica sob Demandas Variáveis*. 2005. 148 f. Thesis (Doctorate in Electrical Engineering) - Universidade Estadual de Campinas, Campinas, 2005.

CHABANLOO, R. M.; MALEKI, M. G.; AGAH, S. M. M.; HABASHI, E. M. Comprehensive coordination of radial distribution network protection in the presence of synchronous distributed generation using fault current limiter. *International Journal of Electrical Power & Energy Systems*, Oxford, v. 99, p. 214-224, 2018.

CHANG, G. W.; CHU, S. Y.; WANG, H. L. An improved backward/forward sweep load flow algorithm for radial distribution systems. *IEEE Transactions on Power Systems*, New York, v. 22, n. 2, p. 882-884, 2007. DOI: 10.1109/TPWRS.2007.894848. ISSN: 0885-8950.

CHATTERJEE, S.; MANDAL, S. A novel comparison of gauss-seidel and newton-raphson methods for load flow analysis. In: *in 2017 International Conference on Power and Embedded Drive Control (ICPEDC)*. Chennai, 2017, 1-7.

CHEN, C. S.; CHO, M. Y. Energy loss reduction by critical switches. *IEEE Transactions on Power Delivery*, New York, v. 8, n. 3, p. 1246-1253, July 1993. ISSN: 0885-8977.

CHIRADEJA, P.; RAMAKUMAR, R. An approach to quantify the technical benefits of distributed generation. *IEEE Transactions on Energy Conversion*, New York, v. 19, n. 4, p. 764–773, Dec 2004. ISSN: 0885-8969.

CIVANLAR, S.; GRAINGER, J. J.; YIN, H.; LEE, S. S. H. Distribution feeder reconfiguration for loss reduction. *IEEE Transactions on Power Delivery*, New York, v. 3, n. 3, p. 1217-1223, Jul 1988. ISSN: 0885-8977.

COMMISSION, C. P. U., Annual report to the governor and the legislature, California Public Utilities Commission, Tech. Rep. California, 2017.

CRUZ, M. R. M.; SANTOS, S. F.; FITIWI, D. Z.; CATALÃO, J. P. S. Coordinated distribution network reconfiguration and distributed generation allocation via genetic algorithm. In: *2017 IEEE International Conference on Environment and Electrical Engineering and 2017 IEEE Industrial and Commercial Power Systems Europe (EEEIC / ICPS Europe)*. Milan, 2017, 1-6.

DAS, D.; KOTHARI, D.; KALAM, A. Simple and efficient method for load flow solution of radial distribution networks. *International Journal of Electrical Power & Energy Systems*, Oxford, v. 17, n. 5, p. 335-346, 1995. DOI: https://doi.org/10.1016/0142-0615(95)00050-0. ISSN: 0142-0615.

DUGAN, R. C.; MCGRANAGHAN, M. F.; SANTOSO, S.; BEATY, H. W. *Electrical power systems quality*. 2. ed. New York: McGraw-Hill, 2003. 521 p.

EL-ELA, A. A.; ALLAM, S.; SHATLA, M. Maximal optimal benefits of distributed generation using genetic algorithms. *Electric Power Systems Research*, Amsterdam, v. 80, n. 7, p. 869-877, 2010. DOI: https://doi.org/10.1016/j.epsr.2009.12.021. ISSN: 0378-7796.

EMINOGLU, U.; HOCAOGLU, M. H. A new power flow method for radial distribution systems including voltage dependent load models. *Electric Power Systems Research*, Amsterdam, v. 76, n. 1, p. 106-114, 2005. DOI: https://doi.org/10.1016/j.epsr.2005.05.008. ISSN: 0378-7796.

EMINOGLU, U.; HOCAOGLU, M. H. Distribution systems forward/backward sweepbased power flow algorithms: A review and comparison study. *Electric Power Components and Systems*, Abingdon, v. 37, n. 1, p. 91-110, 2008. DOI: 10.1080/15325000802322046.

EPE. *Anuário Estatístico de Energia Elétrica 2023 – Ano base 2022*. Brasília: Empresa de Pesquisa Energética, Brasília, 2023.

FAN, J.; BORLASE, S. The evolution of distribution. *IEEE Power and Energy Magazine*, New York, v. 7, n. 2, p. 63-68, 2009. DOI: 10.1109/MPE.2008.931392. ISSN: 1540-7977.

FERDAVANI, A. K.; ZIN, A. A. B. M.; KHAIRUDDIN, A. B.; NAEINI, M. M. A. review on reconfiguration of radial electrical distribution network through heuristic methods. In: *2011 Fourth International Conference on Modeling, Simulation and Applied Optimization*. Kuala Lumpur, 2011, 1-5.

FRASER, P. Distributed generation in liberalised electricity markets. In: *INTERNATIONAL ENERGY AGENCY, Tech. Rep.* Paris , 2002.

GARCIA, P. A. N.; PEREIRA, J. L. R.; CARNEIRO, S.; COSTA, V. M. D.; MARTINS, N. Three-phase power flow calculations using the current injection method. *IEEE Transactions on Power Systems*, New York, v. 15, n. 2, p. 508-514, 2000. DOI: 10.1109/59.867133. ISSN: 0885-8950.

GHARAVI, H.; GHAFURIAN, R. Smart grid: The electric energy system of the future. *IEEE Journals & Magazines*, New York, v. 99, n. 6, p. 917-921, 2011.

GHASEMI, M.; KAZEMI, A.; GILANI, M. A.; SHAFIE-KHAH, M. A stochastic planning model for improving resilience of distribution system considering master-slave distributed generators and network reconfiguration. *IEEE Access*, New York, v. 9, p. 78859-78872, 2021.

GHOSH, S.; DAS, D. Method for load-flow solution of radial distribution networks. *IEE Proceedings - Generation, Transmission and Distribution*, Chichester, v. 146, n. 6, p. 641-648, 1999. DOI: 10.1049/ip-gtd:19990464. ISSN: 1350-2360.

GUO, J.; CHEN, T.; CHAUDHURI, B.; HUI, S. Y. R. Stability of Isolated Microgrids with Renewable Generation and Smart Loads. *IEEE Transactions on Sustainable Energy*, New York, v. 11, n. 4, p. 2845 - 2854, 2020.

GUTIÉRREZ-ALCARAZ, G.; TOVAR-HERNÁNDEZ, J. H. Two-stage heuristic methodology for optimal reconfiguration and volt/var control in the operation of electrical distribution systems. *IET Generation, Transmission Distribution*, Chichester, v. 11, n. 16, p. 3946-3954, 2017. DOI: 10.1049/iet-gtd.2016.1870. ISSN: 1751-8687.

HARIRI, A. M.; HASHEMI-DEZAKI, H.; HEJAZI, M. A. A novel generalized analytical reliability assessment method of smart grids including renewable and non-renewable distributed generations and plug-in hybrid electric vehicles. *Reliability Engineering & System Safety*, London, v. 196, 106746, 2020.

IMRAN, A. M.; KOWSALYA, M. A new power system reconfiguration scheme for power loss minimization and voltage profile enhancement using fireworks algorithm. *International Journal of Electrical Power & Energy Systems*, Oxford, v. 62, n. Supplement C, p. 312-322, 2014. DOI: https://doi.org/10.1016/j.ijepes.2014.04.034. ISSN: 0142-0615.

IMRAN, A. M.; KOWSALYA, M.; KOTHARI, D. A novel integration technique for optimal network reconfiguration and distributed generation placement in power distribution networks. *International Journal of Electrical Power & Energy Systems*, Oxford, v. 63, p. 461-472, 2014. DOI: https://doi.org/10.1016/j.ijepes.2014.06.011. ISSN: 0142-0615.

JAKUS, D.; ČAĐENOVIĆ, R.; BOGDANOVIĆ, M.; SARAJČEV, P.; VASILJ, J. Distribution network reconfiguration using hybrid heuristic genetic algorithm. In: *2017 2nd International Multidisciplinary Conference on Computer and Energy Science (SpliTech)*. Split, 2017, 1-6.

KAGAN, N.; OLIVEIRA, C. C. B.; ROBBA, E. J. *Introdução aos sistemas de distribuição de energia elétrica*. 1. ed. São Paulo, SP: Edgard Blucher, 2005. 328 p.

KASHEM, M. A.; GANAPATHY, V.; JASMON, G. B. Network reconfiguration for enhancement of voltage stability in distribution networks. *IEE Proceedings - Generation, Transmission and Distribution*, Chichester, v. 147, n. 3, p. 171-175, May 2000. ISSN: 1350-2360.

KERSTING, W. H. *Distribution System Modeling and Analysis*. 1. ed. Boca Raton: CRC Press, 2001. 328 p.

KERSTING, W. H. *Distribution System Modeling and Analysis*. 3. ed. Boca Raton: CRC Press, 2012. 439 p.

KERSTING, W. H.; MENDIVE, D. L. An application of ladder network theory to the solution of three phase radial load-flow problem. *IEEE PAS Winter meeting,* New York, p. A76044-76048, 1976.

KHAIRUDDIN, N. A. M.; CIPCIGAN, L. M. Optimal placement and capacity of distributed generators in medium voltage generic uk network. In: *2016 51st International Universities Power Engineering Conference (UPEC)*. Coimbra, 2016, 1-6.

KOSOW, I. L. *Máquinas elétricas e transformadores*. 2. ed. Porto Alegre, RS: Globo RS, 1982.

LEAL, A. G.; JARDINI, J. A.; MAGRINI, L. C.; AHN, S. U.; BATTANI, D. Management system of distribution transformer loading. *IEEE Transmission and Distribution 2002*, New York, 2002.

LEE, R. E.; BROOKS, C. L. A method and its application to evaluate automated distribution control. *IEEE Transactions on Power Delivery*, New York, v. 3, n. 3, p. 1232-1240, Jul 1988. ISSN: 0885-8977.

LI, J.; XIONG, R.; YANG, Q.; LIANG, F.; ZHANG, M.; YUAN, W. Design/test of a hybrid energy storage system for primary frequency control using a dynamic droop method in an isolated microgrid power system. *Applied Energy*, Amsterdam, v. 201, n. C, p. 257-269, 2017.

LIU, J.; SALAMA, M. M. A.; MANSOUR, R. R. An efficient power flow algorithm for distribution systems with polynomial load. *International Journal of Electrical Engineering Education*, Manchester, v. 39, n. 4, p. 371-386, 2002. DOI: 10.7227/IJEEE.39.4.7.

LOHIA, S.; MAHELA, O. P.; OLA, S. R. Optimal capacitor placement in distribution system using genetic algorithm. In: *2016 IEEE 7th Power India International Conference (PIICON)*. Bikaner. 2016, 1-6.

LU, L. Y.; LIU, H. J.; ZHU, H.; CHU, C. C. Intrusion detection in distributed frequency control of isolated microgrids. *IEEE Transactions on Smart Grid*, New York, v. 10, n. 6, p. 6502-6515, 2019.

MA, Y.; TONG, X.; ZHOU, X.; GAO, Z. The review on distribution network reconfiguration. In: *2017 29th Chinese Control And Decision Conference (CCDC)*. Chongqing, 2017, 2292-2297.

MAHINDARA, V. R.; PRIYADI, A.; PUJIANTARA, M.; PURNOMO, M. H.; SABER, A. Y.; MULJADI, E. Protection Coordination Challenges for Microgrid Distribution Network with High Penetration Inverter-Based Resources. In: *2020 IEEE Energy Conversion Congress and Exposition (ECCE)* October 2020: IEEE, Michigan, 1618-1622.

MANTOVANI, J. R. S.; CASARI, F.; ROMERO, R. A. Reconfiguração de sistemas de distribuição radiais utilizando o critério de queda de tensão. *Controle and Automação*, Campinas, v. 11, n. 3, p. 150-159, 2000.

MASHAYEKH, S.; STADLER, M.; CARDOSO, G.; HELENO, M. A mixed integer linear programming approach for optimal DER portfolio, sizing, and placement in multi-energy microgrids. *Applied Energy*, Amsterdam, v. 187, p. 154-168, 2017.

MÉFFE, A. *Metodologia para Cálculo de Perdas Técnicas por segmento do Sistema de Distribuição*. 2001. 152 f. Dissertation (Masters in Electrical Engineering) - Universidade de São Paulo, São Paulo, 2001.

MERLIN, A.; BACK, H. Search for a Minimal-Loss Operating Spanning Tree Configuration in an Urban Power Distribution System. In: *Proc. 5th Power System Computation Conference (PSCC)*. Cambridge, 1975.

MILANOVIĆ, J. V.; ALI, H.; AUNG, M. T. Influence of distributed wind generation and load composition on voltage sags. *IET Generation, Transmission & Distribution*, Chichester, v. 1, n. 1, p. 13-22, 2007.

MIRJALILI, S.; LEWIS, A. The Whale Optimization Algorithm. *Advances in Engineering Software*, Amsterdam, v. 95, p. 51-67, 2016.

MOGHADDAM, M. J. H.; KALAM, A.; SHI, J.; NOWDEH, S. A.; GANDOMAN, F. H.; AHMADI, A. A new model for reconfiguration and distributed generation allocation in distribution network considering power quality indices and network losses. *IEEE Systems Journal*, New York, v. 14, n. 3, p. 3530-3538, 2020.

MOHAMMADI, M. T. A. Y.; FARAMARZI, M. PSO algorithm for sitting and sizing of distributed generation to improve voltage profile and decreasing power losses. In: *2012 Proceedings of 17th Conference on Electrical Power Distribution*. Tehran, 2012, 1-5.

NARA, K.; SHIOSE, A.; KITAGAWA, M.; ISHIHARA, T. Implementation of genetic algorithm for distribution systems loss minimumre-configuration. *IEEE Transactions on Power Systems*, New York, v. 7, n. 3, p. 1044-1051, Aug 1992. ISSN: 0885-8950.

NDAHEPELE, L.; CHOWDHURY, S. Impact of Distributed Generation on Traditional Protection in Distribution and Transmission Systems: A Review. In: *2020 IEEE PES/IAS PowerAfrica*. Nairobi, August 2020: IEEE, 1-5.

NGUYEN, H. L. Newton-raphson method in complex form [power system load flow analysis]. *IEEE Transactions on Power Systems*, New York, v. 12, n. 3, p. 1355-1359, 1997. DOI: 10.1109/59.630481. ISSN: 0885-8950.

NGUYEN, T. T.; TRUONG, A. V. Distribution network reconfiguration for power loss minimization and voltage profile improvement using cuckoo search algorithm. *International Journal of Electrical Power & Energy Systems*, Oxford, v. 68, n. Supplement C, p. 233-242, 2015. DOI: https://doi.org/10.1016/j.ijepes.2014.12.075. ISSN: 0142-0615.

NGUYEN, T. T.; TRUONG, A. V.; PHUNG, T. A. A novel method based on adaptive cuckoo search for optimal network reconfiguration and distributed generation allocation in distribution network. *International Journal of Electrical Power & Energy Systems*, Oxford, v. 78, p. 801-815, 2016.

NICK, M.; CHERKAOUI, R.; PAOLONE, M. Optimal planning of distributed energy storage systems in active distribution networks embedding grid reconfiguration. *IEEE Transactions on Power Systems*, New York, v. 33, n. 2, p. 1577-1590, 2017.

OCHOA, L. F. *Cálculo de Fluxo de Potência em Redes de Distribuição com Modelagem a Quatro Fios*. 2003. 120 f. Dissertation (Masters in Electrical Engineering) - Universidade Estadual Paulista "Júlio de Mesquita Filho", Ilha Solteira, 2003.

OLIVEIRA, M. E. *Avaliação de Metodologias de Cálculo de Perdas Técnicas em Sistemas de Distribuição de Energia Elétrica*. 2009. 137 f. Thesis (Doctorate in Electrical Engineering) - Universidade Estadual Paulista "Júlio de Mesquita Filho", Ilha Solteira, 2009.

PAMSHETTI, V. B.; SINGH, S.; SINGH, S. P. Combined impact of network reconfiguration and volt-var control devices on energy savings in the presence of distributed generation. *IEEE Systems Journal*, New York, v. 14, n. 1, p. 995-1006, 2020.

PANWAR, N. L.; KAUSHIK, S. C.; KOTHARI, S. Role of renewable energy sources in environmental protection: A review. *Renewable and Sustainable Energy Reviews*, Amsterdam, v. 15, n. 3, p. 1513-1524, 2011.

PATEL, V. S.; CHAKRABARTI, S.; SINGH, S. N. A hopfield neural network-based reconfiguration algorithm for power distribution systems. In: *2017 IEEE Region 10 Symposium (TENSYMP)*. Cochin, 2017, 1-5.

PEPERMANS, G.; DRIESEN, J.; HAESELDONCKX, D.; BELMANS, R.; D'HAESELEER, W. Distributed generation: definition, benefits and issues. *Energy Policy*, Amsterdam, v. 33, n. 6, p. 787-798, 2005. DOI: https://doi.org/10.1016/j.enpol.2003.10.004. ISSN: 0301-4215.

PERALTA, R. A. V. *Desenvolvimento de uma metodologia para restauração automática de Redes de Distribuição*. 2015. 93 f. Dissertation (Masters in Electrical Engineering) - Universidade Estadual Paulista "Júlio de Mesquita Filho", Ilha Solteira, 2015.

PEYGHAMI, S.; PALENSKY, P.; BLAABJERG, F. An overview on the reliability of modern power electronic based power systems. *IEEE Open Journal of Power Electronics*, New York, v. 1, p. 34-50, 2020.

QUEIROZ, L. M. O. *Estimação e Análise das Perdas Técnicas na Distribuição de Energia Elétrica*. 2010. 161 f. Thesis (Doctorate in Electrical Engineering) Tese (Doutorado em Engenharia Elétrica)- Universidade Estadual de Campinas, Campinas, 2010.

QUEIROZ, L. M. O.; LYRA, C. Adaptive hybrid genetic algorithm for technical loss reduction in distribution networks under variable demands. *IEEE Transactions on Power Systems*, New York, v. 24, n. 1, p. 445-453, Feb 2009.

QUEZADA, V. H. M.; ABBAD, J. R.; ROMAN, T. G. S. Assessment of energy distribution losses for increasing penetration of distributed generation. *IEEE Transactions on Power Systems*, New York, v. 21, n. 2, p. 533–540, May 2006. ISSN: 0885-8950.

RAHIM, M. N. A.; MOKHLIS, H.; BAKAR, A. H. A.; RAHMAN, M. T.; BADRAN, O.; MANSOR, N. N. Protection coordination toward optimal network reconfiguration and DG sizing. *IEEE Access*, New York, v. 7, p. 163700-163718, 2019.

RAJARAM, R.; KUMAR, K. S.; RAJASEKAR, N. Power system reconfiguration in a radial distribution network for reducing losses and to improve voltage profile using modified plant growth simulation algorithm with distributed generation (DG). *Energy Reports*, Amsterdam, v. 1, p. 116-122, 2015.

RAKESH, R.; VENKATAPAPANA, P.; KEERTHI, S. A hybrid algorithm for optimal allocation of DG in radial distribution system. In: *2017 IEEE Region 10 Symposium (TENSYMP)*. Cochin, 2017, 1-5.

REDDY, A. V. S.; REDDY, M. D. Application of whale optimization algorithm for distribution feeder reconfiguration. *i-manager's Journal on Electrical Engineering (JEE)*, Nagercoil, v. 11, n. 3, p. 17-24, 2018.

REKOWSKI, R.; DOBRZYŃSKI, K.; LUBOŚNY, Z. The impact of the distribution network reconfiguration on active power losses: Selected issues of UPGRID project realization. In: *2017 IEEE 21st International Conference on Intelligent Engineering Systems (INES)*. Larnaca, 2017, 000247-000252.

REMOLINO, A. S.; PAREDES, H. F. R. An efficient method for power flow calculation applied to the reconfiguration of radial distribution systems. In: *2016 IEEE PES Transmission Distribution Conference and Exposition-Latin America (PES T D-LA)*. Morelia, 2016, 1-6.

ROSSONI, A.; DRESCH, R. D. F. V.; BRETAS, A. S.; BETTIOL, A. L.; CARNIATO, A.; PASSOS, L. F. N.; MARTIN, R. P. Load models effects on distribution system losses estimation: A numerical study. In: *2013 IEEE Power & Energy Society General Meeting (PESGM)*. Vancouver, 2013, 1-5. ISSN: 1932-5517.

SAHOO, N.; PRASAD, K. A fuzzy genetic approach for network reconfiguration to enhance voltage stability in radial distribution systems. *Energy Conversion and Management*, Amsterdam, v. 47, n. 18, p. 3288-3306, 2006. ISSN: 0196-8904.

SAMBAIAH, K. S.; JAYABARATHI, T. Optimal reconfiguration and renewable distributed generation allocation in electric distribution systems. *International Journal of Ambient Energy*, Abingdon, v. 42, n. 9, p. 1018-1031, 2021.

SAMPAIO, F. C.; LEÃO, R. P.; SAMPAIO, R. F.; MELO, L. S.; BARROSO, G. C. A multi-agent-based integrated self-healing and adaptive protection system for power distribution systems with distributed generation. *Electric Power Systems Research*, Amsterdam, v. 188, 106525, 2020.

SANCHES, D. S. *Algoritmos Evolutivos Multi-Objetivo para Reconfiguração de Redes em Sistemas de Distribuição de Energia Elétrica*. 2013. 152 f. Thesis (Doctorate in Electrical Engineering) - Universidade de São Paulo, São Carlos, 2013.

SARFI, R. J.; SALAMA, M. M. A.; CHIKHANI, Y. Practical aspects of performing a distribution system loss reduction study. In: *Proceedings 1995 Canadian Conference on Electrical and Computer Engineering*. Montreal, 1995, vol. 1, 164–167. ISSN: 0840-7789.

SCHERER, H. N.; VASSELL, G. S. Transmission of electric power at ultra-high voltages: Current status and future prospects. *Proceedings of the IEEE*, New York, v. 73, n. 8, p. 1252-1278, Aug 1985. ISSN: 0018-9219.

SHAHEEN, A. M.; EL-SEHIEMY, R. A.; KAMEL, S.; ELATTAR, E. E.; ELSAYED, A. M. Improving distribution networks' consistency by optimal distribution system reconfiguration and distributed generations. *IEEE Access*, New York, v. 9, p. 67186-67200, 2021.

SHAHEEN, A. M.; ELSAYED, A. M.; EL-SEHIEMY, R. A.; ABDELAZIZ, A. Y. Equilibrium optimization algorithm for network reconfiguration and distributed generation allocation in power systems. *Applied Soft Computing*, Amsterdam, v. 98, 106867, 2021.

SHI, Q.; LI, F.; OLAMA, M.; DONG, J.; XUE, Y.; STARKE, M.; WINSTEAD, C.; KURUGANTI, T. Network reconfiguration and distributed energy resource scheduling for improved distribution system resilience. *International Journal of Electrical Power & Energy Systems*, Oxford, v. 124, 106355, 2021.

SHIRMOHAMMADI, D.; HONG, H. W.; SEMLYEN, A.; LUO, G. X. A compensation based power flow method for weakly meshed distribution and transmission networks. *IEEE Transactions on Power Systems*, New York, v. 3, n. 2, p. 753-762, May 1988. ISSN: 0885-8950.

SOLIMAN, M.; ABDELAZIZ, A. Y.; EL-HASSANI, R. M. Distribution power system reconfiguration using whale optimization algorithm. *International Journal of Applied Power Engineering (IJAPE)*, Semarang, v. 9, n. 1, p. 48-57, 2020.

SRIKANTHA, P.; KUNDUR, D. Intelligent signal processing and coordination for the adaptive smart grid: An overview of data-driven grid management. *IEEE Signal Processing Magazine*, New York, v. 36, n. 3, p. 82-102, 2019.

SRINIVAS, M. S. Distribution load flows: a brief review. In: *2000 IEEE Power Engineering Society Winter Meeting*. Conference Proceedings (Cat. No.00CH37077). Singapore, 2000, vol. 2, 942-945.

STOTT, B. Review of load-flow calculation methods. *Proceedings of the IEEE*, New York, v. 62, n. 7, p. 916-929, 1974. DOI: 10.1109/PROC.1974.9544. ISSN: 0018-9219.

SWARNKAR, A.; GUPTA, N.; NIAZI, K. R. Adapted ant colony optimization for efficient reconfiguration of balanced and unbalanced distribution systems for loss minimization. *Swarm and Evolutionary Computation*, Amsterdam, v. 1, n. 3, p. 129-137, 2011. https://doi.org/10.1016/j.swevo.2011.05.004.

TAVARES, J. P. M. *Reconfiguração de Sistemas de Distribuição de Energia Elétrica aplicada na Redução das Perdas Técnicas e Melhoria dos Níveis de Tensão*. 2018. 107 f. Dissertation (Bachelor in Electrical Engineering) - Instituto Federal de Educação, Ciência e Tecnologia de Goiás (IFG), Goiânia, 2018.

TENG, J.-H.; CHANG, C.-Y. A novel and fast three-phase load flow for unbalanced radial distribution systems. *IEEE Transactions on Power Systems*, New York, v. 17, n. 4, p. 1238-1244, 2002. DOI: 10.1109/TPWRS.2002.805012. ISSN: 0885-8950.

TOLBA, M. A.; TULSKY, V. N.; DIAB, A. A. Z. Optimal sitting and sizing of renewable distributed generations in distribution networks using a hybrid PSOGSA optimization algorithm. In: *2017 IEEE International Conference on Environment and Electrical Engineering and 2017 IEEE Industrial and Commercial Power Systems Europe (EEEIC / ICPS Europe)*. Milan, 2017, 1-7.

TRAN, T. T.; TRUONG, K. H.; VO, D. N. Stochastic fractal search algorithm for reconfiguration of distribution networks with distributed generations. *Ain Shams Engineering Journal*, Cairo, v. 11, n. 2, p. 389-407, 2020.

TRAN, T. V.; TRUONG, B.-H.; NGUYEN, T. P.; NGUYEN, T. A.; DUONG, T. L.; VO, D. N. Reconfiguration of distribution networks with distributed generations using an improved neural network algorithm. *IEEE Access*, New York, v. 9, p. 165618-165647, 2021.

VIJAYAPRIYA, T.; KOTHARI, D. P. Smart grid: an overview. *Smart Grid and Renewable Energy*, Wuhan, v. 2, n. 4, p. 305-311, 2011.

VIRAL, R.; KHATOD, D. Optimal planning of distributed generation systems in distribution system: A review. *Renewable and Sustainable Energy Reviews*, Amsterdam, v. 16, n. 7, p. 5146-5165, 2012. DOI: https://doi.org/10.1016/j.rser.2012.05.020. ISSN: 1364-0321.

WANG, C.; LEI, S.; JU, P.; CHEN, C.; PENG, C.; HOU, Y. MDP-based distribution network reconfiguration with renewable distributed generation: approximate dynamic programming approach. *IEEE Transactions on Smart Grid*, New York, v. 11, n. 4, p. 3620-3631, 2020.

YU, Q. Applications of flexible ac transmissions system (facts) technology in smartgrid and its emc impact. *In: 2014 IEEE International Symposium on Electromagnetic Compatibility (EMC)*, Raleigh, p. 392-397, 2014. ISSN: 2158-110X.

ZHANG, F.; CHENG, C. S. A modified newton method for radial distribution system power flow analysis. *IEEE Transactions on Power Systems*, New York, v. 12, n. 1, p. 389-397, 1997. DOI: 10.1109/59.575728. ISSN: 0885-8950.

ZHANG, M.; CHEN, J. Islanding and scheduling of power distribution systems with distributed generation. *IEEE Transactions on Power Systems*, New York, v. 30, n. 6, p. 3120-3129, 2014.

APPENDIX A – 33-Bus System Data

The complete data of the distribution system of 33-bus is presented in this appendix that tested in the work.

Soliman et al. (2020) described the 33-bus system data in Table 22.

- Substation bus: 1;
- Base voltage: 12.66 kV;
- Base power: 100 MVA.

Table 22 – The data of 33-bus test system

Bus	P [kW]	Q [kVAr]	Branch Node	From Node	To Node	Resistance [Ω]	Reactance [Ω]
1	0	0	1	1	2	0.0922	0.047
2	100	60	2	2	3	0.493	0.2511
3	90	40	3	3	4	0.366	0.1864
4	120	80	4	4	5	0.3811	0.1941
5	60	30	5	5	6	0.819	0.707
6	60	20	6	6	7	0.1872	0.6188
7	200	100	7	7	8	0.7114	0.2351
8	200	100	8	8	9	1.03	0.74
9	60	20	9	9	10	1.044	0.74
10	60	20	10	10	11	0.1966	0.065
11	45	30	11	11	12	0.3744	0.1238
12	60	35	12	12	13	1.468	1.155
13	60	35	13	13	14	0.5416	0.7129
14	120	80	14	14	15	0.591	0.526
15	60	10	15	15	16	0.7463	0.545
16	60	20	16	16	17	1.289	1.721
17	60	20	17	17	18	0.732	0.574
18	90	40	18	2	19	0.164	0.1565
19	90	40	19	19	20	1.5042	1.3554

20	90	40	20	20	21	0.4095	0.4784
21	90	40	21	21	22	0.7089	0.9373
22	90	40	22	3	23	0.4512	0.3083
23	90	50	23	23	24	0.898	0.7091
24	420	200	24	24	25	0.896	0.7011
25	420	200	25	6	26	0.203	0.1034
26	60	25	26	26	27	0.2842	0.1447
27	60	25	27	27	28	1.059	0.9337
28	60	20	28	28	29	0.8042	0.7006
29	120	70	29	29	30	0.5075	0.2585
30	200	600	30	30	31	0.9744	0.963
31	150	70	31	31	32	0.3105	0.3619
32	210	100	32	32	33	0.341	0.5302
33	60	40	33	8	21	2	2
34	0	0	34	9	15	2	2
35	0	0	35	12	22	2	2
36	0	0	36	18	33	0.5	0.5
37	**3715**	**2300**	37	25	29	0.5	0.5

Source: Soliman et al. (2020).

APPENDIX B – 69-Bus System Data

The complete data of the distribution system of 69-bus is presented in this appendix that tested in the work.

Soliman et al. (2020) described the 69-bus system data in Table 23.

- Substation bus: 1;
- Base voltage: 12.66 kV;
- Base power: 100 MVA.

Table 23 – The data of 69-bus test system

Bus	P [kW]	Q [kVAr]	Branch Node	From Node	To Node	Resistance [Ω]	Reactance [Ω]
1	0	0	1	1	2	0.0005	0.0012
2	0	0	2	2	3	0.0005	0.0012
3	0	0	3	3	4	0.0015	0.0036
4	0	0	4	4	5	0.0251	0.0294
5	0	0	5	5	6	0.366	0.1864
6	2.6	2.2	6	6	7	0.3811	0.1941
7	40.4	30	7	7	8	0.0922	0.047
8	75	54	8	8	9	0.0493	0.0251
9	30	22	9	9	10	0.819	0.2707
10	28	19	10	10	11	0.1872	0.0619
11	145	104	11	11	12	0.7114	0.2351
12	145	104	12	12	13	1.03	0.34
13	8	5	13	13	14	1.044	0.345
14	8	5.5	14	14	15	1.058	0.3496
15	0	0	15	15	16	0.1966	0.065
16	45.5	30	16	16	17	0.3744	0.1238
17	60	35	17	17	18	0.0047	0.0016
18	60	35	18	18	19	0.3276	0.1083
19	0	0	19	19	20	0.2106	0.069

20	1	0.6	20	20	21	0.3416	0.1129
21	114	81	21	21	22	0.014	0.0046
22	5	3.5	22	22	23	0.1591	0.0526
23	0	0	23	23	24	0.3463	0.1145
24	28	20	24	24	25	0.7488	0.2475
25	0	0	25	25	26	0.3089	0.1021
26	14	10	26	26	27	0.1732	0.0572
27	14	10	27	3	28	0.0044	0.0108
28	26	18.6	28	28	29	0.064	0.1565
29	26	18.6	29	29	30	0.3978	0.1315
30	0	0	30	30	31	0.0702	0.0232
31	0	0	31	31	32	0.351	0.116
32	0	0	32	32	33	0.839	0.2816
33	14	10	33	33	34	1.708	0.5646
34	19.5	14	34	34	35	1.474	0.4873
35	6	4	35	3	36	0.0044	0.0108
36	26	18.55	36	36	37	0.064	0.1565
37	26	18.55	37	37	38	0.1053	0.123
38	0	0	38	38	39	0.0304	0.0355
39	24	17	39	39	40	0.0018	0.0021
40	24	17	40	40	41	0.7283	0.8509
41	1.2	1	41	41	42	0.31	0.3623
42	0	0	42	42	43	0.041	0.0478
43	6	4.3	43	43	44	0.0092	0.0116
44	0	0	44	44	45	0.1089	0.1373
45	39.22	26.3	45	45	46	0.0009	0.0012
46	39.22	26.3	46	4	47	0.0034	0.0084
47	0	0	47	47	48	0.0851	0.2083
48	79	56.4	48	48	49	0.2898	0.7091
49	384.7	274.5	49	49	50	0.0822	0.2011
50	384.7	274.5	50	8	51	0.0928	0.0473
51	40.5	28.3	51	51	52	0.3319	0.1114
52	3.6	2.7	52	9	53	0.174	0.0886

53	4.35	3.5	53	53	54	0.203	0.1034
54	26.4	19	54	54	55	0.2842	0.1447
55	24	17.2	55	55	56	0.2813	0.1433
56	0	0	56	56	57	1.59	0.5337
57	0	0	57	57	58	0.7837	0.263
58	0	0	58	58	59	0.3042	0.1006
59	100	72	59	59	60	0.3861	0.1172
60	0	0	60	60	61	0.5075	0.2585
61	1244	888	61	61	62	0.0974	0.0496
62	32	23	62	62	63	0.145	0.0738
63	0	0	63	63	64	0.7105	0.3619
64	227	162	64	64	65	1.041	0.5302
65	59	42	65	11	66	0.2012	0.0611
66	18	13	66	66	67	0.0047	0.0014
67	18	13	67	12	68	0.7394	0.2444
68	28	20	68	68	69	0.0047	0.0016
69	28	20	69	11	43	0.5	0.5
70	0	0	70	13	21	0.5	0.5
71	0	0	71	15	46	1	1
72	0	0	72	50	59	2	2
73	**3802**	**2694.1**	73	27	65	1	1

Source: Soliman et al. (2020).

APPENDIX C – 136-Bus System Data

The complete data of the distribution system of 136-bus is presented in this appendix that tested in the work.

Mantovani et al. (2000) described the 136-bus system data in Table 24.

- Substation bus: 136;
- Base voltage: 13.80 kV;
- Base power: 100 MVA.

Table 24 – The data of 136-bus test system

Bus	P [kW]	Q [kVAr]	Branch Node	From Node	To Node	Resistance [Ω]	Reactance [Ω]
1	0	0	1	136	1	0.33205	0.76653
2	47.78	19.009	2	1	2	0.00188	0.00433
3	42.551	16.929	3	2	3	0.22324	0.51535
4	87.022	34.622	4	3	4	0.09943	0.22953
5	311.31	123.855	5	4	5	0.15571	0.35945
6	148.869	59.228	6	5	6	0.16321	0.37677
7	238.672	94.956	7	6	7	0.11444	0.26417
8	62.299	24.786	8	6	8	0.05675	0.05666
9	124.598	49.571	9	8	9	0.52124	0.27418
10	140.175	55.768	10	8	10	0.10877	0.1086
11	116.813	46.474	11	10	11	0.39803	0.20937
12	249.203	99.145	12	10	12	0.91744	0.31469
13	291.447	115.952	13	10	13	0.11823	0.11805
14	303.72	120.835	14	13	14	0.50228	0.26421
15	215.396	85.695	15	13	15	0.05675	0.05666
16	198.586	79.007	16	15	16	0.29379	0.15454
17	0	0	17	136	17	0.33205	0.76653
18	0	0	18	17	18	0.00188	0.00433
19	0	0	19	18	19	0.22324	0.51535

20	30.127	14.729	20	19	20	0.10881	0.25118
21	230.972	112.92	21	20	21	0.71078	0.37388
22	60.256	29.458	22	20	22	0.18197	0.42008
23	230.972	112.92	23	22	23	0.30326	0.15952
24	120.507	58.915	24	22	24	0.02439	0.0563
25	0	0	25	24	25	0.04502	0.10394
26	56.981	27.857	26	25	26	0.01876	0.04331
27	364.665	178.281	27	26	27	0.11823	0.11805
28	0	0	28	27	28	0.02365	0.02361
29	124.647	60.939	29	28	29	0.18954	0.0997
30	56.981	27.857	30	29	30	0.39803	0.20937
31	0	0	31	28	31	0.05675	0.05666
32	85.473	41.787	32	31	32	0.09477	0.04985
33	0	0	33	32	33	0.41699	0.21934
34	396.735	193.96	34	33	34	0.11372	0.05982
35	0	0	35	31	35	0.07566	0.07555
36	181.152	88.563	36	35	36	0.3696	0.19442
37	242.172	118.395	37	36	37	0.26536	0.13958
38	75.316	36.821	38	35	38	0.05675	0.05666
39	0	0	39	136	39	0.33205	0.76653
40	1.254	0.531	40	39	40	0.11819	0.27283
41	6.274	2.66	41	40	41	2.96288	1.01628
42	0	0	42	40	42	0.00188	0.00433
43	117.88	49.971	43	42	43	0.06941	0.16024
44	62.668	26.566	44	43	44	0.81502	0.42872
45	172.285	73.034	45	43	45	0.06378	0.14724
46	458.556	194.388	46	45	46	0.13132	0.30315
47	262.962	111.473	47	46	47	0.06191	0.14291
48	235.761	99.942	48	47	48	0.11444	0.26417
49	0	0	49	48	49	0.28374	0.28331
50	109.215	46.298	50	49	50	0.28374	0.28331
51	0	0	51	48	51	0.04502	0.10394
52	72.809	30.865	52	51	52	0.02626	0.06063

53	258.473	109.57	53	52	53	0.06003	0.13858
54	69.169	29.322	54	53	54	0.03002	0.06929
55	21.843	9.26	55	54	55	0.02064	0.04764
56	0	0	56	52	56	0.10881	0.25118
57	20.527	8.702	57	56	57	0.25588	0.1346
58	150.548	63.819	58	57	58	0.41699	0.21934
59	220.687	93.552	59	58	59	0.50228	0.26421
60	92.384	39.163	60	59	60	0.3317	0.17448
61	0	0	61	60	61	0.20849	0.10967
62	226.693	96.098	62	47	62	0.13882	0.32047
63	0	0	63	136	63	0.0075	0.01732
64	294.016	116.974	64	63	64	0.27014	0.62362
65	83.015	33.028	65	64	65	0.3827	0.88346
66	83.015	33.028	66	65	66	0.33018	0.7622
67	103.77	41.285	67	66	67	0.3283	0.75787
68	176.408	70.184	68	67	68	0.17072	0.39409
69	83.015	33.028	69	68	69	0.55914	0.29412
70	217.917	86.698	70	68	70	0.05816	0.13425
71	23.294	9.267	71	70	71	0.7013	0.3689
72	5.075	2.019	72	71	72	1.02352	0.53839
73	72.638	28.899	73	70	73	0.06754	0.15591
74	405.99	161.5235	74	73	74	1.32352	0.45397
75	0	0	75	136	75	0.01126	0.02598
76	100.182	42.468	76	75	76	0.72976	1.68464
77	142.523	60.417	77	76	77	0.22512	0.51968
78	96.042	40.713	78	77	78	0.20824	0.48071
79	300.454	127.366	79	78	79	0.0469	0.10827
80	141.238	59.873	80	79	80	0.6195	0.61857
81	279.847	118.631	81	80	81	0.34049	0.33998
82	87.312	37.013	82	81	82	0.56862	0.29911
83	243.849	103.371	83	81	83	0.10877	0.1086
84	247.75	105.025	84	83	84	0.56862	0.29911
85	0	0	85	136	85	0.01126	0.02598

86	89.878	38.101	86	85	86	0.41835	0.96575
87	1137.28	482.108	87	86	87	0.10499	0.13641
88	458.339	194.296	88	86	88	0.43898	1.01338
89	385.197	163.29	89	88	89	0.0752	0.02579
90	0	0	90	89	90	0.07692	0.17756
91	79.608	33.747	91	90	91	0.33205	0.76653
92	87.312	37.013	92	91	92	0.08442	0.19488
93	0	0	93	92	93	0.1332	0.30748
94	74.001	31.37	94	93	94	0.2932	0.29276
95	232.05	98.369	95	94	95	0.21753	0.21721
96	141.819	60.119	96	95	96	0.26482	0.26443
97	0	0	97	93	97	0.10318	0.23819
98	76.449	32.408	98	97	98	0.13507	0.31181
99	0	0	99	136	99	0.00938	0.02165
100	51.322	21.756	100	99	100	0.16884	0.38976
101	59.874	25.381	101	100	101	0.11819	0.27283
102	9.065	3.843	102	101	102	2.28608	0.78414
103	2.092	0.887	103	101	103	0.45587	1.05236
104	16.735	7.094	104	103	104	0.696	1.60669
105	1506.522	638.634	105	104	105	0.45774	1.05669
106	313.023	132.694	106	105	106	0.20298	0.26373
107	79.831	33.842	107	106	107	0.21348	0.27737
108	51.322	21.756	108	107	108	0.54967	0.28914
109	0	0	109	108	109	0.54019	0.28415
110	202.435	85.815	110	107	110	0.0455	0.05911
111	60.823	25.784	111	110	111	0.47385	0.24926
112	45.618	19.338	112	111	112	0.86241	0.45364
113	0	0	113	112	113	0.56862	0.29911
114	157.07	66.584	114	108	114	0.77711	0.40878
115	0	0	115	114	115	1.08038	0.5683
116	250.148	106.041	116	109	116	1.09933	0.57827
117	0	0	117	116	117	0.47385	0.24926
118	69.809	29.593	118	104	118	0.32267	0.74488

119	32.072	13.596	119	118	119	0.14633	0.33779
120	61.084	25.894	120	119	120	0.12382	0.28583
121	0	0	121	136	121	0.01126	0.02598
122	94.622	46.26	122	121	122	0.6491	1.49842
123	49.858	24.375	123	122	123	0.04502	0.10394
124	123.164	60.214	124	123	124	0.5264	0.18056
125	78.35	38.304	125	123	125	0.02064	0.04764
126	145.475	71.121	126	125	126	0.53071	0.27917
127	21.369	10.447	127	125	127	0.09755	0.2252
128	74.789	36.564	128	127	128	0.11819	0.27283
129	227.926	111.431	129	127	129	0.13882	0.32047
130	35.614	17.411	130	129	130	0.04315	0.09961
131	249.295	121.877	131	130	131	0.09192	0.2122
132	316.722	154.842	132	131	132	0.16134	0.37244
133	333.817	163.199	133	132	133	0.37832	0.37775
134	249.295	121.877	134	133	134	0.39724	0.39664
135	0	0	135	134	135	0.2932	0.29276
136	0	0	136	7	73	0.13132	0.30315
137	0	0	137	9	24	0.26536	0.13958
138	0	0	138	15	83	0.14187	0.14166
139	0	0	139	38	135	0.08512	0.08499
140	0	0	140	25	51	0.04502	0.10394
141	0	0	141	50	96	0.14187	0.14166
142	0	0	142	55	98	0.14187	0.14166
143	0	0	143	62	120	0.0394	0.09094
144	0	0	144	66	79	0.12944	0.29882
145	0	0	145	79	131	0.01688	0.03898
146	0	0	146	84	135	0.3317	0.17448
147	0	0	147	91	104	0.14187	0.14166
148	0	0	148	90	129	0.07692	0.17756
149	0	0	149	90	103	0.07692	0.17756
150	0	0	150	92	104	0.07692	0.17756
151	0	0	151	92	132	0.07692	0.17756

152	0	0	152	96	120	0.26482	0.26443
153	0	0	153	110	47	0.49696	0.64567
154	0	0	154	126	76	0.17059	0.08973
155	0	0	155	128	77	0.05253	0.12126
156	**18313.81**	**7932.534**	156	135	98	0.2932	0.29276

Source: Mantovani et al. (2000).

APPENDIX D – 415-Bus System Data

The complete data of the distribution system of 415-bus is presented in this appendix that tested in the work.

Bernal-Agustin (1998) described the 415-bus system data in Table 25.

- Substation bus: 1;
- Base voltage: 10.00 kV;
- Base power: 100 MVA.

Table 25 – The data of 415-bus test system

Bus	P [kW]	Q [kVAr]	Branch Node	From Node	To Node	Resistance [Ω]	Reactance [Ω]
1	0.1	0	1	384	68	0.0310675	0.02142
2	0.1	0	2	89	67	0.1078225	0.07434
3	122	59	3	225	224	0.069445	0.04788
4	0.1	0	4	21	72	0.193715	0.13356
5	0.1	0	5	66	384	0.0347225	0.02394
6	114	55	6	3	20	0.610385	0.42084
7	51	25	7	224	222	0.069445	0.04788
8	83	40	8	72	74	0.02193	0.01512
9	0.1	0	9	70	382	0.0310675	0.02142
10	122	59	10	20	51	0.08772	0.06048
11	122	59	11	222	221	0.08772	0.06048
12	77	37	12	76	72	0.054825	0.0378
13	0.1	0	13	382	66	0.032895	0.02268
14	68	33	14	51	52	0.069445	0.04788
15	71	34	15	221	220	0.084065	0.05796
16	0.1	0	16	75	81	0.084065	0.05796
17	0.1	0	17	59	70	0.0537285	0.037044
18	77	37	18	52	56	0.11696	0.08064
19	30	14	19	1	273	0.0142545	0.009828

20	13	6	20	81	76	0.0529975	0.03654
21	1	0	21	68	85	0.02924	0.02016
22	194	94	22	56	27	0.09503	0.06552
23	77	37	23	1	274	0.115498	0.079632
24	77	37	24	74	75	0.105995	0.07308
25	77	37	25	68	93	0.084065	0.05796
26	122	59	26	27	31	0.10234	0.07056
27	104	51	27	274	275	0.0836995	0.057708
28	0.1	0	28	72	73	0.098685	0.06804
29	77	37	29	60	58	0.010965	0.00756
30	243	118	30	31	40	0.105995	0.07308
31	77	37	31	275	209	0.139621	0.096264
32	77	37	32	73	80	0.0731	0.0504
33	0.1	0	33	65	71	0.0712725	0.04914
34	121	58	34	40	47	0.091375	0.063
35	194	94	35	275	276	0.1158635	0.079884
36	122	59	36	73	77	0.076755	0.05292
37	77	37	37	69	65	0.0310675	0.02142
38	0.1	0	38	51	54	0.054825	0.0378
39	0.1	0	39	276	264	0.1151325	0.07938
40	96	47	40	77	78	0.05117	0.03528
41	122	59	41	59	69	0.021199	0.014616
42	70	34	42	54	24	0.0731	0.0504
43	58	28	43	263	264	0.068714	0.047376
44	0.1	0	44	79	83	0.24123	0.16632
45	122	59	45	63	61	0.10965	0.0756
46	122	59	46	24	29	0.09503	0.06552
47	122	59	47	262	263	0.0630936	0.0532656
48	86	42	48	82	80	0.0731	0.0504
49	77	37	49	71	63	0.022661	0.015624
50	0.1	0	50	29	34	0.1151325	0.07938
51	122	59	51	261	262	0.037973	0.032058
52	122	59	52	78	79	0.02193	0.01512

53	122	59	53	61	60	0.04386	0.03024
54	0.1	0	54	34	47	0.1736125	0.1197
55	42	20	55	259	261	0.0511175	0.043155
56	122	59	56	83	90	0.1209805	0.083412
57	13	6	57	58	62	0.129387	0.089208
58	77	37	58	47	21	0.084065	0.05796
59	50	24	59	257	259	0.068714	0.047376
60	0.1	0	60	77	59	0.38743	0.26712
61	60	29	61	64	67	0.0449565	0.030996
62	71	34	62	20	44	0.01462	0.01008
63	122	59	63	372	239	0.0265811	0.0224406
64	77	37	64	123	1	0.013524	0.015953
65	95	46	65	67	68	0.086258	0.059472
66	121	58	66	44	25	0.127925	0.0882
67	77	37	67	264	265	0.072369	0.049896
68	103	50	68	120	94	0.2538284	0.2584552
69	52	25	69	62	64	0.0603075	0.04158
70	57	27	70	25	35	0.127925	0.0882
71	171	83	71	369	347	0.13158	0.09072
72	121	58	72	120	123	0.294875	0.30025
73	39	19	73	58	20	0.59211	0.40824
74	119	58	74	35	38	0.08041	0.05544
75	49	24	75	369	370	0.208335	0.14364
76	0.1	0	76	114	115	0.047515	0.03276
77	50	24	77	1	92	0.388892	0.268128
78	44	21	78	38	41	0.1041675	0.07182
79	82	40	79	370	348	0.1187875	0.0819
80	132	64	80	115	112	0.040205	0.02772
81	194	94	81	92	2	0.3410115	0.235116
82	0.1	0	82	41	43	0.11696	0.08064
83	122	59	83	383	251	0.010965	0.00756
84	3	1	84	94	113	0.032895	0.02268
85	52	25	85	92	87	0.0128524	0.0108504

86	103	50	86	43	48	0.08041	0.05544
87	21	10	87	383	370	0.018275	0.0126
88	21	10	88	113	114	0.076755	0.05292
89	21	10	89	2	17	0.08772	0.06048
90	5	3	90	48	50	0.0731	0.0504
91	0.1	0	91	208	277	0.067252	0.046368
92	0.1	0	92	106	95	0.084065	0.05796
93	21	10	93	6	7	0.040205	0.02772
94	18	9	94	20	33	0.06579	0.04536
95	122	59	95	277	278	0.032895	0.02268
96	116	56	96	95	112	0.032895	0.02268
97	7	3	97	7	3	0.051901	0.035784
98	64	31	98	84	33	0.0420325	0.02898
99	49	24	99	277	279	0.048246	0.033264
100	16	8	100	94	111	0.06579	0.04536
101	77	37	101	18	5	0.1224425	0.08442
102	119	58	102	28	36	0.091375	0.063
103	71	34	103	279	280	0.034357	0.023688
104	77	37	104	111	106	0.06579	0.04536
105	194	94	105	5	6	0.0493425	0.03402
106	122	59	106	36	45	0.13158	0.09072
107	55	27	107	280	281	0.062135	0.04284
108	38	18	108	119	121	0.0102235	0.008631
109	22	10	109	17	18	0.11696	0.08064
110	0.1	0	110	49	45	0.04386	0.03024
111	77	37	111	281	235	0.0493425	0.03402
112	122	59	112	94	119	0.056028	0.066091
113	38	18	113	2	14	0.0164475	0.01134
114	122	59	114	55	23	0.076755	0.05292
115	27	13	115	281	282	0.0537285	0.037044
116	64	31	116	118	84	0.040205	0.02772
117	0.1	0	117	8	9	0.09503	0.06552
118	0.1	0	118	23	28	0.069445	0.04788

119	0.1	0	119	235	234	0.083334	0.057456
120	0.1	0	120	119	122	0.05117	0.03528
121	79	38	121	9	3	0.01462	0.01008
122	247	119	122	33	55	0.04386	0.03024
123	0.1	0	123	235	236	0.0420325	0.02898
124	0.1	0	124	122	118	0.201025	0.1386
125	0.1	0	125	16	19	0.157165	0.10836
126	0.1	0	126	21	50	0.03655	0.0252
127	0.1	0	127	208	236	0.076755	0.05292
128	0.1	0	128	104	105	0.049657	0.041922
129	77	37	129	19	8	0.02193	0.01512
130	122	59	130	32	44	0.25585	0.1764
131	62	30	131	232	349	0.075946	0.064116
132	105	51	132	84	104	0.0731	0.0504
133	122	59	133	14	16	0.098685	0.06804
134	77	37	134	37	32	0.105995	0.07308
135	77	37	135	349	207	0.032131	0.027126
136	0.1	0	136	105	108	0.06579	0.04536
137	85	41	137	2	13	0.032131	0.027126
138	8	4	138	42	37	0.0676175	0.04662
139	122	59	139	380	229	0.0411861	0.0347706
140	35	17	140	109	108	0.049657	0.041922
141	55	27	141	4	12	0.067183	0.056718
142	153	74	142	46	42	0.025585	0.01764
143	316	153	143	229	228	0.0630936	0.0532656
144	105	51	144	84	109	0.047515	0.03276
145	20	10	145	12	15	0.105156	0.088776
146	95	46	146	46	50	0.03655	0.0252
147	38	18	147	232	231	0.0968575	0.06678
148	83	40	148	110	84	0.04386	0.03024
149	50	24	149	15	11	0.1329055	0.112203
150	77	37	150	21	49	0.135235	0.09324
151	122	59	151	232	293	0.0749275	0.05166

152	102	49	152	103	110	0.076755	0.05292
153	60	29	153	13	4	0.0452755	0.038223
154	77	37	154	39	30	0.11696	0.08064
155	194	94	155	293	236	0.069445	0.04788
156	56	27	156	107	103	0.054825	0.0378
157	122	59	157	11	86	0.035052	0.029592
158	0.1	0	158	49	39	0.08772	0.06048
159	3	1	159	221	344	0.02924	0.02016
160	1	0	160	84	107	0.06579	0.04536
161	52	25	161	86	91	0.09503	0.06552
162	194	94	162	53	22	0.040205	0.02772
163	10	5	163	304	306	0.069445	0.04788
164	128	62	164	97	116	0.04386	0.03024
165	16	8	165	10	11	0.046736	0.039456
166	37	18	166	30	26	0.054825	0.0378
167	154	75	167	378	377	0.1114775	0.07686
168	0.1	0	168	84	99	0.13158	0.09072
169	0.1	0	169	3	10	0.1078225	0.07434
170	78	38	170	26	53	0.1005125	0.0693
171	0.1	0	171	304	378	0.0588455	0.040572
172	27	13	172	101	96	0.105995	0.07308
173	103	50	173	10	88	0.1095375	0.092475
174	122	59	174	22	33	0.04386	0.03024
175	72	35	175	309	307	0.098685	0.06804
176	0.1	0	176	100	101	0.05848	0.04032
177	122	59	177	88	89	0.08041	0.05544
178	194	94	178	21	57	0.215645	0.14868
179	0.1	0	179	314	317	0.0815065	0.056196
180	77	37	180	102	100	0.054825	0.0378
181	82	40	181	99	102	0.05117	0.03528
182	53	26	182	187	167	0.084709	0.071514
183	122	59	183	314	318	0.072369	0.049896
184	64	31	184	138	194	0.0127925	0.00882

185	86	42	185	96	117	0.0785825	0.05418
186	82	40	186	167	175	0.090551	0.076446
187	0.1	0	187	301	305	0.04386	0.03024
188	167	81	188	155	151	0.069445	0.04788
189	0.1	0	189	117	97	0.040205	0.02772
190	0.1	0	190	175	181	0.084709	0.071514
191	131	64	191	310	315	0.061404	0.042336
192	21	10	192	126	124	0.02924	0.02016
193	21	10	193	98	94	0.040205	0.02772
194	21	10	194	160	180	0.04386	0.03024
195	21	10	195	310	305	0.082603	0.056952
196	0.1	0	196	1	351	0.22661	0.15624
197	0.1	0	197	116	98	0.062135	0.04284
198	0.1	0	198	180	177	0.054825	0.0378
199	0.1	0	199	129	346	0.261698	0.180432
200	0.1	0	200	1	350	0.22661	0.15624
201	52	25	201	57	147	0.157165	0.10836
202	202	98	202	169	162	0.076755	0.05292
203	202	98	203	90	370	0.157896	0.108864
204	73	35	204	350	203	0.023392	0.016128
205	81	39	205	153	141	0.073025	0.06165
206	115	56	206	162	183	0.084065	0.05796
207	118	57	207	382	383	0.1502205	0.103572
208	318	154	208	351	379	0.023392	0.016128
209	161	78	209	147	142	0.105995	0.07308
210	126	61	210	183	182	0.032895	0.02268
211	59	29	211	66	252	0.192984	0.133056
212	24	12	212	203	204	0.0511175	0.043155
213	24	12	213	142	136	0.08041	0.05544
214	5	2	214	160	181	0.091375	0.063
215	126	61	215	384	243	0.227341	0.156744
216	56	27	216	204	205	0.062135	0.04284
217	62	30	217	132	153	0.08772	0.06048

218	0.1	0	218	181	178	0.05848	0.04032
219	32	15	219	85	244	0.1399865	0.096516
220	158	77	220	203	206	0.1034034	0.0872964
221	126	61	221	136	132	0.149855	0.10332
222	202	98	222	171	163	0.064262	0.054252
223	41	20	223	352	414	0.0705415	0.048636
224	81	39	224	379	380	0.1034034	0.0872964
225	126	61	225	57	149	0.069445	0.04788
226	202	98	226	163	184	0.075946	0.064116
227	18	9	227	414	385	0.0720035	0.049644
228	202	98	228	206	207	0.0598805	0.050553
229	106	51	229	57	125	0.091375	0.063
230	175	85	230	160	129	0.227838	0.192348
231	174	84	231	414	401	0.0727345	0.050148
232	113	55	232	1	375	0.010965	0.00756
233	202	98	233	127	124	0.02924	0.02016
234	0.1	0	234	129	141	0.032131	0.027126
235	202	98	235	401	386	0.059211	0.040824
236	403	195	236	208	209	0.0383775	0.02646
237	202	98	237	128	127	0.27047	0.18648
238	126	61	238	131	157	0.03655	0.0252
239	0.1	0	239	401	402	0.070907	0.048888
240	29	14	240	209	210	0.11696	0.08064
241	9	4	241	125	128	0.02193	0.01512
242	5	2	242	130	131	0.054825	0.0378
243	0.1	0	243	402	387	0.0566525	0.03906
244	18	9	244	209	211	0.0559215	0.038556
245	45	22	245	200	119	0.076755	0.05292
246	32	16	246	141	130	0.046736	0.039456
247	61	30	247	402	403	0.0595765	0.041076
248	81	39	248	211	1	0.056287	0.038808
249	126	61	249	200	201	0.00731	0.00504
250	23	11	250	157	133	0.113305	0.07812

251	14	7	251	403	388	0.083334	0.057456
252	18	9	252	375	202	0.149855	0.10332
253	126	61	253	158	200	0.02193	0.01512
254	5	3	254	133	140	0.105995	0.07308
255	26	13	255	403	404	0.0683485	0.047124
256	18	9	256	202	1	0.48246	0.33264
257	126	61	257	124	158	0.10234	0.07056
258	81	39	258	140	147	0.15351	0.10584
259	0.1	0	259	368	345	0.1151325	0.07938
260	126	61	260	373	352	0.1041675	0.07182
261	41	20	261	199	192	0.01462	0.01008
262	0.1	0	262	129	154	0.035052	0.029592
263	28	14	263	345	346	0.05848	0.04032
264	30	14	264	352	212	0.1136705	0.078372
265	81	39	265	199	197	0.069445	0.04788
266	202	98	266	137	144	0.09503	0.06552
267	318	154	267	345	369	0.0529975	0.03654
268	176	85	268	352	353	0.2138175	0.14742
269	126	61	269	159	199	0.27047	0.18648
270	6	3	270	144	148	0.09503	0.06552
271	31	15	271	400	404	0.047515	0.03276
272	60	29	272	353	213	0.201025	0.1386
273	56	27	273	197	191	0.010965	0.00756
274	126	61	274	154	156	0.032131	0.027126
275	118	57	275	404	405	0.040205	0.02772
276	126	61	276	353	214	0.0500735	0.034524
277	202	98	277	159	190	0.2359	0.2402
278	10	5	278	156	137	0.084065	0.05796
279	126	61	279	405	389	0.0588455	0.040572
280	202	98	280	1	215	0.3475905	0.239652
281	318	154	281	159	161	0.084065	0.05796
282	82	40	282	143	150	0.098685	0.06804
283	126	61	283	405	406	0.071638	0.049392

284	22	10	284	215	216	0.105995	0.07308
285	13	6	285	161	172	0.08772	0.06048
286	71	34	286	150	148	0.02193	0.01512
287	101	49	287	406	390	0.045322	0.031248
288	113	54	288	216	217	0.099314	0.083844
289	126	61	289	172	188	0.091375	0.063
290	0.1	0	290	134	139	0.119761	0.101106
291	34	17	291	406	391	0.0731	0.0504
292	83	40	292	216	218	0.06579	0.04536
293	59	29	293	188	168	0.091375	0.063
294	126	61	294	139	143	0.062135	0.04284
295	145	70	295	404	407	0.083334	0.057456
296	202	98	296	218	219	0.002924	0.002016
297	50	24	297	176	179	0.06579	0.04536
298	41	20	298	154	134	0.078867	0.066582
299	202	98	299	407	392	0.0785825	0.05418
300	77	37	300	219	220	0.08041	0.05544
301	161	78	301	168	176	0.113305	0.07812
302	477	231	302	148	57	0.1462	0.1008
303	68	33	303	407	408	0.048977	0.033768
304	14	7	304	220	223	0.0709803	0.0599238
305	4	2	305	161	185	0.13158	0.09072
306	0.1	0	306	129	151	0.032895	0.02268
307	66	32	307	408	409	0.0668865	0.046116
308	0.1	0	308	223	237	0.081788	0.069048
309	60	29	309	185	164	0.091375	0.063
310	95	46	310	145	146	0.032895	0.02268
311	0.1	0	311	409	393	0.073831	0.050904
312	19	9	312	237	238	0.0622173	0.0525258
313	67	32	313	164	165	0.032895	0.02268
314	18	9	314	146	149	0.054825	0.0378
315	33	16	315	409	394	0.0690795	0.047628
316	21	10	316	237	372	0.0537464	0.0453744

317	33	16	317	165	173	0.13889	0.09576
318	42	20	318	152	135	0.076755	0.05292
319	52	25	319	408	410	0.0551905	0.038052
320	43	21	320	239	240	0.005842	0.004932
321	126	61	321	173	179	0.113305	0.07812
322	107	52	322	135	145	0.142545	0.09828
323	202	98	323	410	415	0.06579	0.04536
324	126	61	324	239	243	0.0835406	0.0705276
325	24	12	325	179	160	0.069445	0.04788
326	101	49	326	135	195	0.0091375	0.0063
327	81	39	327	410	411	0.064328	0.044352
328	155	75	328	243	355	0.0054825	0.00378
329	23	11	329	159	182	0.054096	0.063812
330	31	15	330	151	152	0.054825	0.0378
331	126	61	331	411	395	0.0595765	0.041076
332	13	6	332	355	354	0.127925	0.0882
333	56	27	333	182	186	0.0483	0.056975
334	120	58	334	1	190	0.14154	0.14412
335	126	61	335	411	412	0.0676175	0.04662
336	403	195	336	354	242	0.018275	0.0126
337	81	39	337	186	166	0.037744	0.038432
338	177	86	338	190	189	0.0731	0.0504
339	151	73	339	412	399	0.0566525	0.03906
340	9	4	340	354	241	0.0731	0.0504
341	29	14	341	166	170	0.037744	0.038432
342	14	7	342	189	198	0.10965	0.0756
343	23	11	343	412	398	0.071638	0.049392
344	45	22	344	243	356	0.0091375	0.0063
345	0.1	0	345	170	174	0.02921	0.02466
346	36	17	346	198	196	0.03655	0.0252
347	5	2	347	412	413	0.0873545	0.060228
348	9	4	348	356	357	0.05117	0.03528
349	80	39	349	174	180	0.063693	0.064854

350	0.1	0	350	189	193	0.023392	0.016128
351	0.1	0	351	413	397	0.0705415	0.048636
352	0.1	0	352	357	244	0.0127925	0.00882
353	0.1	0	353	159	184	0.22661	0.15624
354	0.1	0	354	149	138	0.127925	0.0882
355	0.1	0	355	413	396	0.069445	0.04788
356	0.1	0	356	357	245	0.0054825	0.00378
357	0.1	0	357	184	187	0.035052	0.029592
358	0.1	0	358	138	155	0.105995	0.07308
359	0.1	0	359	290	289	0.062866	0.043344
360	0.1	0	360	243	246	0.0365125	0.030825
361	0.1	0	361	246	247	0.052632	0.036288
362	0.1	0	362	265	266	0.1078225	0.07434
363	0.1	0	363	289	288	0.046784	0.032256
364	0.1	0	364	306	310	0.126463	0.087192
365	0.1	0	365	247	248	0.0727345	0.050148
366	0.1	0	366	266	267	0.099416	0.068544
367	0.1	0	367	288	300	0.1867705	0.128772
368	0.1	0	368	310	320	0.0127925	0.00882
369	0.1	0	369	243	249	0.0487807	0.0411822
370	0.1	0	370	267	268	0.156434	0.107856
371	0.1	0	371	300	286	0.10965	0.0756
372	0.1	0	372	310	314	0.072369	0.049896
373	0.1	0	373	249	358	0.043129	0.029736
374	0.1	0	374	268	269	0.0549647	0.0559666
375	0.1	0	375	1	373	0.027778	0.019152
376	0.1	0	376	314	309	0.0698105	0.048132
377	86	41	377	358	359	0.0054825	0.00378
378	86	41	378	269	365	0.07077	0.07206
379	0.1	0	379	300	285	0.081141	0.055944
380	0.1	0	380	309	313	0.0785825	0.05418
381	0.1	0	381	359	250	0.0201025	0.01386
382	0.1	0	382	365	366	0.025585	0.01764

383	0.1	0	383	300	301	0.0932025	0.06426
384	0.1	0	384	313	317	0.0683485	0.047124
385	68	33	385	359	251	0.1407175	0.09702
386	15	7	386	366	270	0.1005125	0.0693
387	56	27	387	301	302	0.055556	0.038304
388	12	6	388	317	319	0.123539	0.085176
389	50	24	389	251	252	0.1882325	0.12978
390	115	56	390	366	271	0.0164475	0.01134
391	14	7	391	302	303	0.045322	0.031248
392	5	2	392	319	318	0.066521	0.045864
393	19	9	393	251	360	0.098685	0.06804
394	34	17	394	365	363	0.0483595	0.049241
395	10	5	395	303	304	0.195177	0.134568
396	40	19	396	318	315	0.069445	0.04788
397	28	14	397	360	253	0.049708	0.034272
398	14	7	398	363	362	0.018872	0.019216
399	17	8	399	304	305	0.208335	0.14364
400	41	20	400	315	311	0.083334	0.057456
401	0.1	0	401	253	254	0.0458597	0.0387162
402	0.1	0	402	363	381	0.26316	0.18144
403	0.1	0	403	305	308	0.050439	0.034776
404	0.1	0	404	311	304	0.105264	0.072576
405	0.1	0	405	254	361	0.0588455	0.040572
406	0.1	0	406	362	272	0.0164475	0.01134
407	0.1	0	407	308	316	0.2218585	0.152964
408	0.1	0	408	296	260	0.0478805	0.033012
409	0.1	0	409	361	256	0.040205	0.02772
410	0.1	0	410	362	1	0.02415	0.0284875
411	0.1	0	411	316	312	0.105264	0.072576
412	0.1	0	412	260	287	0.035819	0.024696
413	0.1	0	413	254	255	0.0274125	0.0189
414	0.1	0	414	1	364	0.28509	0.19656
415	19	9	415	312	307	0.072369	0.049896

416	0	0	416	260	324	0.1078225	0.07434
417	0	0	417	254	257	0.078867	0.066582
418	0	0	418	364	284	0.1041675	0.07182
419	0	0	419	307	300	0.078217	0.053928
420	0	0	420	324	326	0.0054825	0.00378
421	0	0	421	257	258	0.105995	0.07308
422	0	0	422	364	285	0.05848	0.04032
423	0	0	423	334	336	0.0712725	0.04914
424	0	0	424	324	266	0.103802	0.071568
425	0	0	425	257	283	0.0537464	0.0453744
426	0	0	426	381	268	0.3095785	0.213444
427	0	0	427	336	323	0.054825	0.0378
428	0	0	428	324	325	0.048246	0.033264
429	0	0	429	283	282	0.0663067	0.0559782
430	0	0	430	268	327	0.0383775	0.02646
431	0	0	431	336	337	0.0646935	0.044604
432	0	0	432	324	323	0.08772	0.06048
433	0	0	433	282	234	0.055499	0.046854
434	0	0	434	327	328	0.054825	0.0378
435	0	0	435	337	338	0.02924	0.02016
436	0	0	436	323	322	0.0676175	0.04662
437	0	0	437	234	233	0.0277495	0.023427
438	0	0	438	268	297	0.050439	0.034776
439	0	0	439	338	339	0.0420325	0.02898
440	0	0	440	322	321	0.09503	0.06552
441	0	0	441	233	376	0.011684	0.009864
442	0	0	442	297	296	0.050439	0.034776
443	0	0	443	339	265	0.067983	0.046872
444	0	0	444	321	299	0.070176	0.048384
445	0	0	445	230	231	0.0455676	0.0384696
446	0	0	446	296	295	0.0741965	0.051156
447	0	0	447	265	367	0.008772	0.006048
448	0	0	448	299	296	0.038012	0.026208

449	0	0	449	230	228	0.026289	0.022194
450	0	0	450	296	298	0.0376465	0.025956
451	0	0	451	367	340	0.0010965	0.000756
452	0	0	452	322	329	0.031433	0.021672
453	0	0	453	228	371	0.046736	0.039456
454	0	0	454	295	294	0.022661	0.015624
455	0	0	455	340	341	0.0274125	0.0189
456	0	0	456	329	330	0.0266815	0.018396
457	0	0	457	371	374	0.0394335	0.033291
458	0	0	458	294	292	0.0917405	0.063252
459	0	0	459	341	342	0.113305	0.07812
460	0	0	460	330	331	0.041667	0.028728
461	0	0	461	374	227	0.003655	0.00252
462	0	0	462	268	292	0.098685	0.06804
463	0	0	463	334	335	0.0559215	0.038556
464	0	0	464	331	332	0.0274125	0.0189
465	0	0	465	374	226	0.0023368	0.0019728
466	0	0	466	292	290	0.016813	0.011592
467	0	0	467	341	368	0.179095	0.12348
468	0	0	468	329	333	0.05848	0.04032
469	0	0	469	226	225	0.0274125	0.0189
470	0	0	470	290	291	0.0054825	0.00378
471	0	0	471	376	230	0.0277495	0.023427
472	0	0	472	333	334	0.041667	0.028728
473	**27372.4**	**13237**	473	368	343	0.0091375	0.0063

Source: Bernal-Agustin (1998).